SAR Basic Concepts:

Estimation of Vertical Structure Parameters

Konstantinos Papathanassiou
kostas.papathanassiou@dlr.de

Microwaves and Radar Institute (DLR-HR)
German Aerospace Center (DLR)

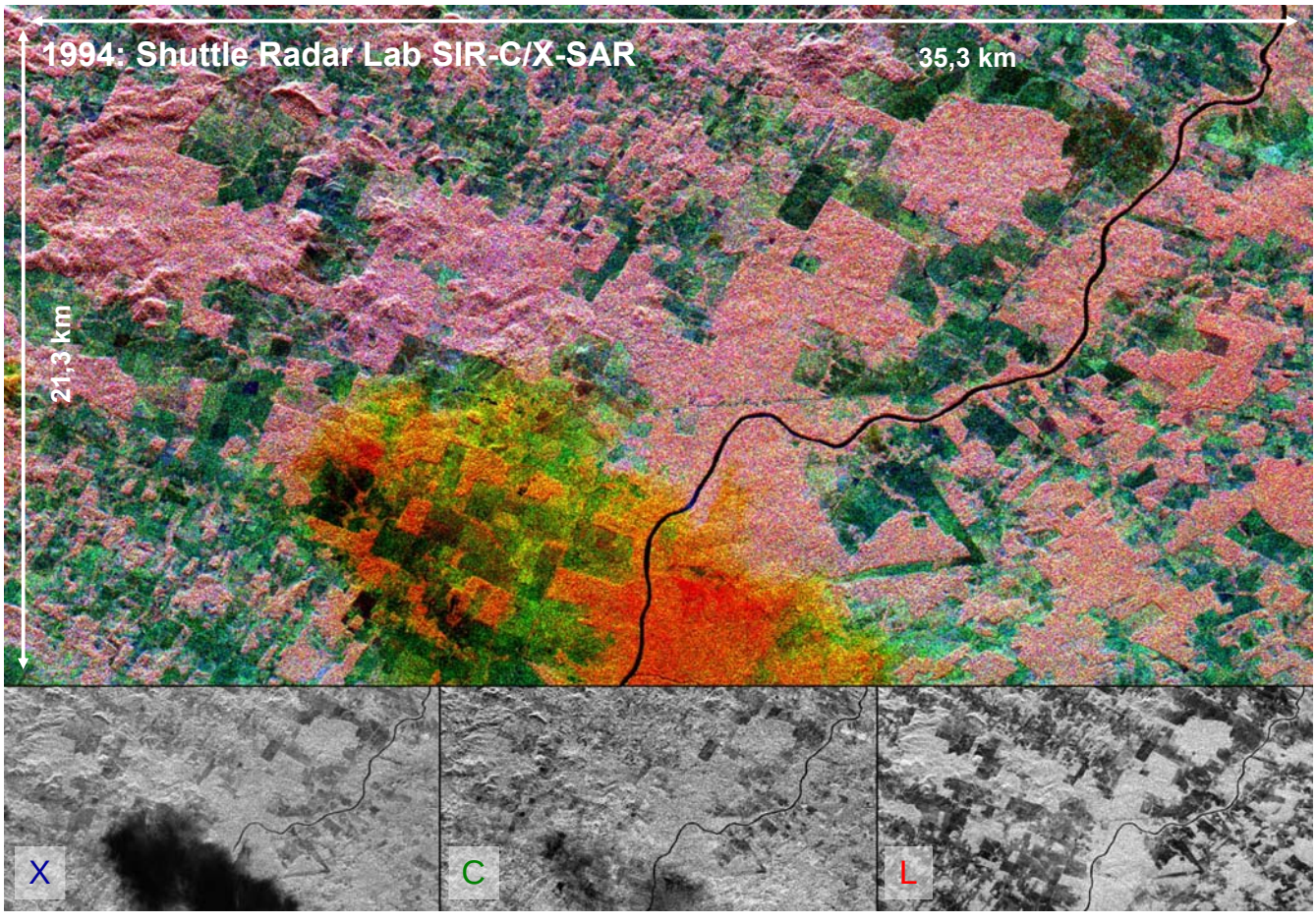

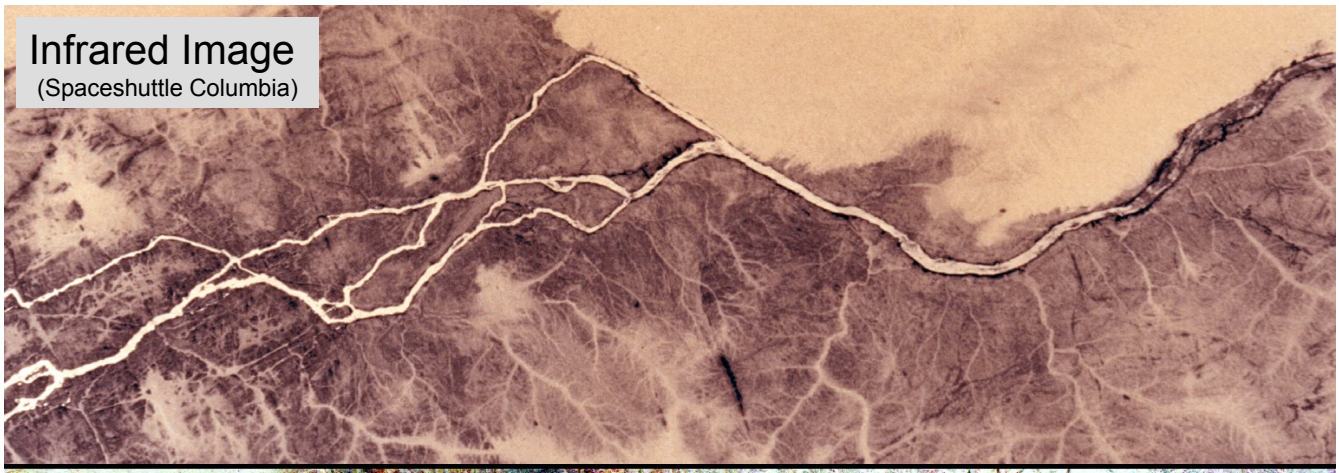
Infrared Image
(Spaceshuttle Columbia)

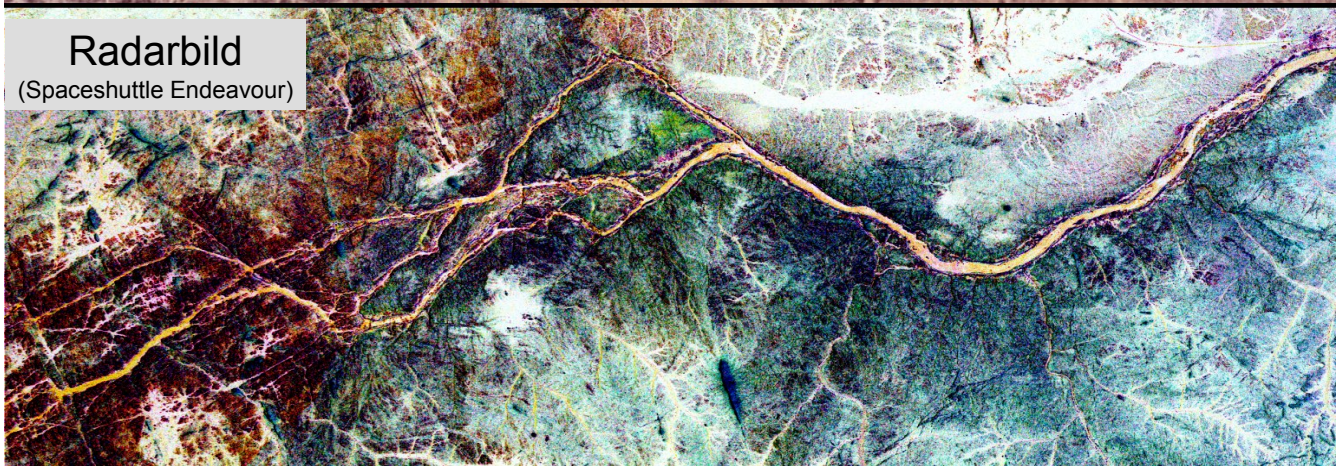
Radarbild
(Spaceshuttle Endeavour)

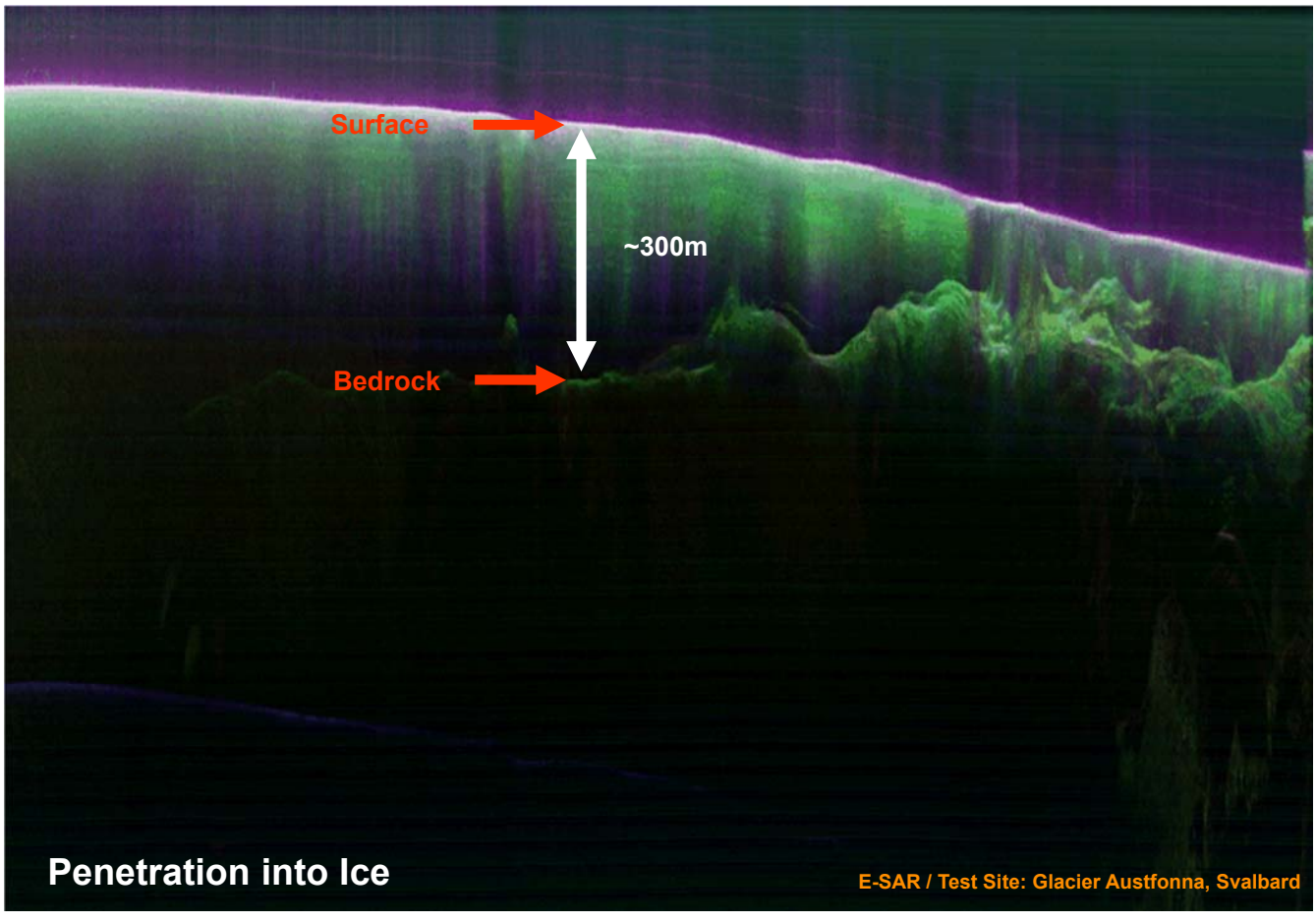
Surface
~300m
Bedrock
Penetration into Ice
E-SAR / Test Site: Glacier Austfonna, Svalbard

Penetration into Vegetation

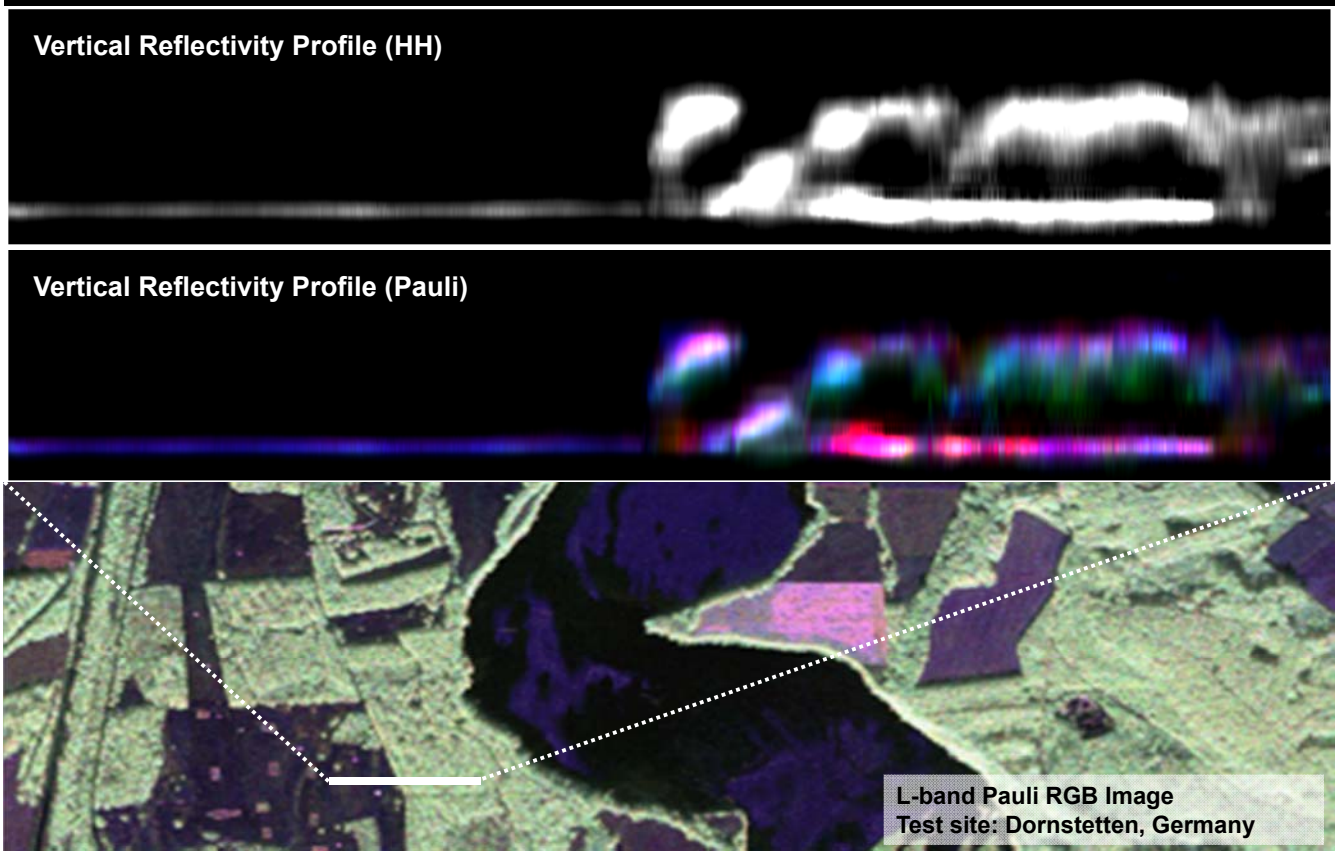

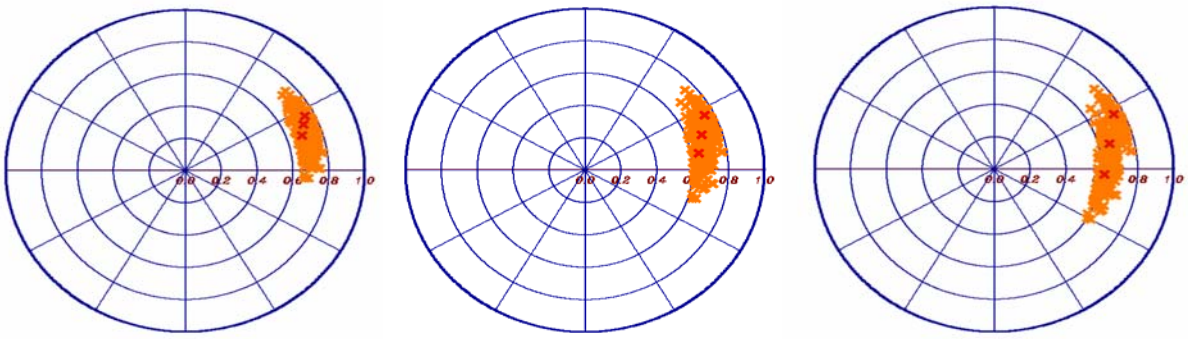

Cross-Range Resolution

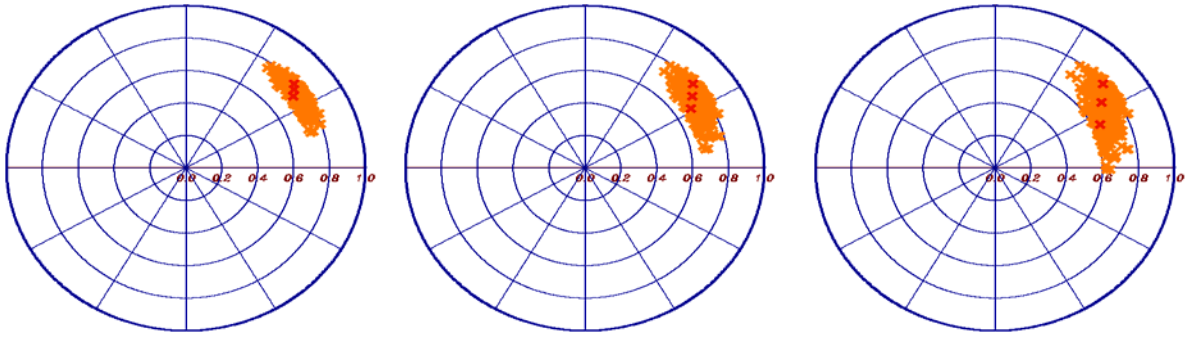

Vertical Resolution: Nadir Looking Case

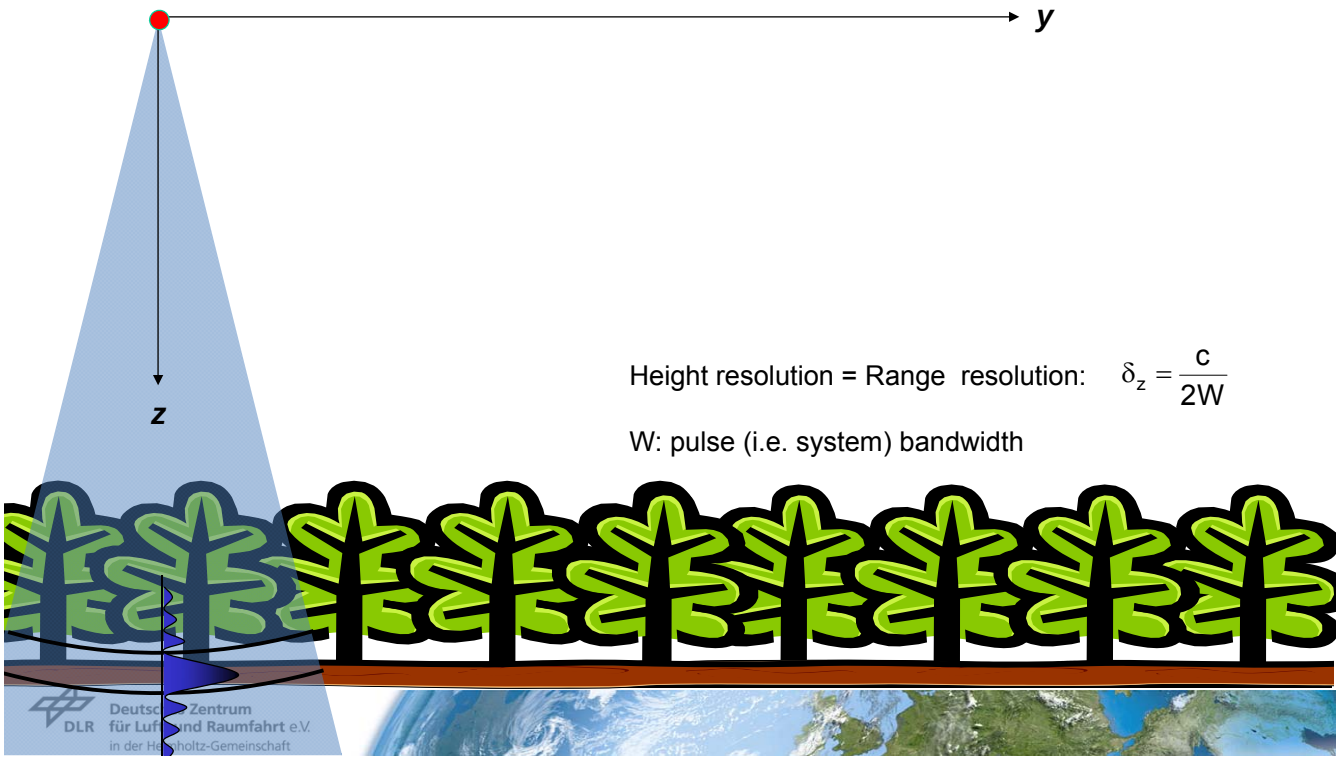

Height resolution = Range resolution: $\delta_z = \frac{c}{2W}$

W: pulse (i.e. system) bandwidth

Vertical Resolution: Side Looking Case

(Slant) range resolution: $\delta_r = \frac{c}{2W}$

W: pulse (i.e. system) bandwidth

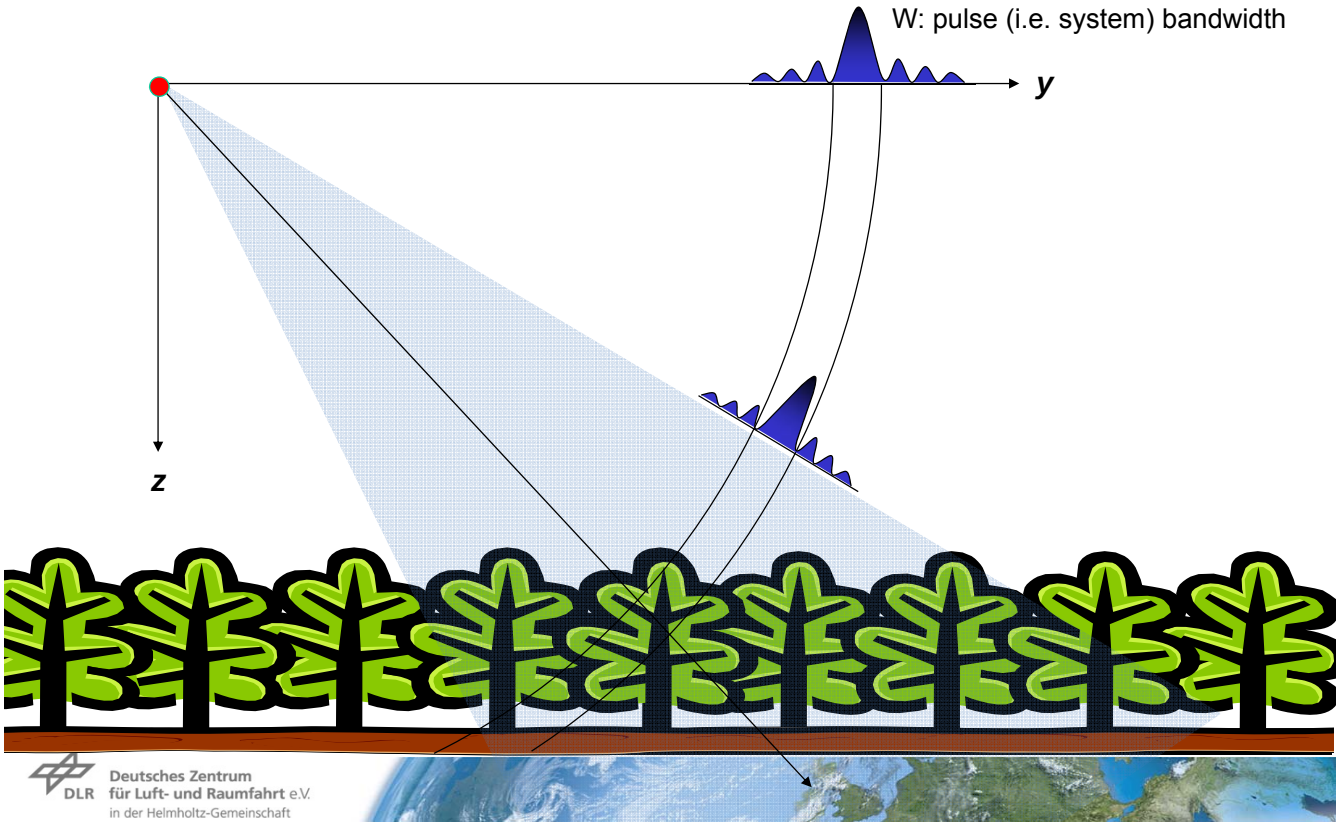

Vertical Resolution: SAR Tomography

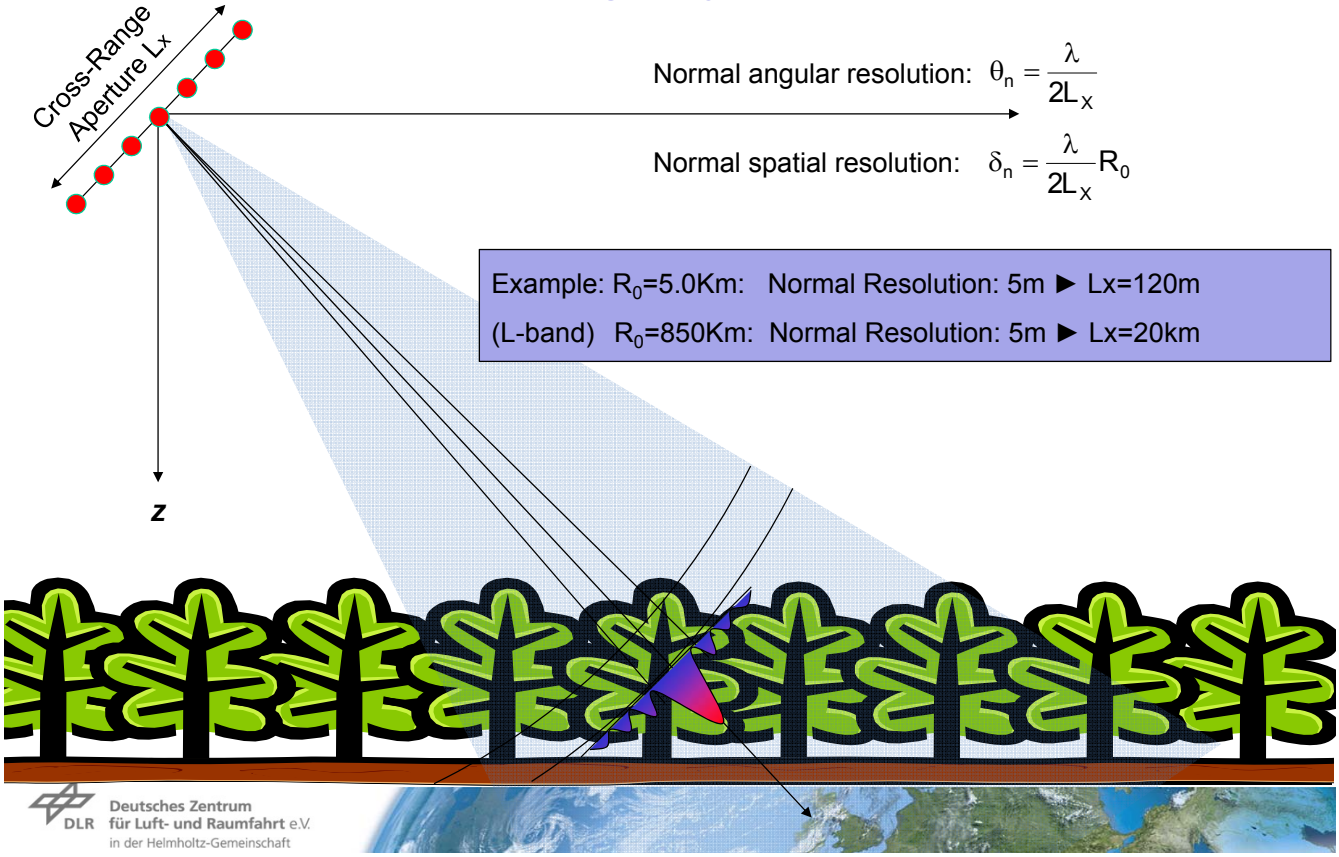

Normal angular resolution: $\theta_n = \frac{\lambda}{2L_X}$

Normal spatial resolution: $\delta_n = \frac{\lambda}{2L_X} R_0$

Example: R_0=5.0Km: Normal Resolution: 5m ► Lx=120m

(L-band) R_0=850Km: Normal Resolution: 5m ► Lx=20km

Deutsches Zentrum DLR für Luft- und Raumfahrt e.V. in der Helmholtz-Gemeinschaft

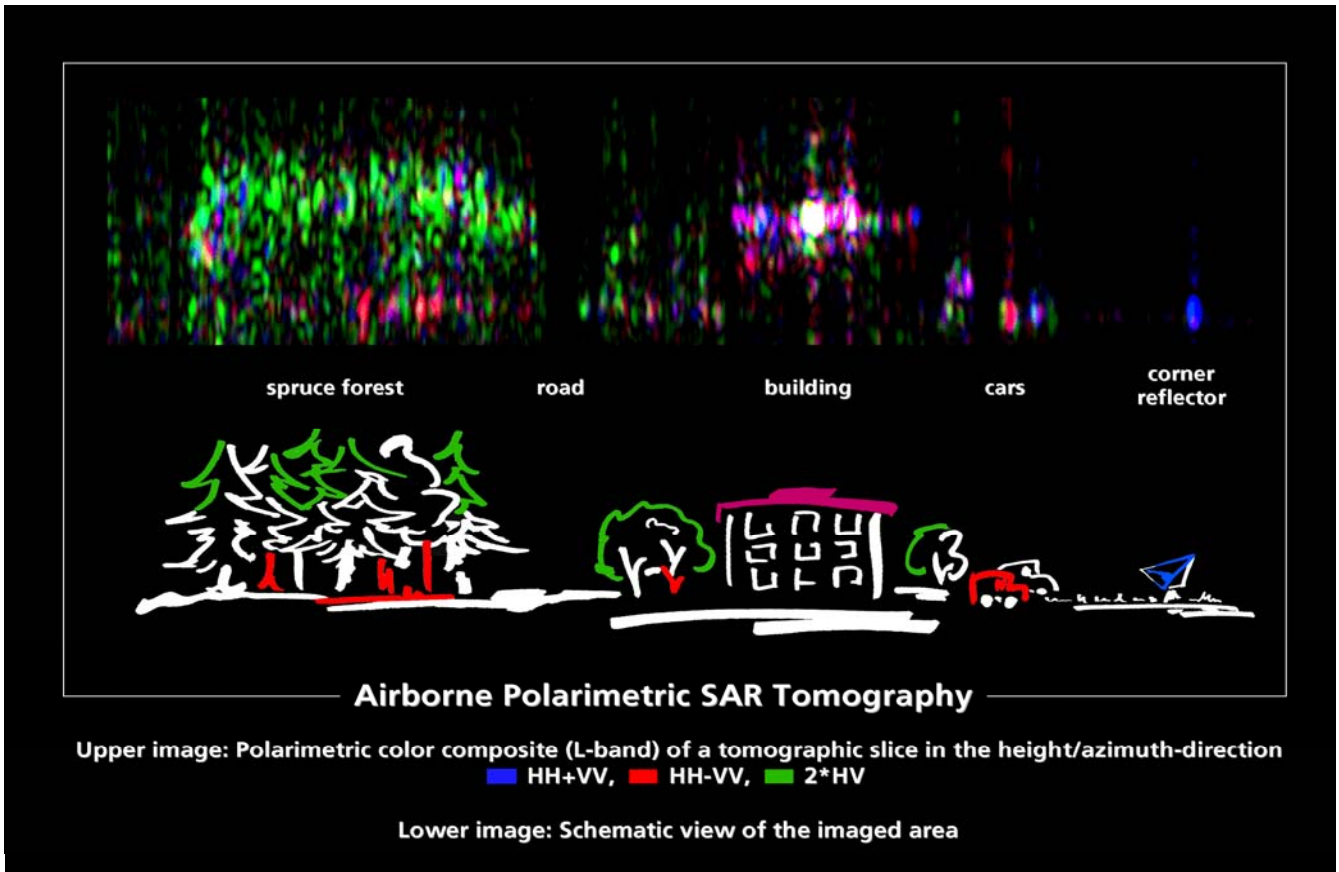

Airborne Polarimetric SAR Tomography

Upper image: Polarimetric color composite (L-band) of a tomographic slice in the height/azimuth-direction
HH+VV, HH-VV, 2*HV

Lower image: Schematic view of the imaged area

Reigber, A. et al: "First Demonstration of Airborne SAR Tomography using Multibaseline L-Band Data". IEEE Trans. on Geosc. and Remote Sensing, Vol. 38 (5), Sept. 2000

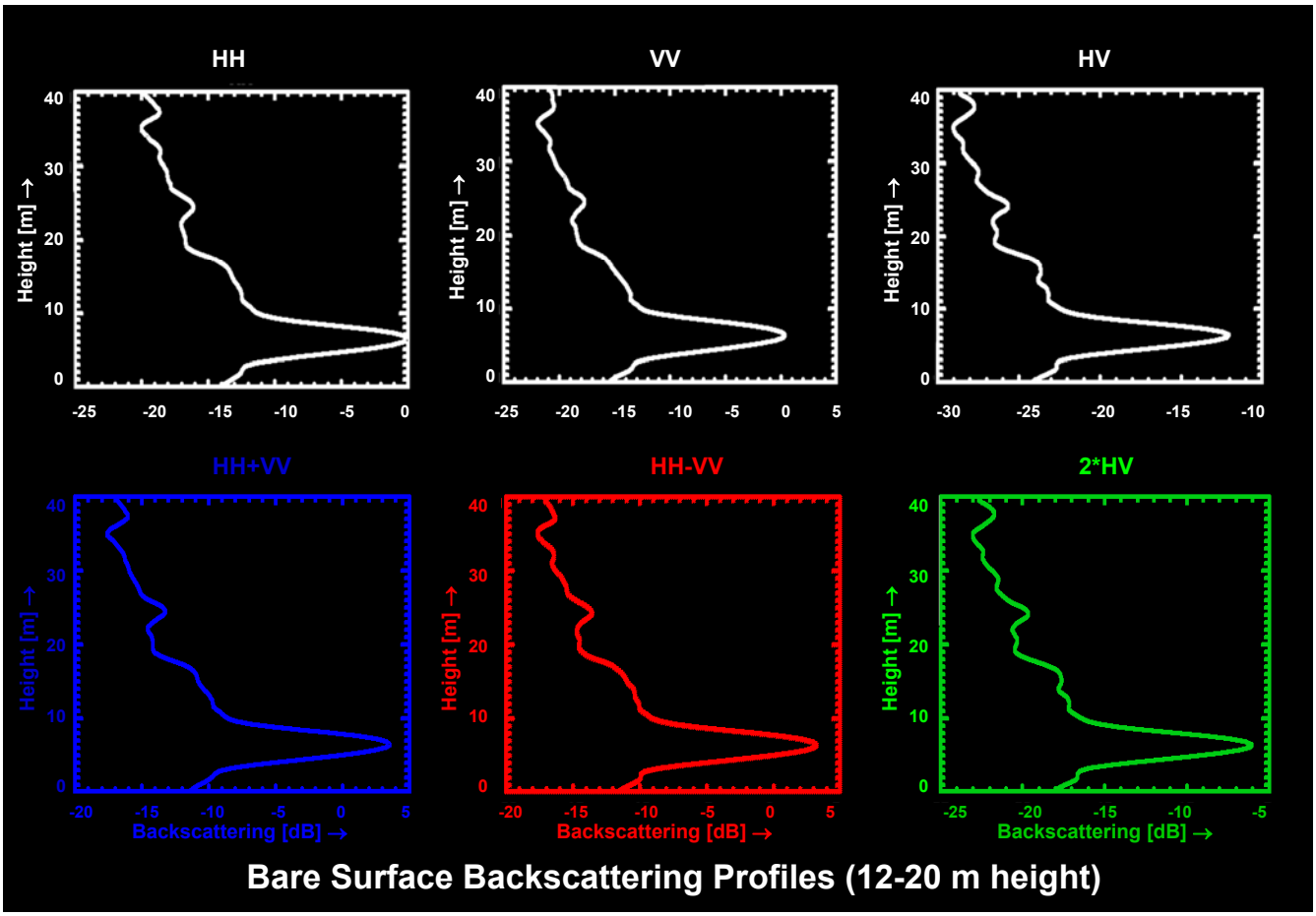

Bare Surface Backscattering Profiles (12-20 m height)

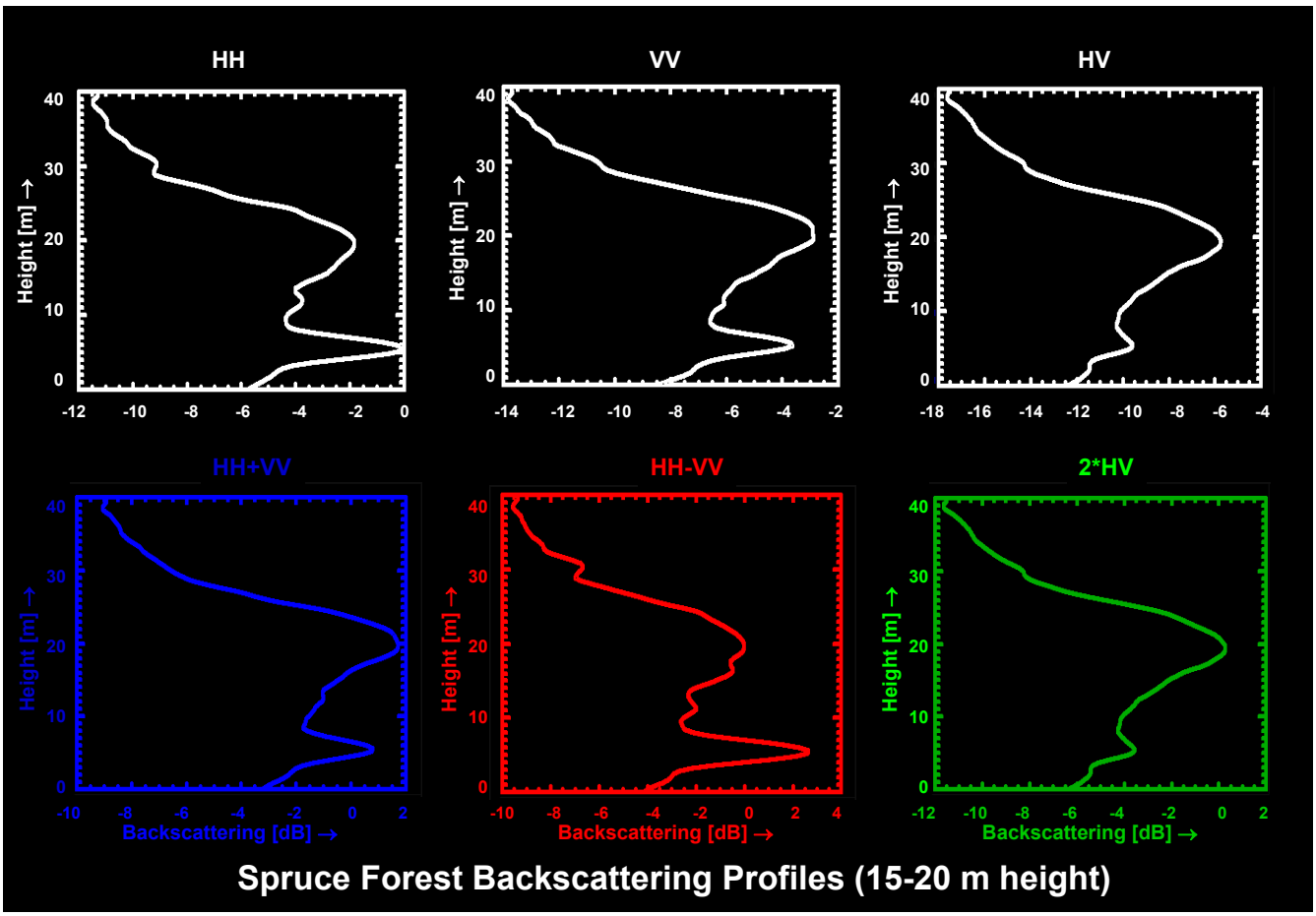

Spruce Forest Backscattering Profiles (15-20 m height)

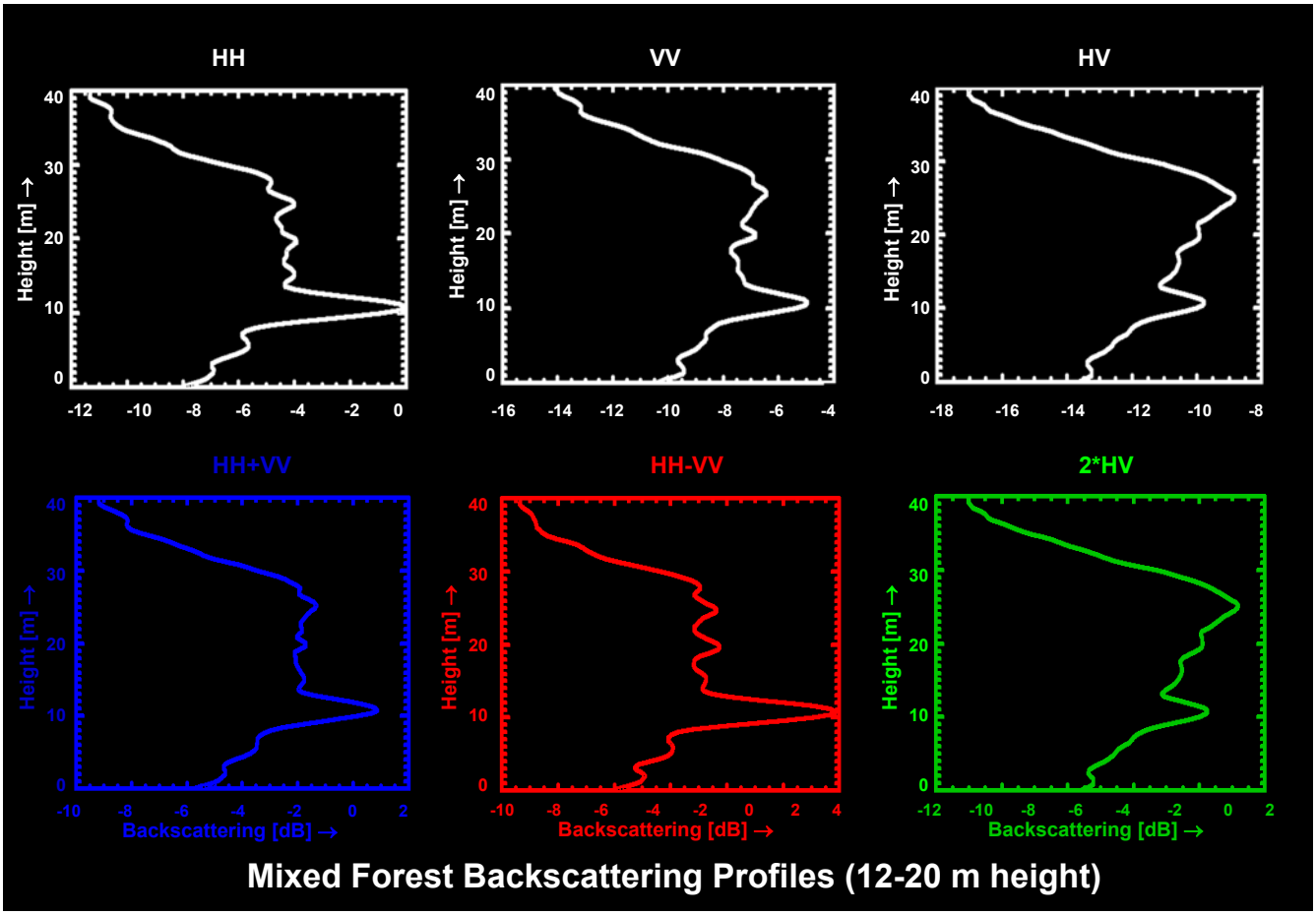

Vertical Resolution

(Slant) range resolution: $\delta_r = \frac{c}{2W}$

W: pulse (i.e. system) bandwidth

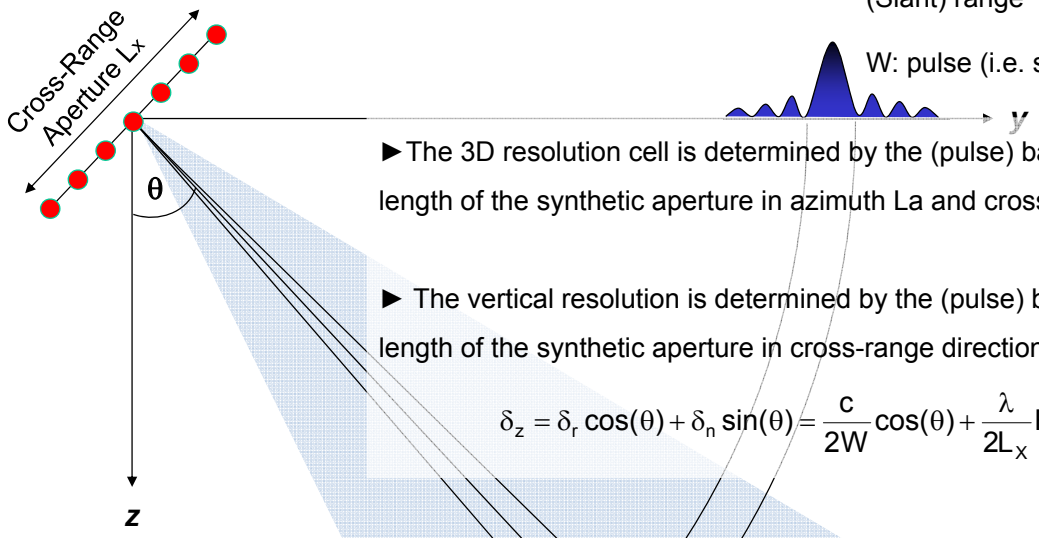

► The 3D resolution cell is determined by the (pulse) bandwidth W and the length of the synthetic aperture in azimuth La and cross-range direction Lx.

► The vertical resolution is determined by the (pulse) bandwidth W and the length of the synthetic aperture in cross-range direction Lx.

$$\delta_z = \delta_r \cos(\theta) + \delta_n \sin(\theta) = \frac{c}{2W}\cos(\theta) + \frac{\lambda}{2L_X} R_0 \sin(\theta)$$

Normal spatial resolution: $\delta_n = \frac{\lambda}{2L_x} R_0$

The Effect of System Bandwidth

(Slant) range resolution: $\delta_r = \frac{c}{2W}$

W: pulse (i.e. system) bandwidth

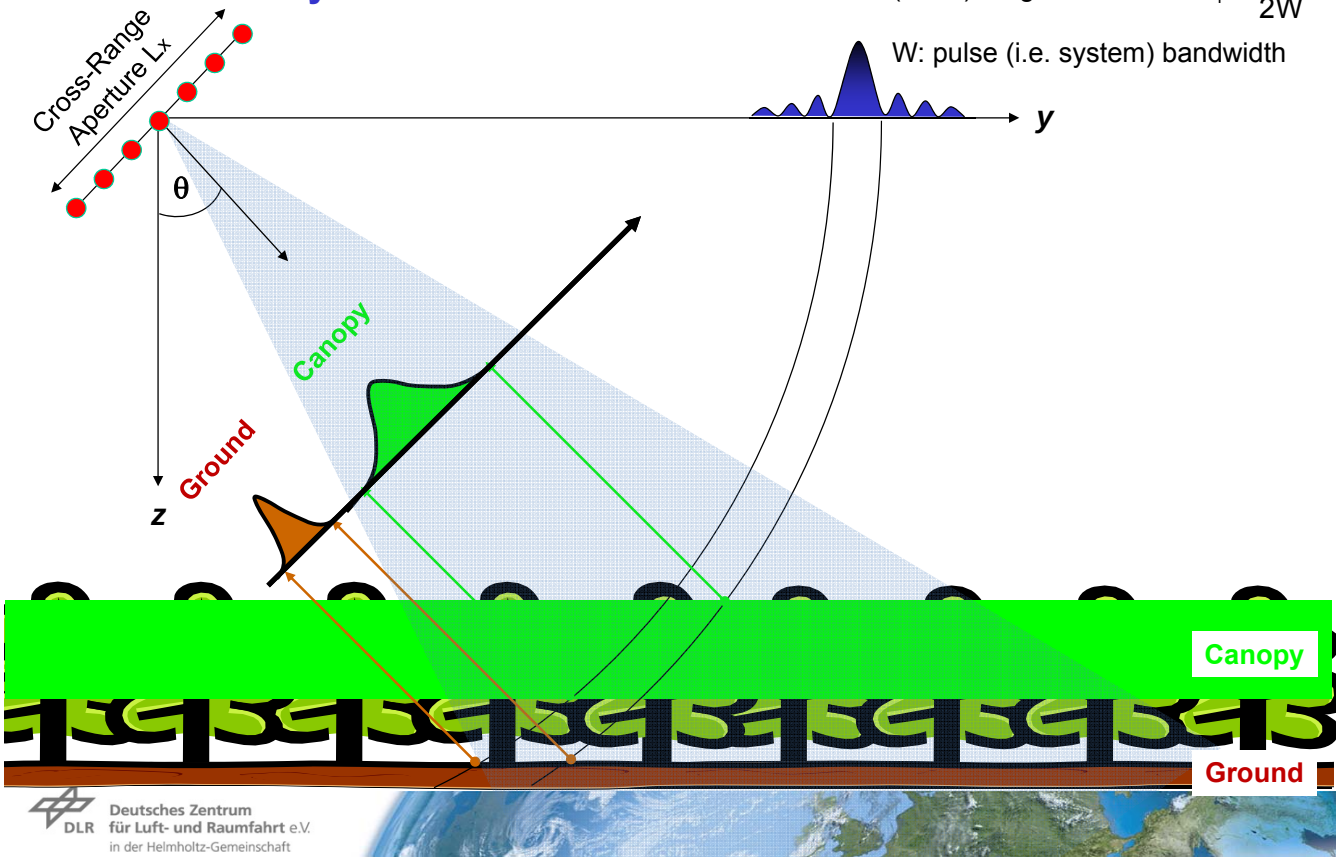

The Effect of System Bandwidth II.

(Slant) range resolution: $\delta_r = \frac{c}{2W}$

W: pulse (i.e. system) bandwidth

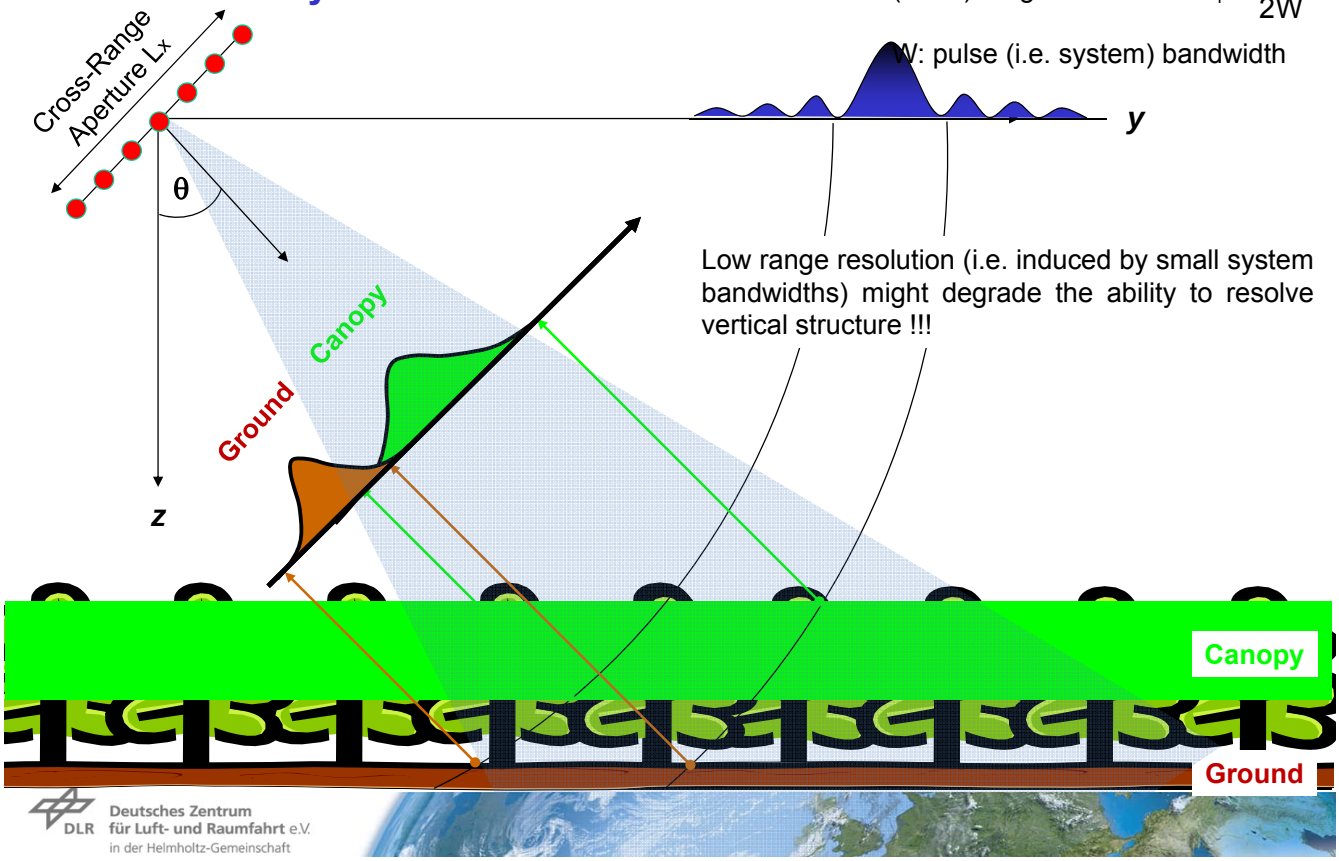

Low range resolution (i.e. induced by small system bandwidths) might degrade the ability to resolve vertical structure !!!

The Effect of System Bandwidth

150Mhz Bandwidth / 7 Tracks

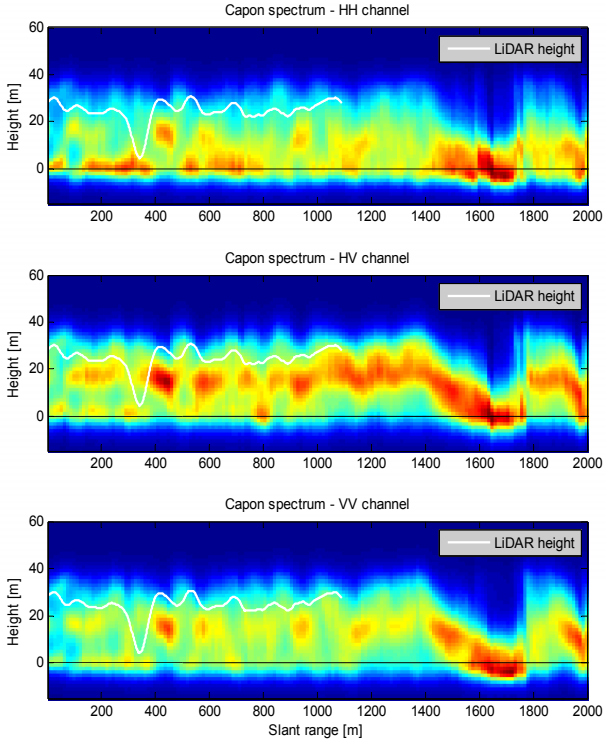

6Mhz Bandwidth / 7 Tracks

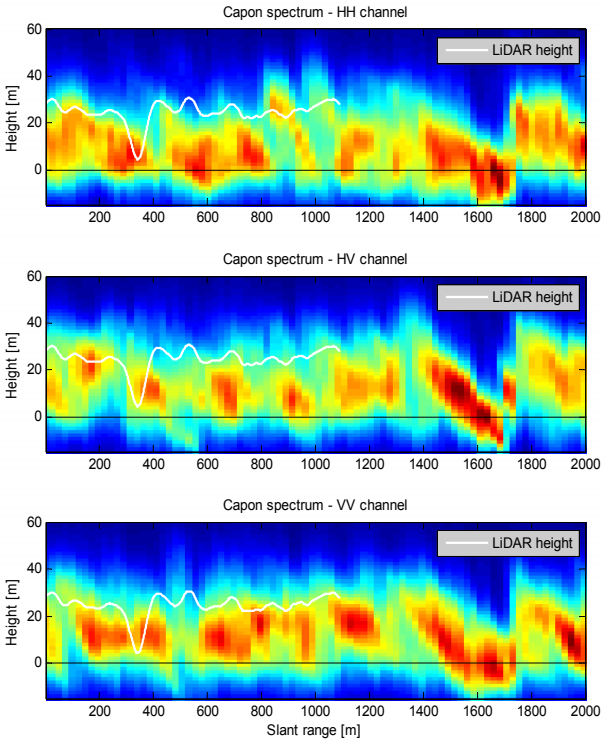

Vertical Resolution

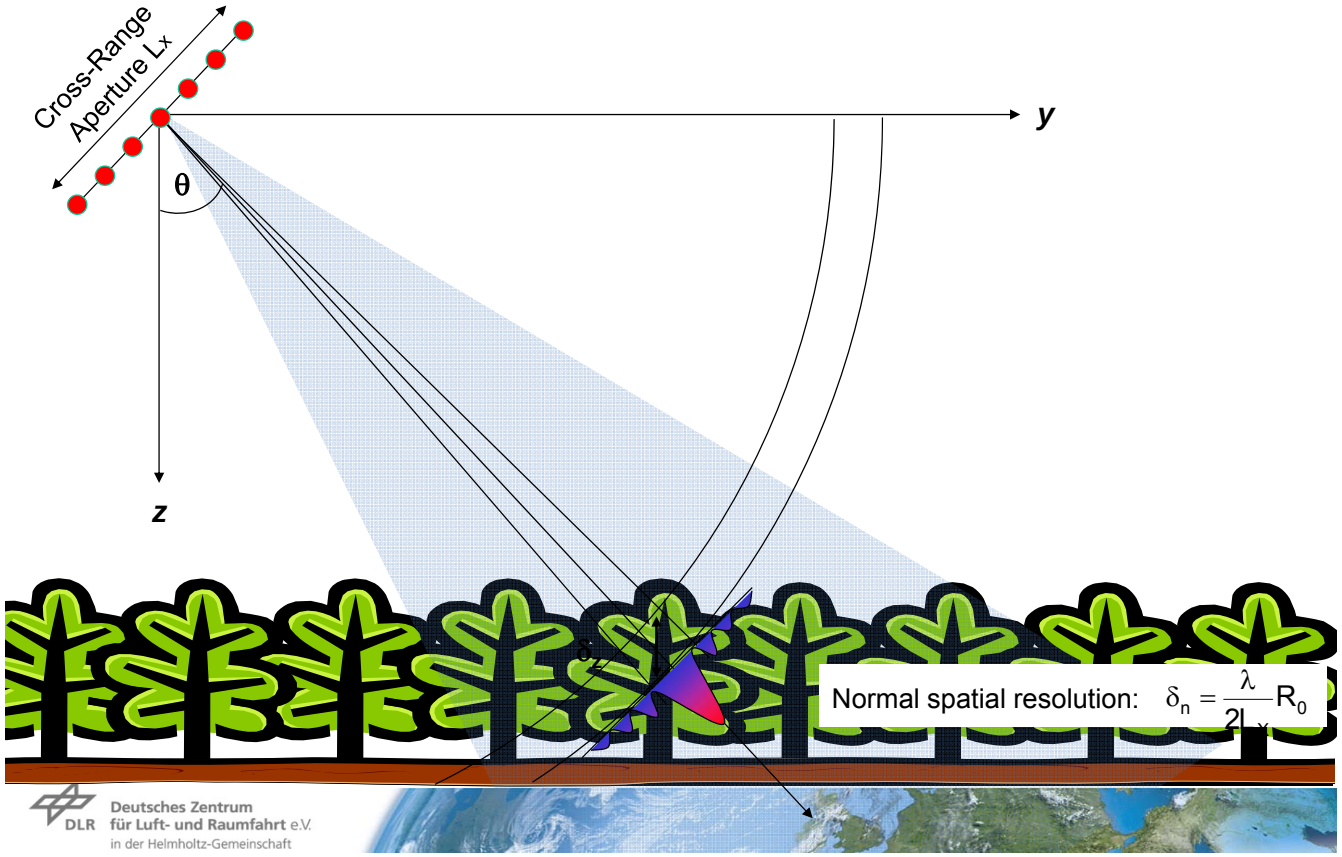

Vertical Resolution

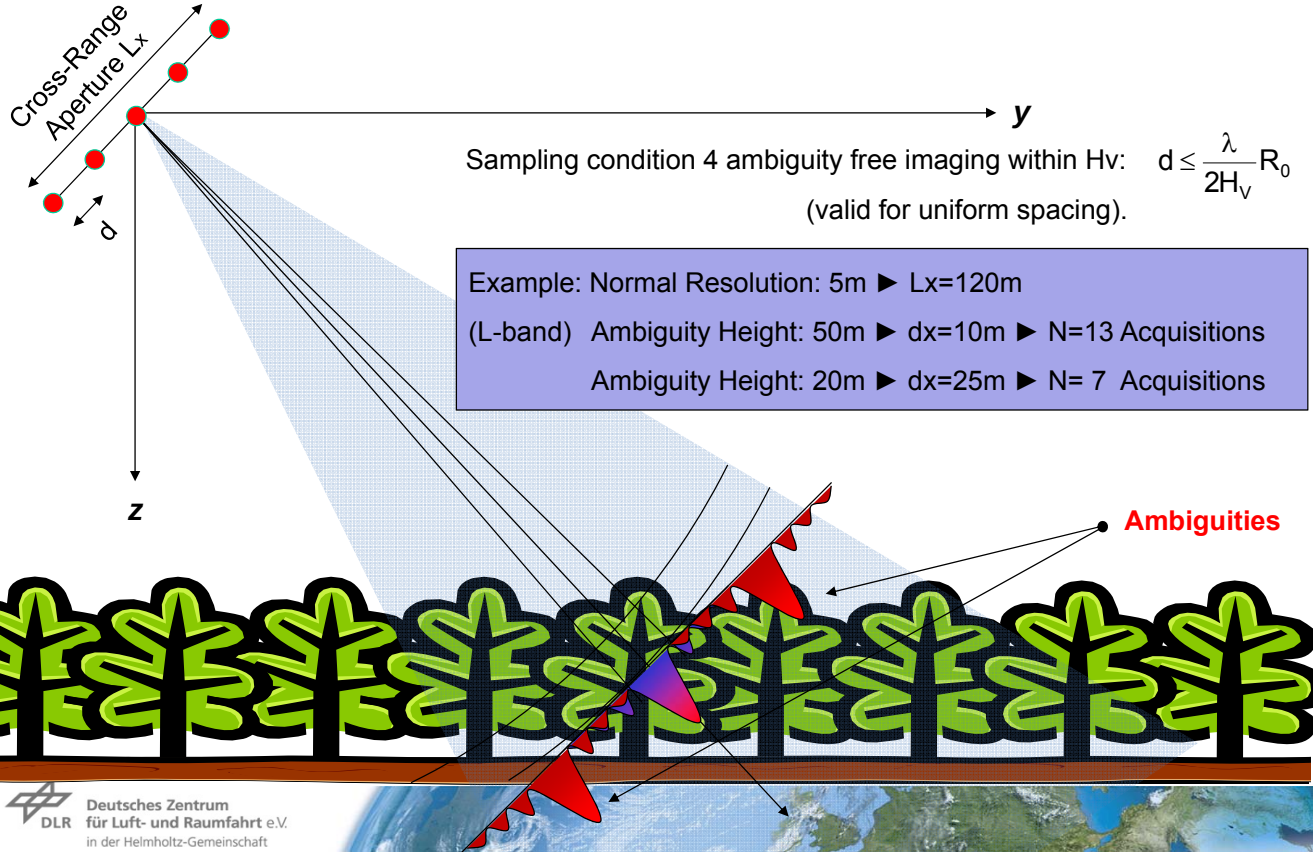

Sampling condition 4 ambiguity free imaging within Hv: $d \le \frac{\lambda}{2H_V} R_0$

(valid for uniform spacing).

Example: Normal Resolution: 5m ► Lx=120m

(L-band) Ambiguity Height: 50m ► dx=10m ► N=13 Acquisitions

Ambiguity Height: 20m ► dx=25m ► N= 7 Acquisitions

Sidelobe / Ambiguity Suppression

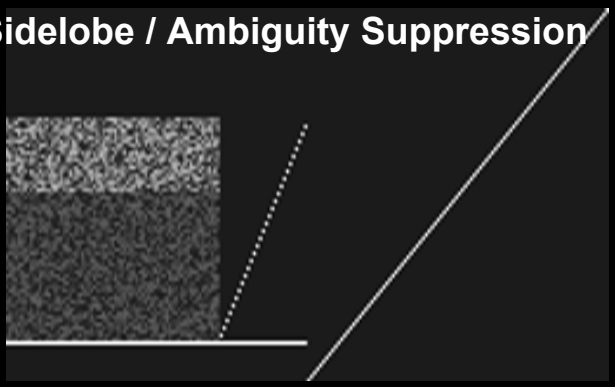

Simulated scatterer distribution

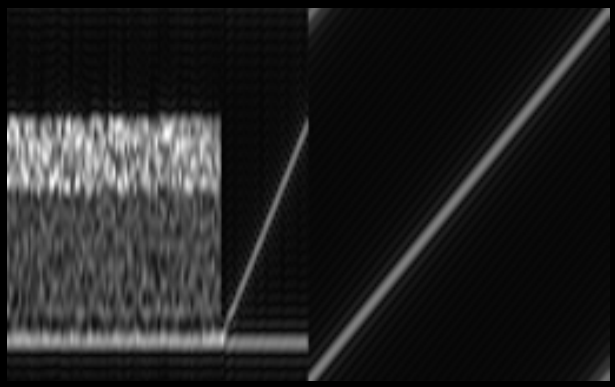

Reconstruction
25 equally spaced tracks with 10m mutual distance

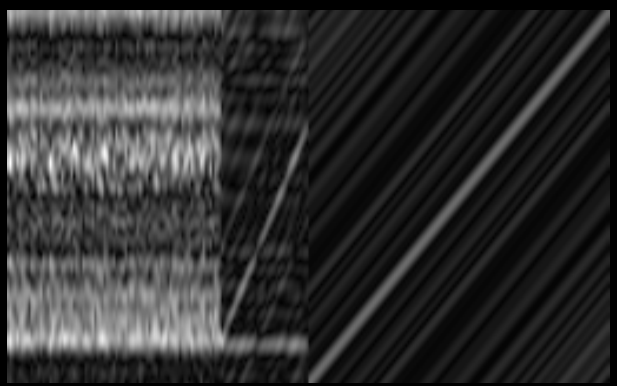

Reconstruction
from 14 unevenly distributed tracks

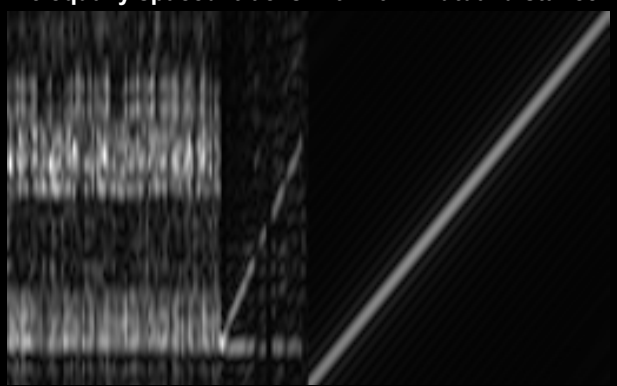

Reconstruction
from 14 unevenly distributed tracks after resampling

SAR Interferometry

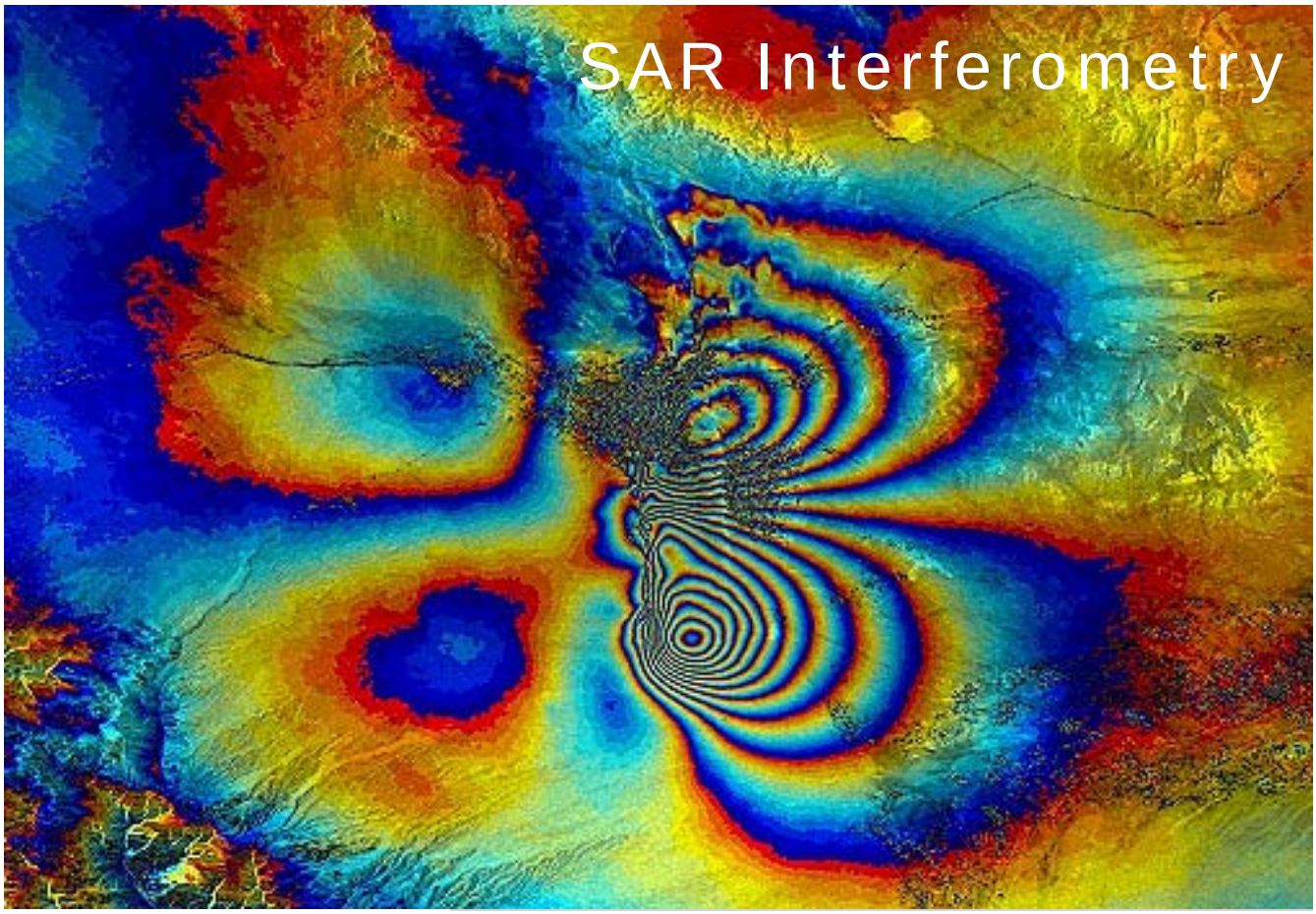

SAR Interferometry

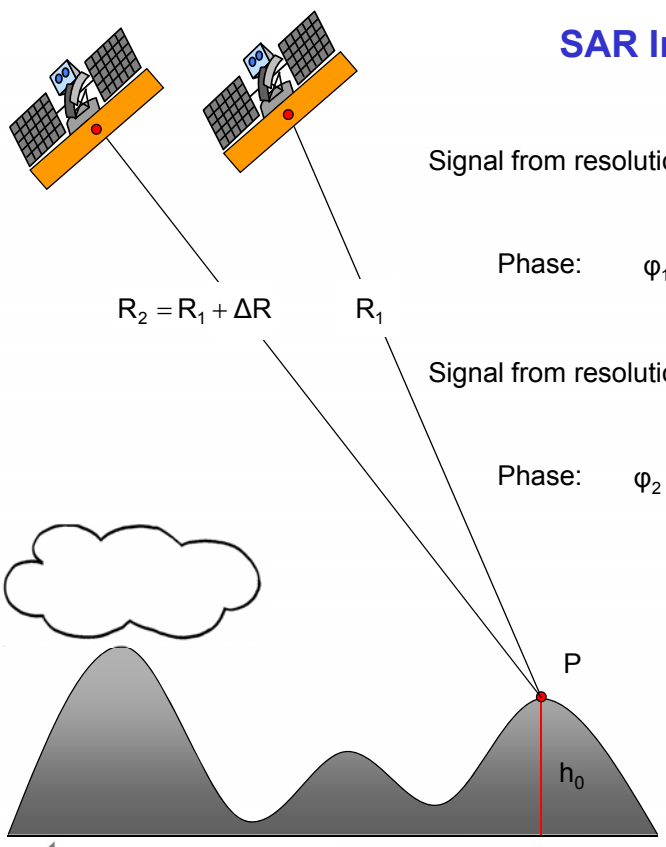

Signal from resolution cell P in Image 1: $i_1 = |i_1| \exp[-i(2\frac{2\pi}{\lambda}R_1) + \varphi_{S1}]$

Phase: $\varphi_1 = \arg(i_1) = (2\frac{2\pi}{\lambda}R_1) + \varphi_{S1}$

Signal from resolution cell P in Image 2: $i_2 = |i_2| \exp[-i(2\frac{2\pi}{\lambda}R_2) + \varphi_{S2}]$

Phase: $\varphi_2 = \arg(i_2) = (2\frac{2\pi}{\lambda}R_2) + \varphi_{S2}$

SAR Interferometry

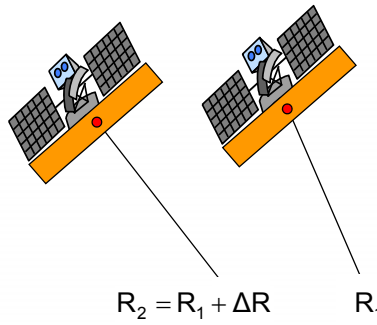

$R_2 = R_1 + \Delta R$ R_1

Signal from resolution cell P in Image 1: $i_1 = |i_1| \exp[-i(2\frac{2\pi}{\lambda}R_1) + \varphi_{S1}]$

Phase: $\varphi_1 = \arg(i_1) = (2\frac{2\pi}{\lambda}R_1) + \varphi_{S1}$

Signal from resolution cell P in Image 2: $i_2 = |i_2| \exp[-i(2\frac{2\pi}{\lambda}R_2) + \varphi_{S2}]$

Phase: $\varphi_2 = \arg(i_2) = (2\frac{2\pi}{\lambda}R_2) + \varphi_{S2}$

Assuming $\varphi_{S1} = \varphi_{S2}$!!!

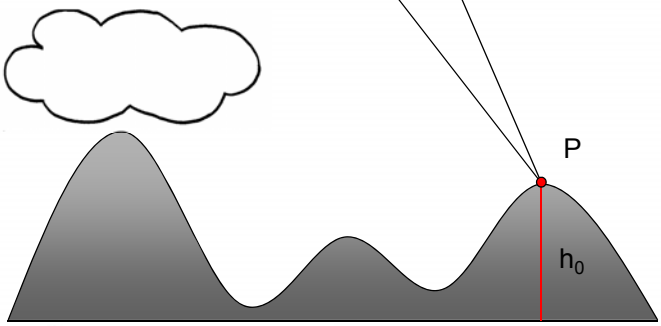

P

h_0

Interferogram: $i_1 i_2^* = |i_1 i_2^*| \exp[-i(2\frac{2\pi}{\lambda}\Delta R)]$

Phase: $\varphi_{Int} = \frac{\mathrm{Re}\{i_1 i_2^*\}}{\mathrm{Im}\{i_1 i_2^*\}} = 2\frac{2\pi}{\lambda}\Delta R$

Deterministic !!!

SAR Interferometry

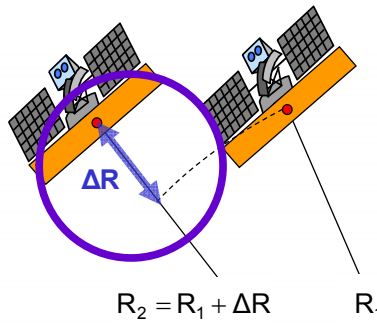

ΔR

$R_2 = R_1 + \Delta R$ R_1

Interferometric Phase: $\varphi = 2\frac{2\pi}{\lambda}\Delta R$

The interferometric phase φ is another way to measure the (relative) distance Δr:

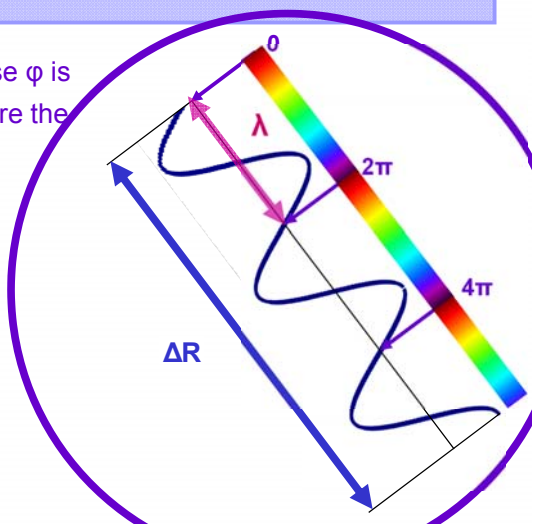

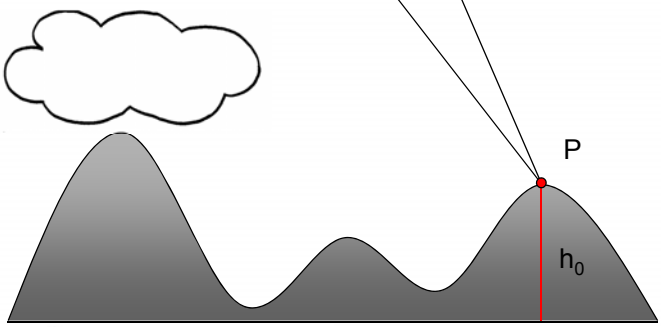

P

h_0

Phase measurements in interferometric systems can be made with a degree level accuracy. At radar wavelengths of 1-90cm (Ku to P-band) this corresponds to millimeter accuracy !!!

DEM Generation

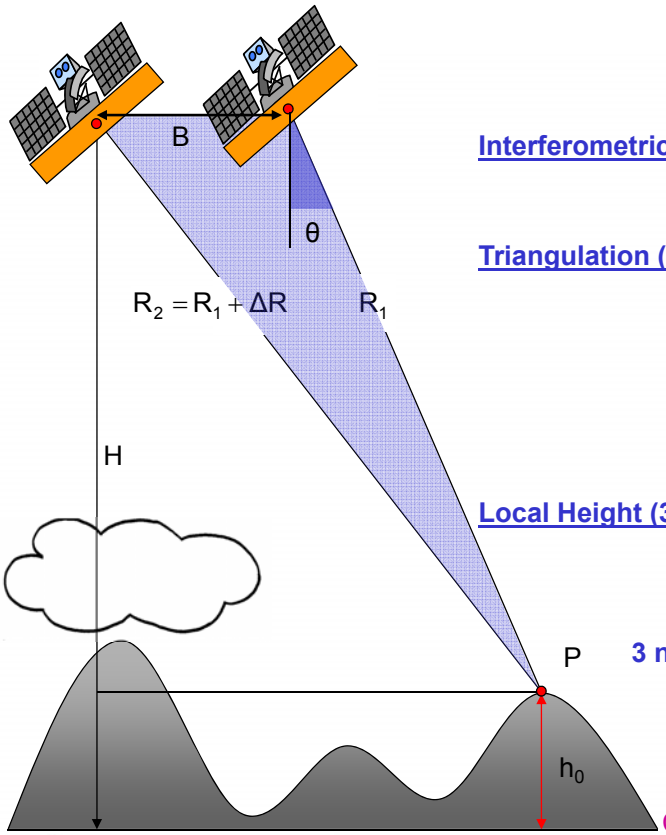

Interferometric Phase (1): $\varphi = 2\frac{2\pi}{\lambda}\Delta R + 2\pi N \quad N = 0, \pm 1, \pm 2$

Triangulation (2): $(R_1 + \Delta R)^2 = R_1^2 + B^2 - 2R_1 B\cos(\pi/2 + \theta) \rightarrow$

$$\rightarrow \sin(\theta) = \frac{(R_1 + \Delta R)^2 - R_1^2 - B^2}{2R_1 B}$$

Local Height (3): $h_0 = H - (R_1 + \Delta R)\cos(\theta)$

3 non-linear Equations for 3 Unknowns (h_0, θ, ΔR)

B … Spatial baseline and

R_1 … Range distance in Image 1are known

Critical is the fact that the interferometric phase φ is initially measured modulo 2π ► Phase Unwrapping

ERS – Bachu / China ~ 100 km × 80 km

Amplitude Image 1

Amplitude Image 2

ERS – Bachu / China ~ 100 km × 80 km

Amplitude Image 1

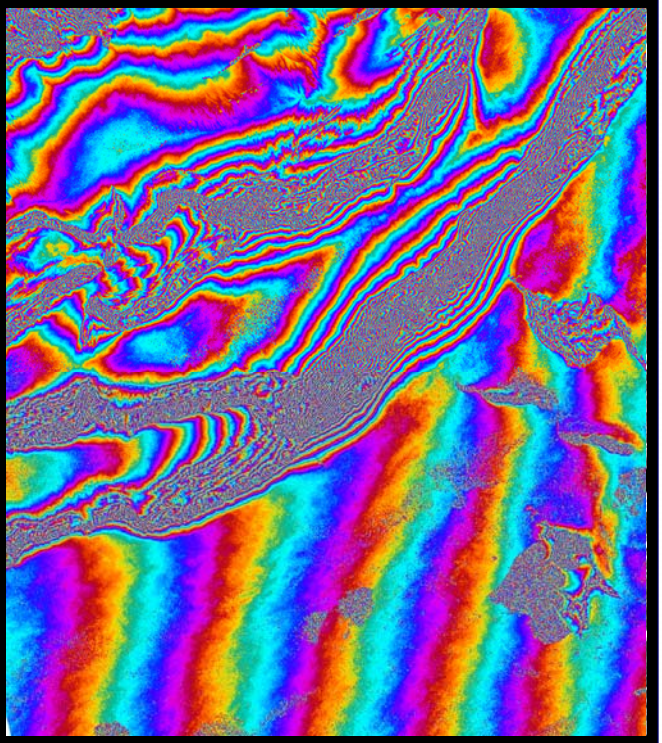

Interferometric Phase Image

ERS – Bachu / China ~ 100 km × 80 km

Amplitude Image

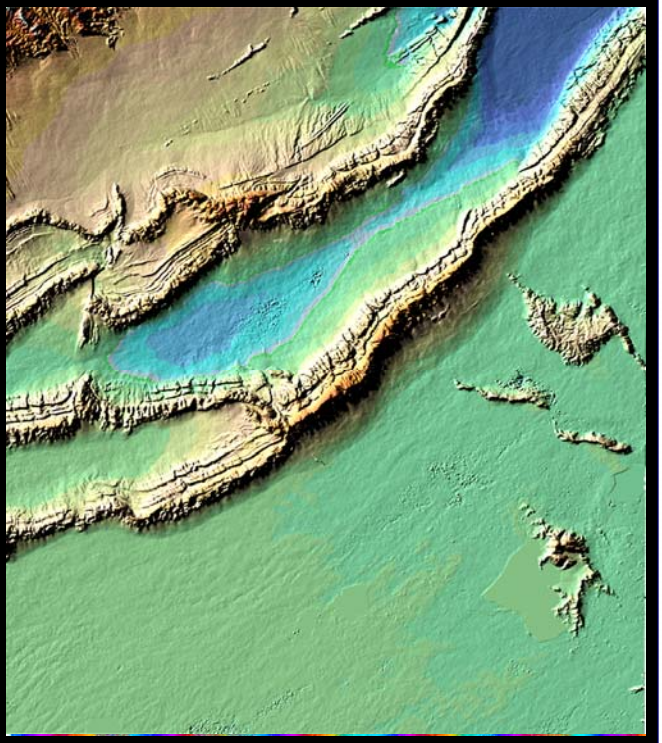

Digital Elevation Model with false colors

Deutsches Zentrum
DLR für Luft- und Raumfahrt e.V.
in der Helmholtz-Gemeinschaft

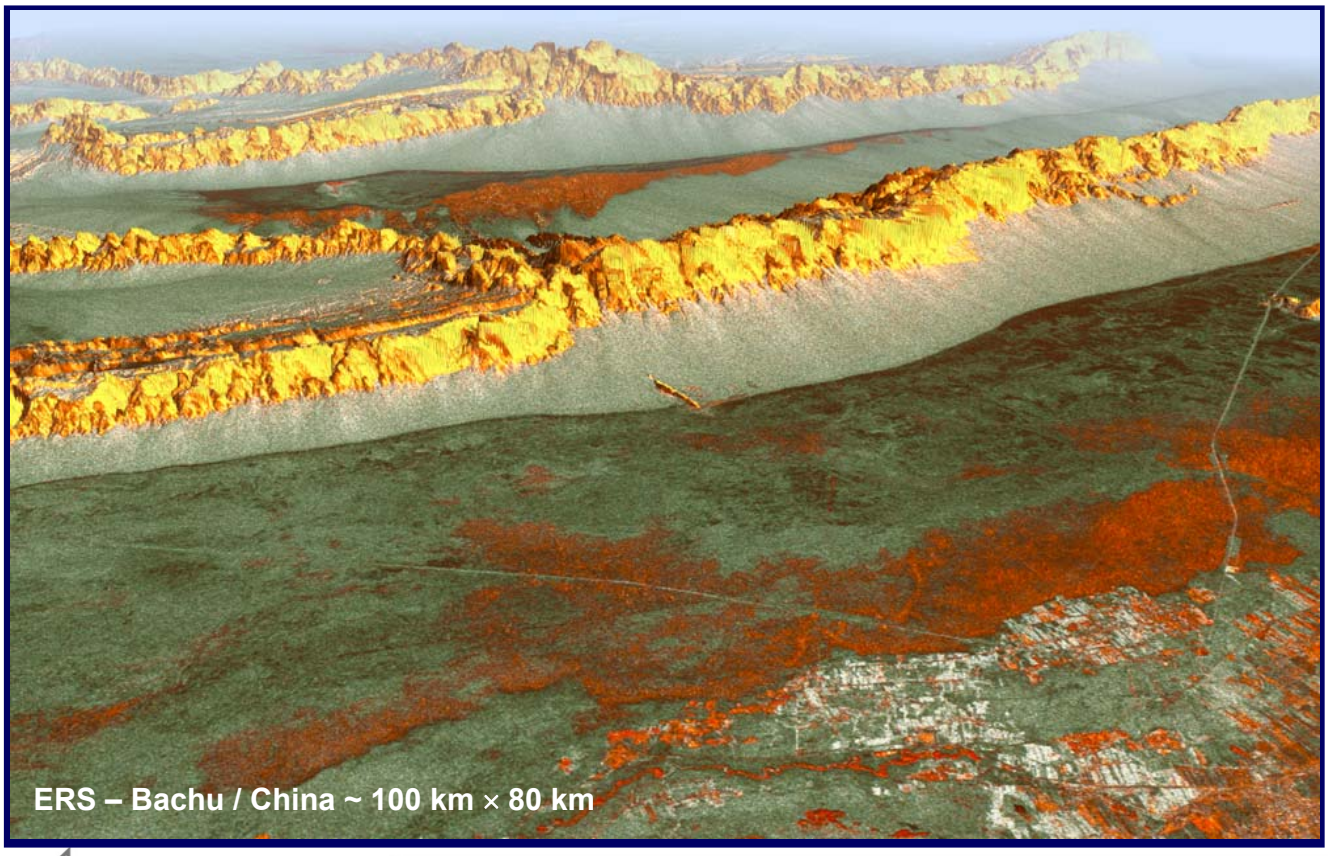

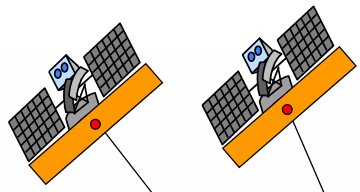

Interferometric Coherence

Image 1: $i_1 = |i_1| \exp[-i(2\frac{2\pi}{\lambda}R_1) + \varphi_{S1}]$

Image 2: $i_2 = |i_2| \exp[-i(2\frac{2\pi}{\lambda}R_2) + \varphi_{S2}]$

Interferometric Coherence: Normalised Complex Correlation Coefficient

$$\tilde{\gamma} = \frac{E\{ i_1 i_2^* \}}{\sqrt{E\{ i_1 i_1^* \} E\{ i_2 i_2^* \}}} = \frac{|E\{ i_1 i_2^* \}| \exp(i\varphi)}{\sqrt{E\{|i_1|^2\} E\{|i_2|^2\}}} \qquad 0 \le |\tilde{\gamma}| \le 1$$

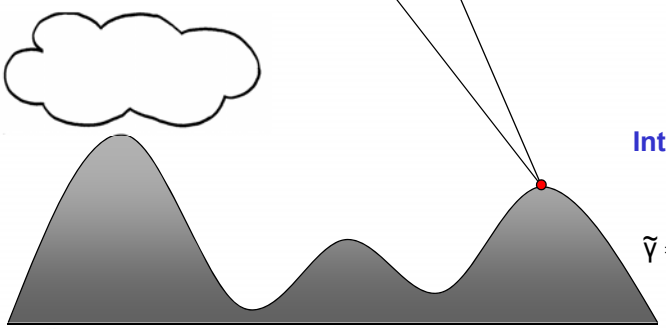

Interferometric Coherence Estimation:

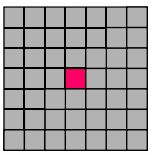

$$\tilde{\gamma} = \frac{\sum_W i_1[i,j]\ i_2^*[i,j]}{\sqrt{\sum_W |i_1[i,j]|^2 \sum_W |i_2[i,j]|^2}} = \frac{< i_1 i_2^* >}{\sqrt{< i_1 i_1^* > < i_2 i_2^* >}}$$

Interferometric coherence

… as a Measure of Interferogram Quality:

Standard Deviation of the InSAR Phase φ:

$$\sigma_\varphi = \sqrt{\int_{-\pi}^{\pi} \varphi^2 \, pdf(\varphi) \cdot d\varphi}$$

depends on ► the underlying coherence &

► the number of looks N.

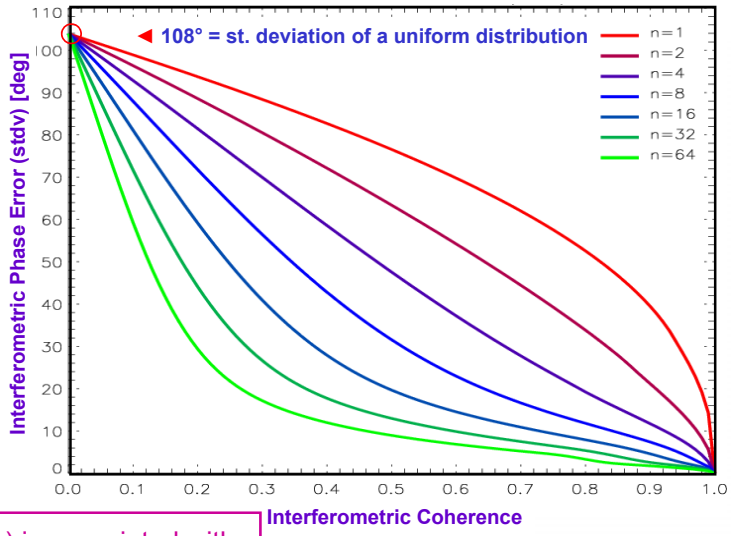

A increase in decorrelation (= loss in coherence) is associated with an increase in the phase variance;

► Increased phase variance leads to increased height errors.

where: $pdf(\varphi,N) = \frac{\Gamma(N+1/2)(1-|\gamma|^2)^2\beta}{2\sqrt{\pi}\Gamma(N)(1-\beta^2)^{N+1/2}} + \frac{(1-|\gamma|^2)^N}{2\pi} F(N,1;1/2;\beta^2)$

► F is a Gauss hypergeometric function and $\beta = |\gamma| \cos(\varphi - \overline{\varphi})$

► **N is the number of Looks**

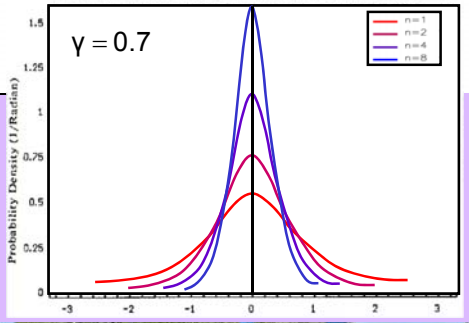

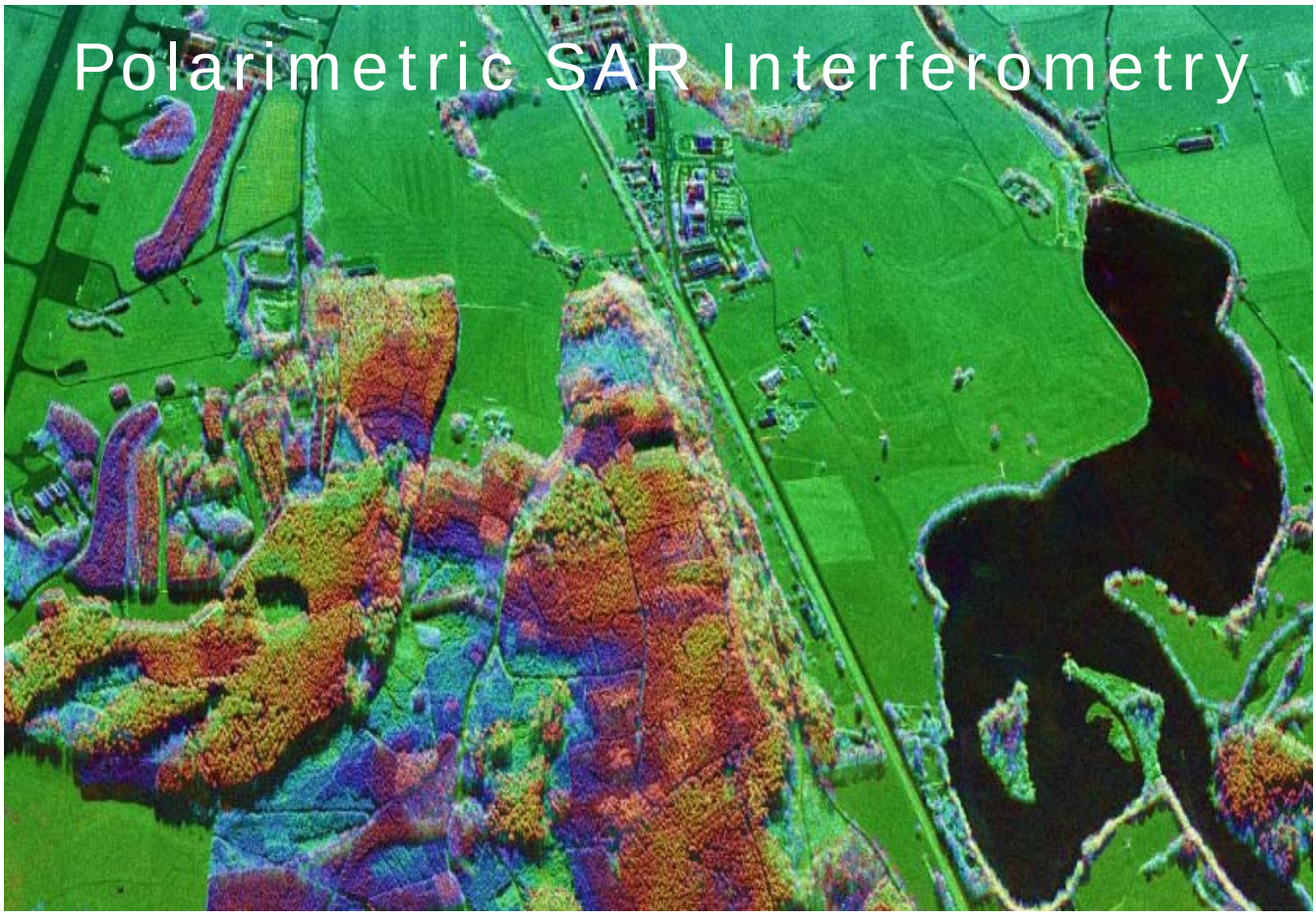

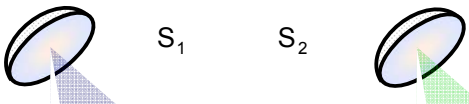

Interferometric Coherence

$$\tilde{\gamma}(S_1, S_2) = \frac{< S_1 S_2^* >}{\sqrt{< S_1 S_1^* > < S_2 S_2^* >}}$$

SAR Interferometry for Volume Structure

Volume Coherence

$$\tilde{\gamma}_{Vol}(f(z)) = e^{ik_z z_o} \frac{\int_o^{h_v} f(z)\, e^{ik_z z} dz}{\int_o^{h_v} f(z)\, dz}$$

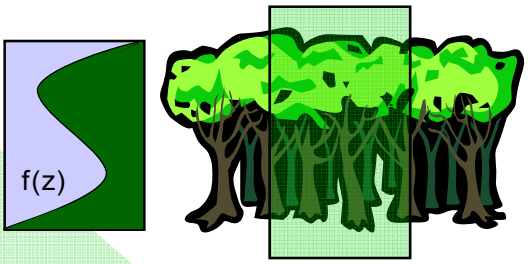

f(z) … vertical reflectivity function

Vertical Wavenumber: $\kappa_z = \frac{\kappa \Delta\theta}{\sin(\theta_0)}$

$$\tilde{\gamma} = \tilde{\gamma}_{Temporal}\ \gamma_{SNR}\ \tilde{\gamma}_{Volume}$$

- $\tilde{\gamma}_{Temporal}$ … temporal decorrelation
- γ_{SNR} … additive noise decorrelation
- $\tilde{\gamma}_{Volume}$ … geometric decorrelation

Baseline 3

$$\tilde{\gamma}_{Vol}(k_{z3}) = e^{ik_z z_o} \frac{\int_o^{h_v} f(z)\, e^{ik_{z3} z} dz}{\int_o^{h_v} f(z)\, dz}$$

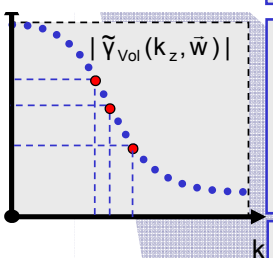

$$\tilde{\gamma}_{Vol}(k_{z1}) = e^{ik_{z1} z_o} \frac{\int_o^{h_v} f(z)\, e^{ik_{z1} z} dz}{\int_o^{h_v} f(z)\, dz}$$

Baseline 2

$$\tilde{\gamma}_{Vol}(k_{z2}) = e^{ik_z z_o} \frac{\int_o^{h_v} f(z)\, e^{ik_{z2} z} dz}{\int_o^{h_v} f(z)\, dz}$$

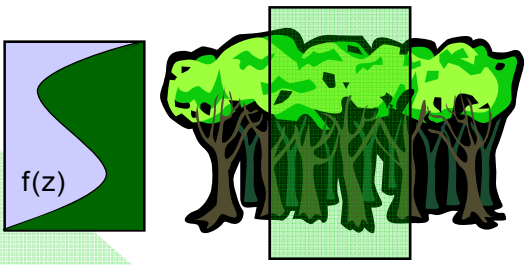

f(z) … vertical reflectivity function

Vertical Wavenumber: $\kappa_z = \frac{\kappa \Delta\theta}{\sin(\theta_0)}$

Multibaseline SAR Interferometry

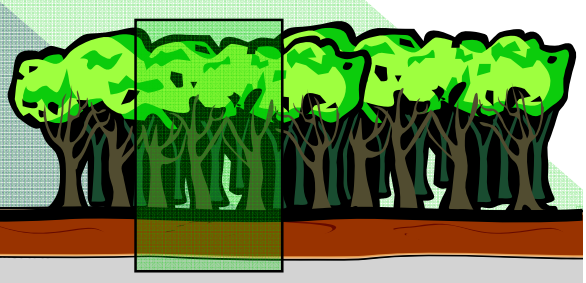

Amplitude Image

25° Incidence Angle 55°

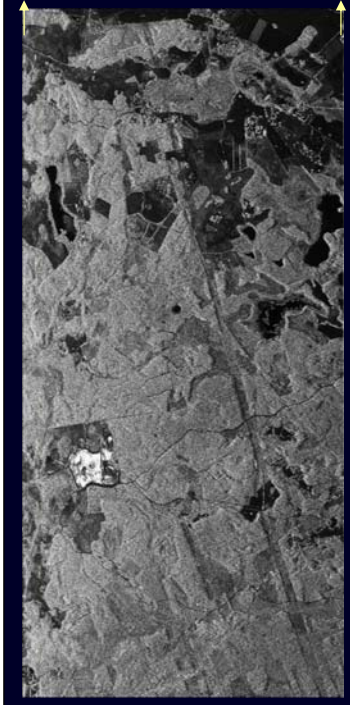

Amplitude Image HH

Interferometric Coherence: Volume Decorrelation

25° Incidence Angle 55°

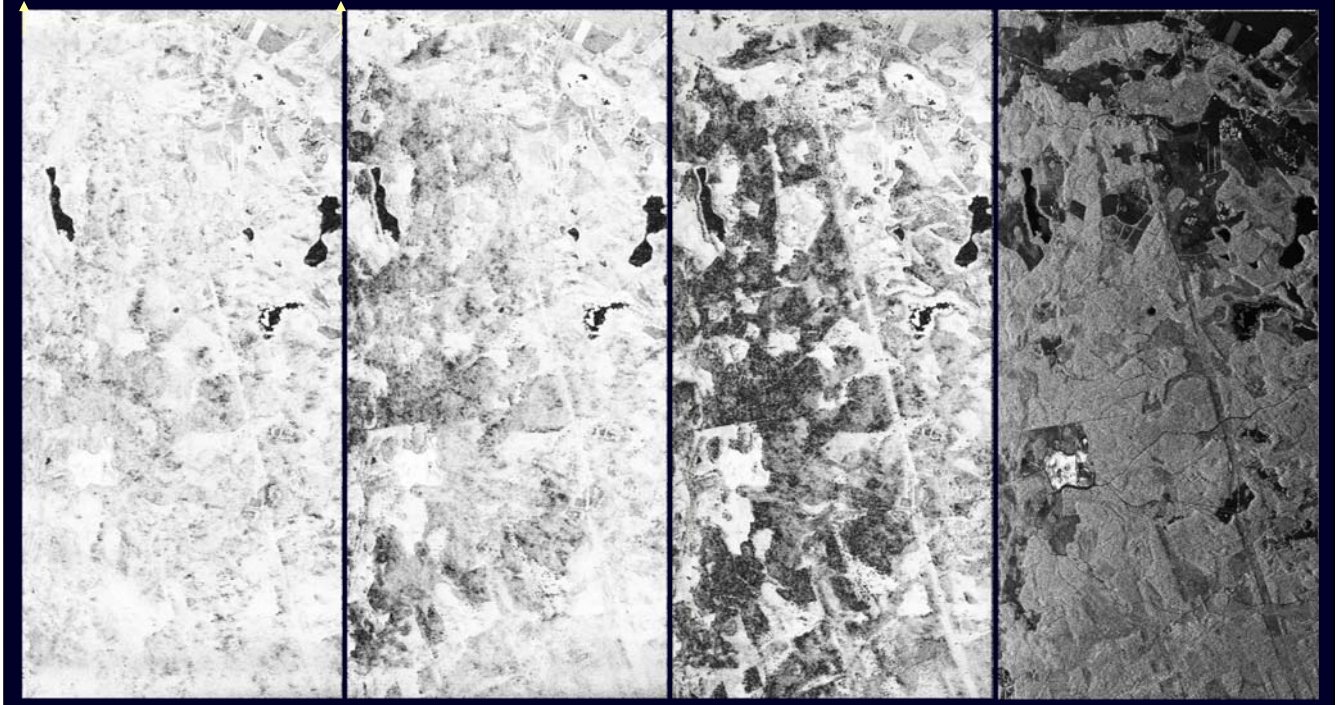

Spatial Baseline 3m 8m 16m 24m

Deutsches Zentrum
DLR für Luft- und Raumfahrt e.V.
in der Helmholtz-Gemeinschaft

Polarimetric SAR Interferometry

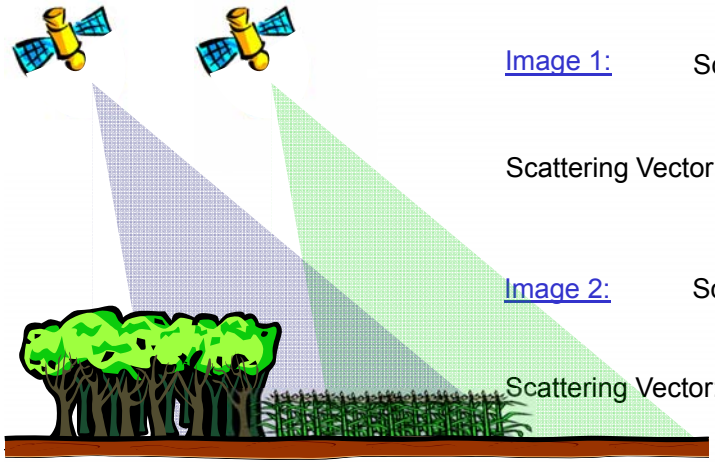

Image 1: Scattering Matrix: $[S_1] = \begin{bmatrix} S^1_{HH} & S^1_{HV} \\ S^1_{VH} & S^1_{VV} \end{bmatrix}$

Scattering Vector: $\vec{k}_1 = \frac{1}{\sqrt{2}}[S^1_{HH} + S^1_{VV} \quad S^1_{HH} - S^1_{VV} \quad 2S^1_{HV}]^T$

Image 2: Scattering Matrix: $[S_2] = \begin{bmatrix} S^2_{HH} & S^2_{HV} \\ S^2_{VH} & S^2_{VV} \end{bmatrix}$

Scattering Vector: $\vec{k}_2 = \frac{1}{\sqrt{2}}[S^2_{HH} + S^2_{VV} \quad S^2_{HH} - S^2_{VV} \quad 2S^2_{HV}]^T$

Image formation: $i_1 = \vec{w}_1^{+} \cdot \vec{k}_1$ and $i_2 = \vec{w}_2^{+} \cdot \vec{k}_2$ where $\vec{w}_i$ are complex unitary vectors

Interferogram formation: $i_1 \; i_2^* = (\vec{w}_1^{+} \cdot \vec{k}_1)(\vec{w}_2^{+} \cdot \vec{k}_2)^{+} = \vec{w}_1^{+}(\vec{k}_1 \cdot \vec{k}_2^{+})\vec{w}_2 = \vec{w}_1^{+}[\Omega]\vec{w}_2$

Interferometric Coherence: $\tilde{\gamma}(\vec{w}_1, \vec{w}_2) = \frac{< i_1 \, i_2^* >}{\sqrt{< i_1 \, i_1^* > < i_2 \, i_2^* >}} = \frac{< \vec{w}_1^{+}[\Omega]\vec{w}_2 \; >}{\sqrt{< (\vec{w}_1^{+}[T_{11}]\vec{w}_1 \;) > < (\vec{w}_2^{+}[T_{22}]\vec{w}_2 \;) >}}$

Interferometric Coherence: Volume Decorrelation

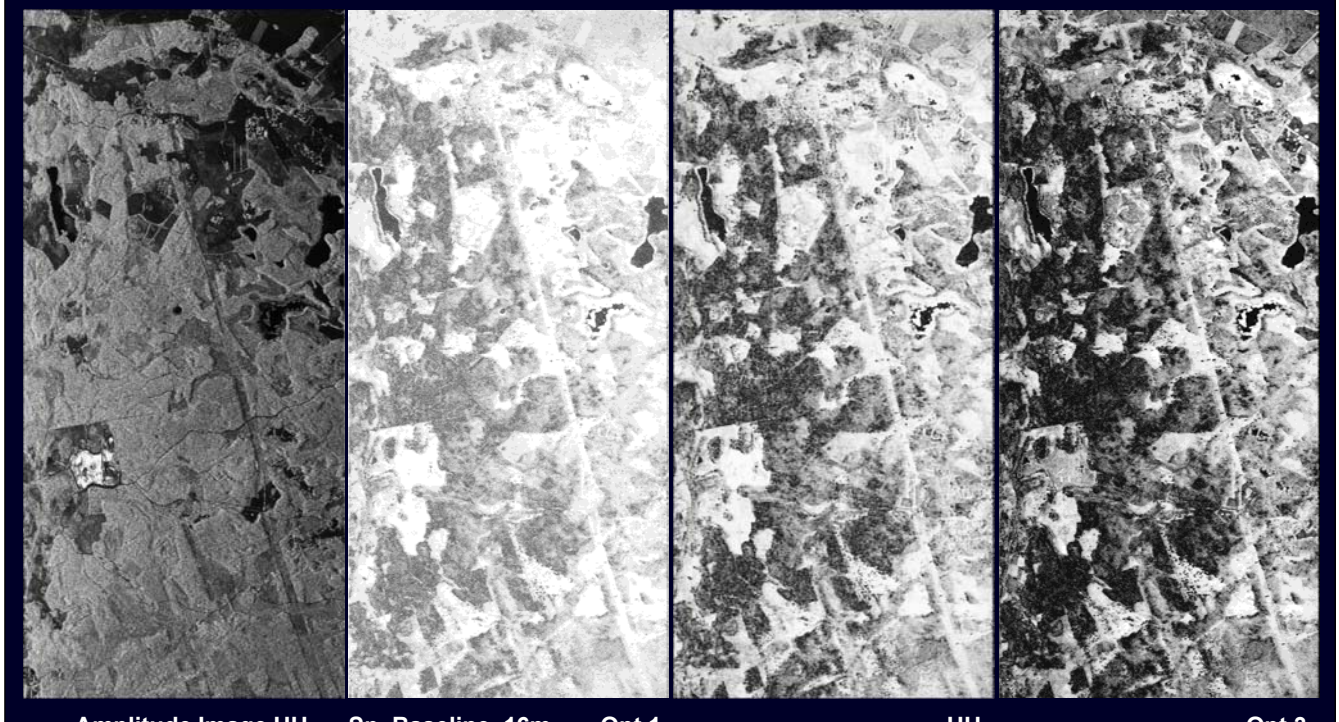

Amplitude Image HH | Sp. Baseline 16m | Opt 1 | HH | Opt 3

Polarisation 3

$$\tilde{\gamma}_{Vol}(f(z)) = e^{ik_z z_o} \frac{\int_o^{h_v} f(z)\, e^{ik_z z} dz}{\int_o^{h_v} f(z)\, dz}$$

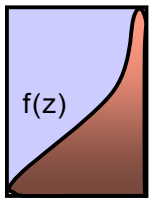

Polarisation 1

$$\tilde{\gamma}_{Vol}(f(z)) = e^{ik_z z_o} \frac{\int_o^{h_v} f(z)\, e^{ik_z z} dz}{\int_o^{h_v} f(z)\, dz}$$

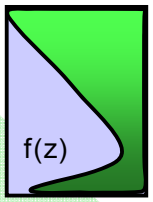

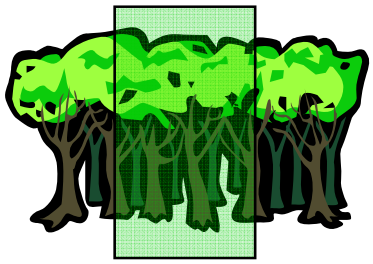

Polarisation 2

$$\tilde{\gamma}_{Vol}(f(z)) = e^{ik_z z_o} \frac{\int_o^{h_v} f(z)\, e^{ik_z z} dz}{\int_o^{h_v} f(z)\, dz}$$

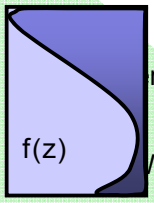

rtical reflectivity function

Vavenumber: $\kappa_z = \frac{\kappa \Delta\theta}{\sin(\theta_0)}$

f(z) … vertical reflectivity function

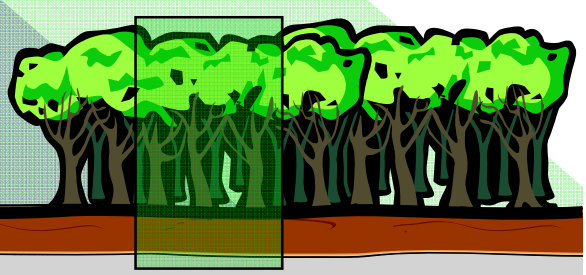

Polarimetric SAR Interferometry

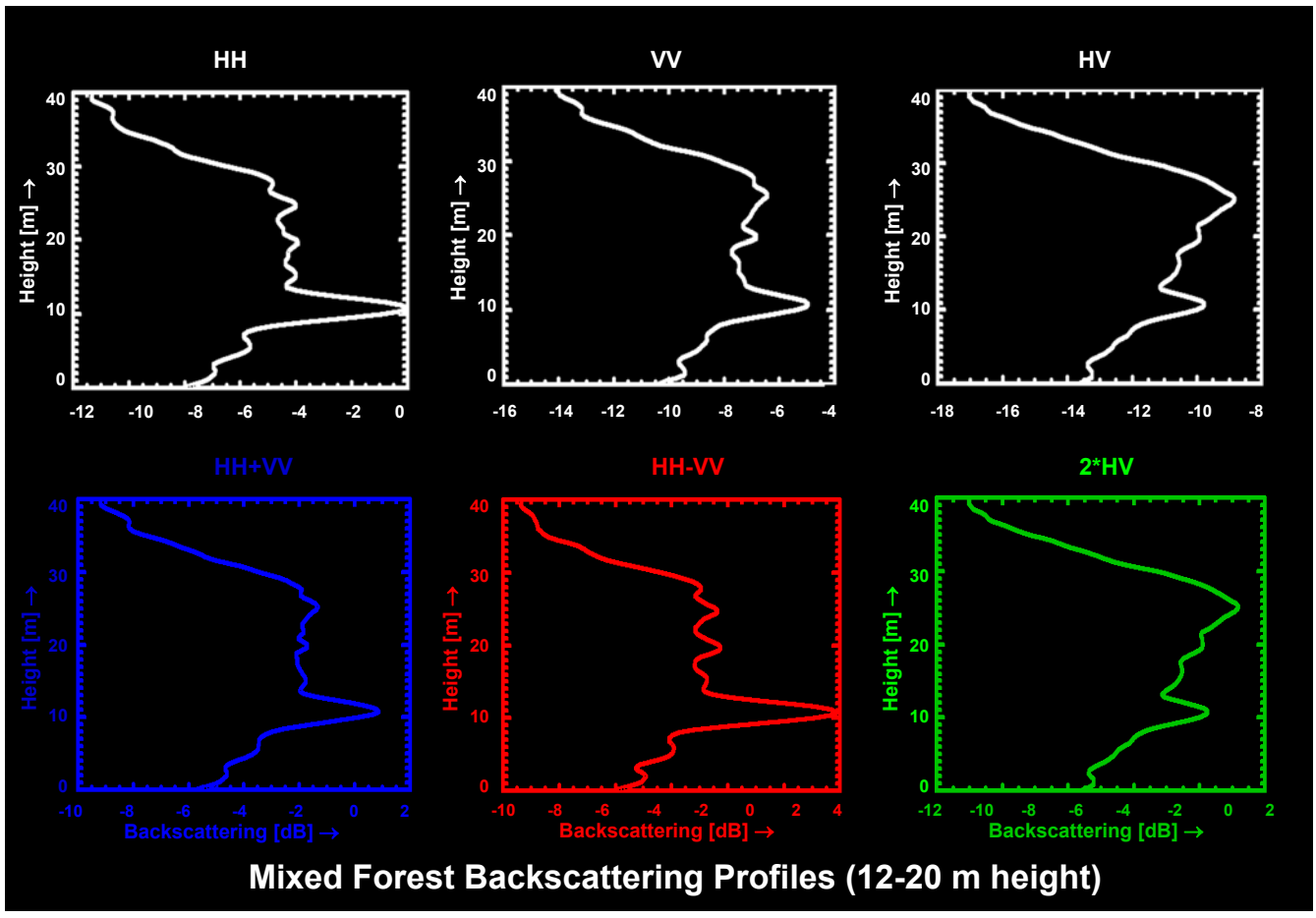

Mixed Forest Backscattering Profiles (12-20 m height)

Structure Parameters & Applications

Forest	• Forest Height • Forest (Vertical) Structure • Forest Biomass • Underlying Topography	• Forest Ecology • Forest Management • Ecosystem Modeling • Climate Change
Agriculture	• Underlying Soil Moisture • Moisture of Vegetation Layer • Height of Vegetation Layer • Soil Roughness	• Farming Management • Ecosystem Modeling • Water Cycle / CC • Desertification
Snow & Ice	• Ice Layer Structure • Penetration Depth (Ice) • Snow Layer Thickness • Snow Water Equivalent	• Ecosystem Change • Water Cycle • Water Management

PoI-InSAR In Orbit

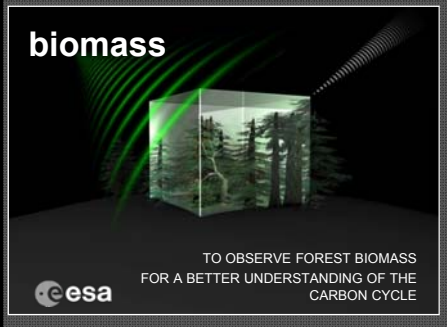

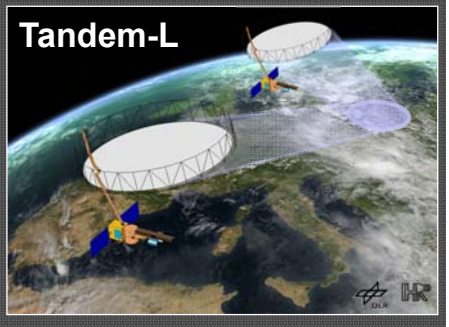

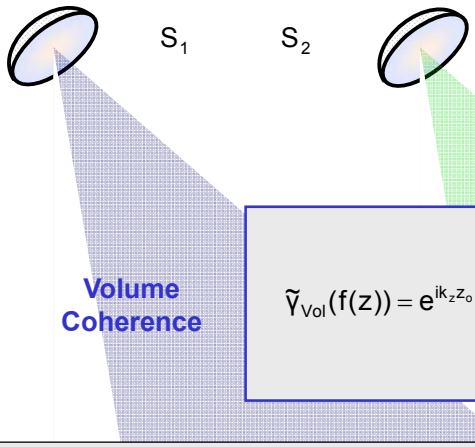

Interferometric Coherence

$$\tilde{\gamma}(S_1, S_2) = \frac{< S_1 S_2^* >}{\sqrt{< S_1 S_1^* > < S_2 S_2^* >}}$$

Volume Coherence

$$\tilde{\gamma}_{Vol}(f(z)) = e^{ik_z z_o} \frac{\int_o^{h_v} f(z)\, e^{ik_z z} dz}{\int_o^{h_v} f(z)\, dz}$$

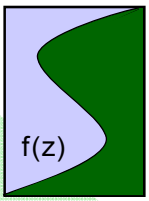

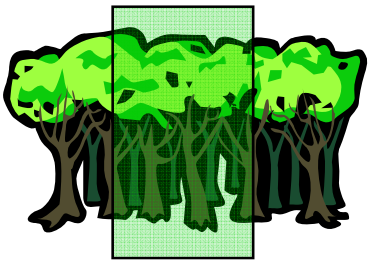

2 Layer Inversion Model

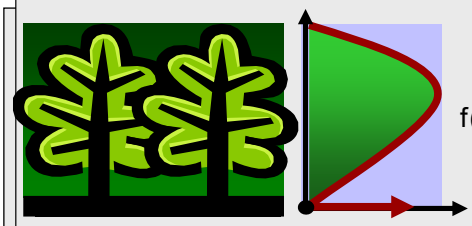

$$f(z) = f_0 e^{\left(\frac{2\,\sigma(z)\,z}{\cos\theta_0}\right)} + m'_G \delta(z - z_0)$$

$$\tilde{\gamma}_{Vol}(\vec{w}) = \exp(i\varphi_0)\frac{\tilde{\gamma}_V + m(\vec{w})}{1 + m(\vec{w})}$$

Volume Coherence

$$\tilde{\gamma}_V = \frac{I}{I_0}$$

$$I = \int_0^{h_V} \exp(i\kappa_z z') \exp\left(\frac{2\,\sigma(z)\,z'}{\cos\theta_0}\right) dz' \qquad I_0 = \int_0^{h_V} \exp\left(\frac{2\,\sigma(z)\,z'}{\cos\theta_0}\right) dz'$$

$$m(\vec{w}) = \frac{m_G(\vec{w})}{m_V(\vec{w}) I_0} \qquad \kappa_z = \frac{\kappa \Delta\theta}{\sin(\theta_0)}$$

- $\sigma(z)$ has to be parameterised
- Volume Height h_V
- Topography φ_0
- G/V Ratio $m(\vec{w})$

Traunstein Test Site

Forest type	Temperate
Topography	Moderate slopes
Height	25 ~ 35m
Species	N. Spruce, E. Beech, White Fir
Biomass	40 ~ 450 t/ha

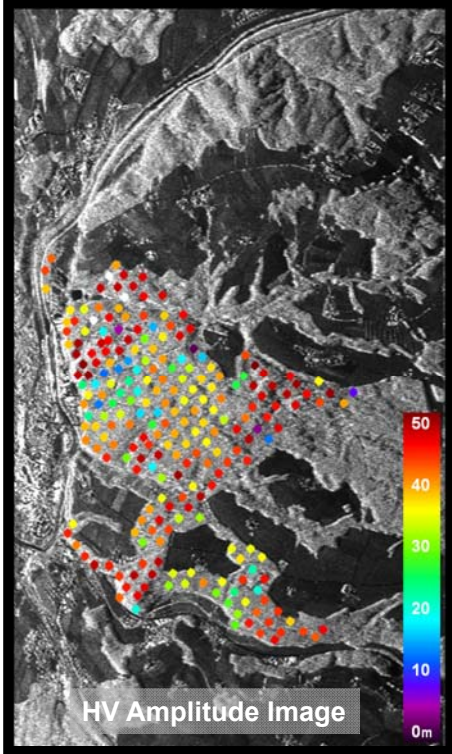

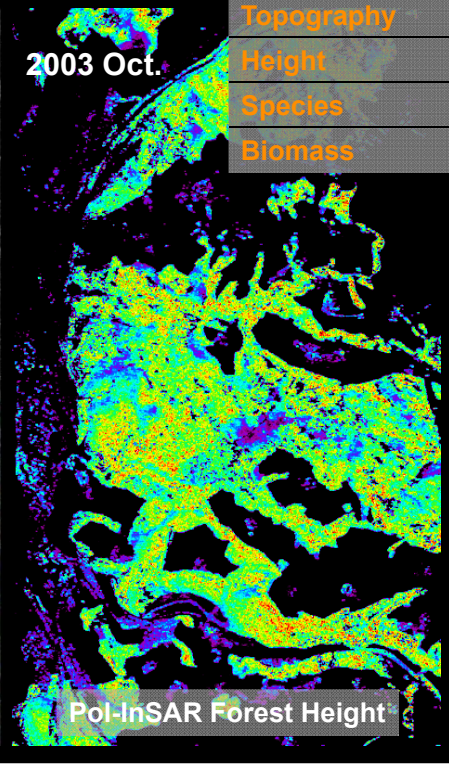

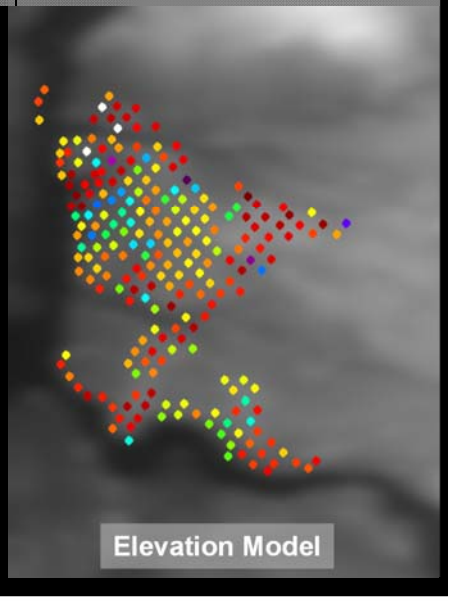

Traunstein Test Site

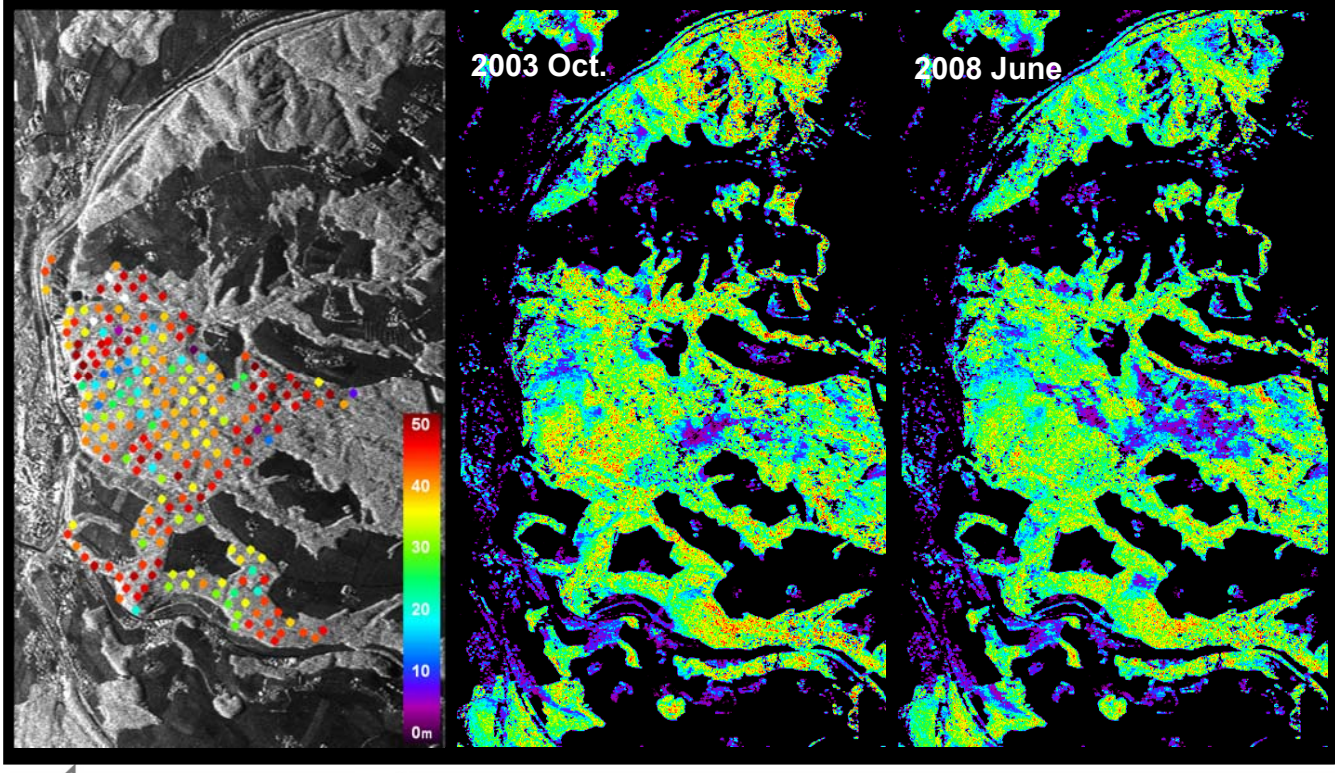

INDREX-II: Mawas Test Site

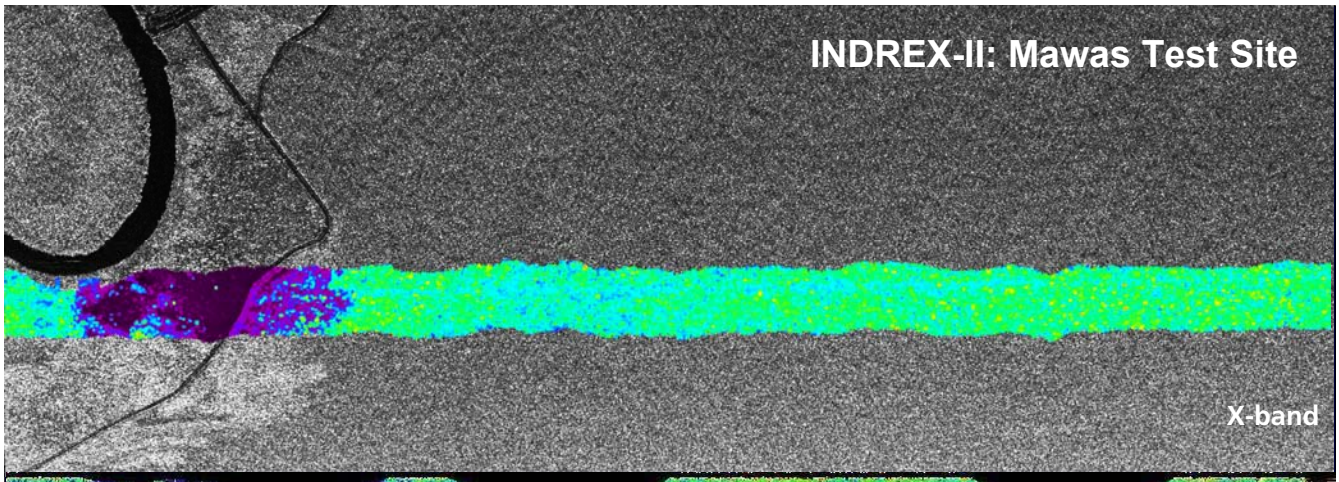

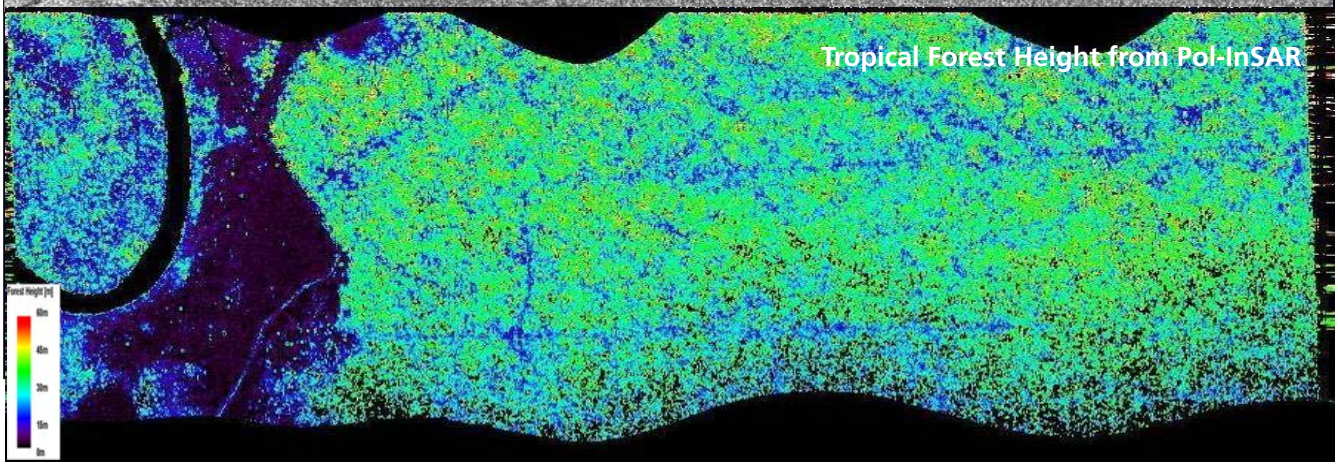

Polarimetric Coherence Tomography

f(z) … vertical reflectivity function

Volume Coherence

$$\tilde{\gamma}_{Vol}(f(z)) = e^{ik_z z_o} \frac{\int_o^{h_v} f(z)\, e^{ik_z z} dz}{\int_o^{h_v} f(z)\, dz}$$

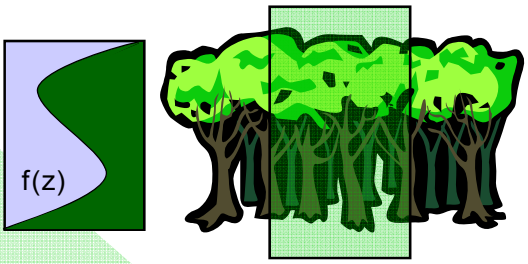

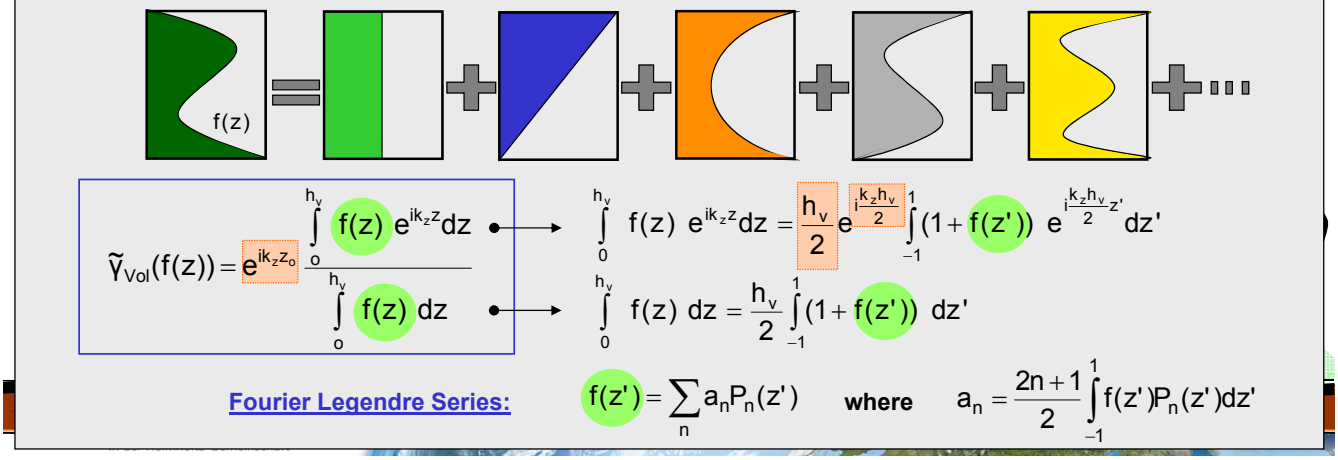

$$\tilde{\gamma}_{Vol}(f(z)) = e^{ik_z z_o} \frac{\int_o^{h_v} f(z)\, e^{ik_z z} dz}{\int_o^{h_v} f(z)\, dz}$$

$$\int_0^{h_v} f(z)\, e^{ik_z z} dz = \frac{h_v}{2} e^{i\frac{k_z h_v}{2}} \int_{-1}^{1} (1 + f(z'))\, e^{i\frac{k_z h_v}{2} z'} dz'$$

$$\int_0^{h_v} f(z)\, dz = \frac{h_v}{2} \int_{-1}^{1} (1 + f(z'))\, dz'$$

Fourier Legendre Series: $f(z') = \sum_n a_n P_n(z')$ where $a_n = \frac{2n+1}{2} \int_{-1}^{1} f(z') P_n(z') dz'$

Vertical Forest Profile Reconstruction

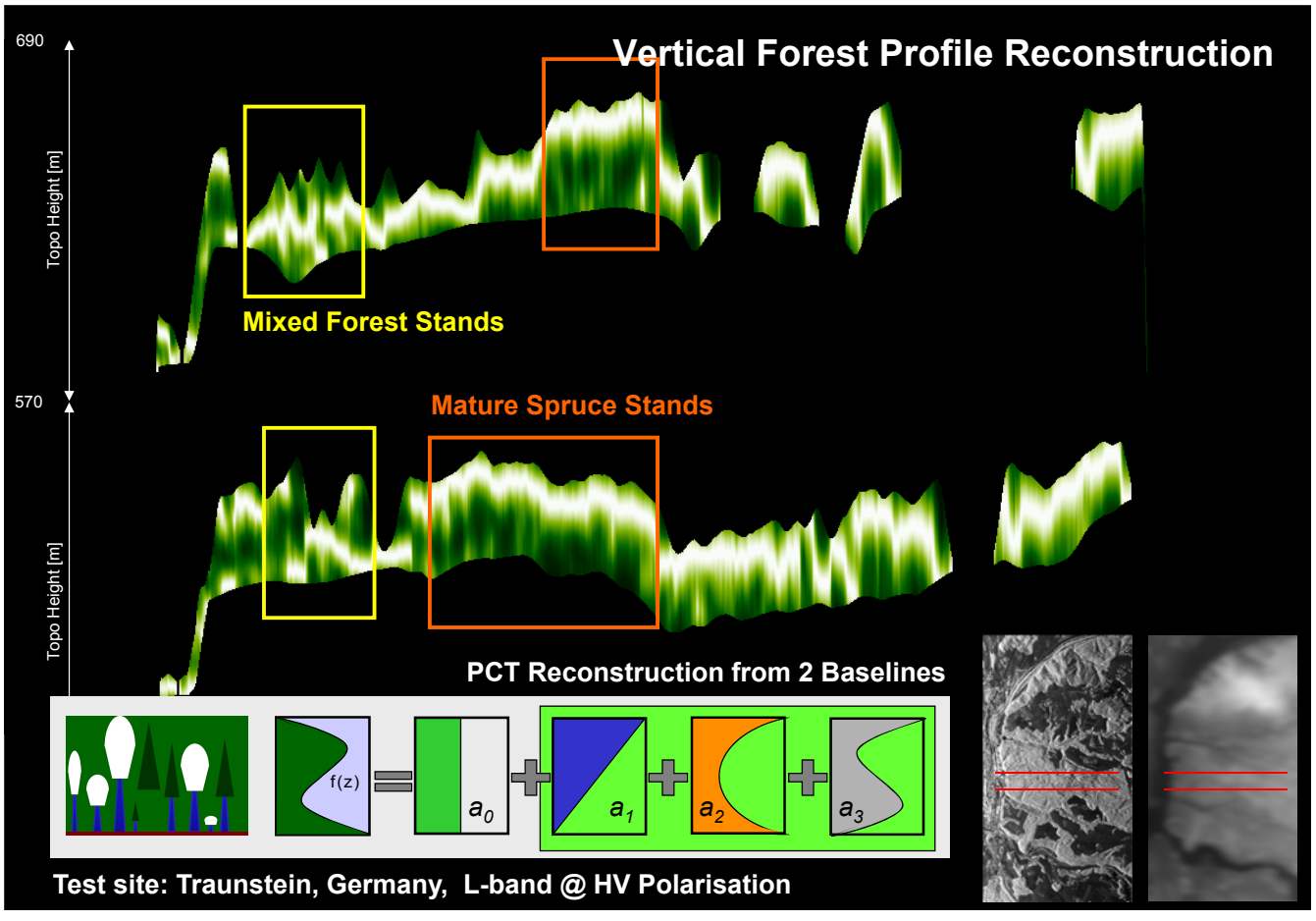

What do we measure ?

Biomass Profile | **Airborne Lidar Profile** | **Terrestrial Lidar Profile** | **L-band Profile**

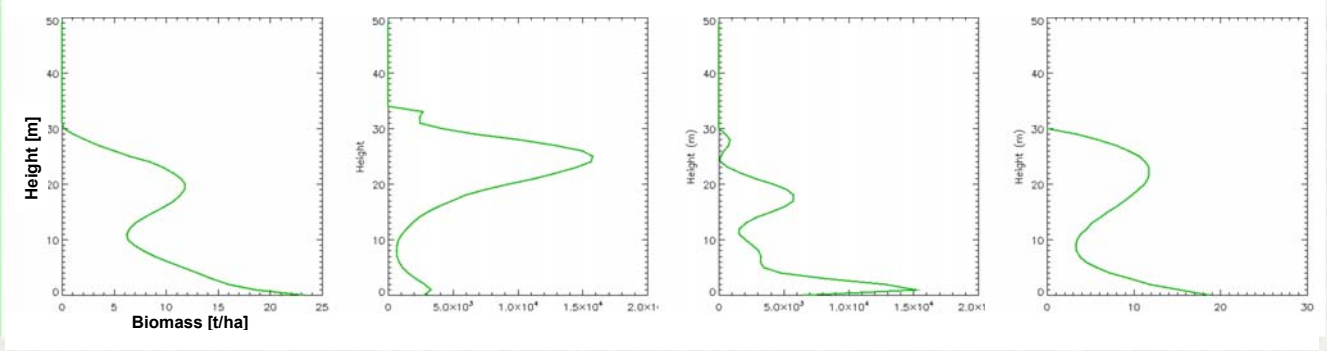

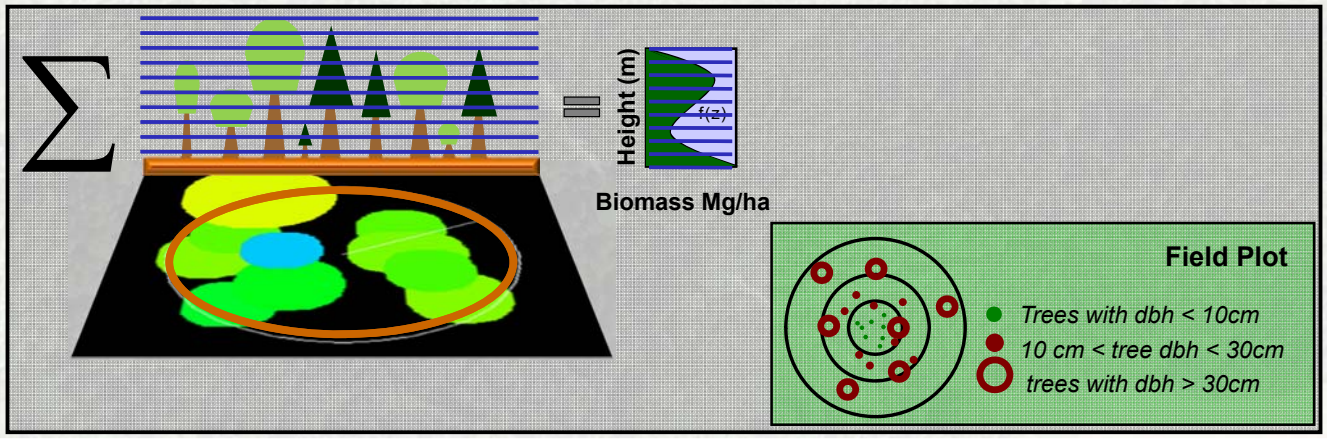

Structure-to-Biomass Allometry

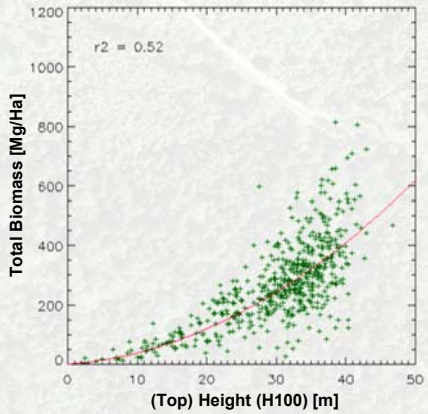

$$B = la * 1.66\, H^{1.50}$$

$$B = 3.11 * \sum_{i=0}^{H} \sum_{j=1}^{3} a_j * P_j(z_i)$$

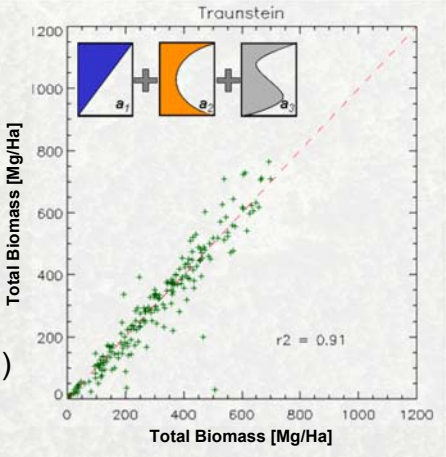

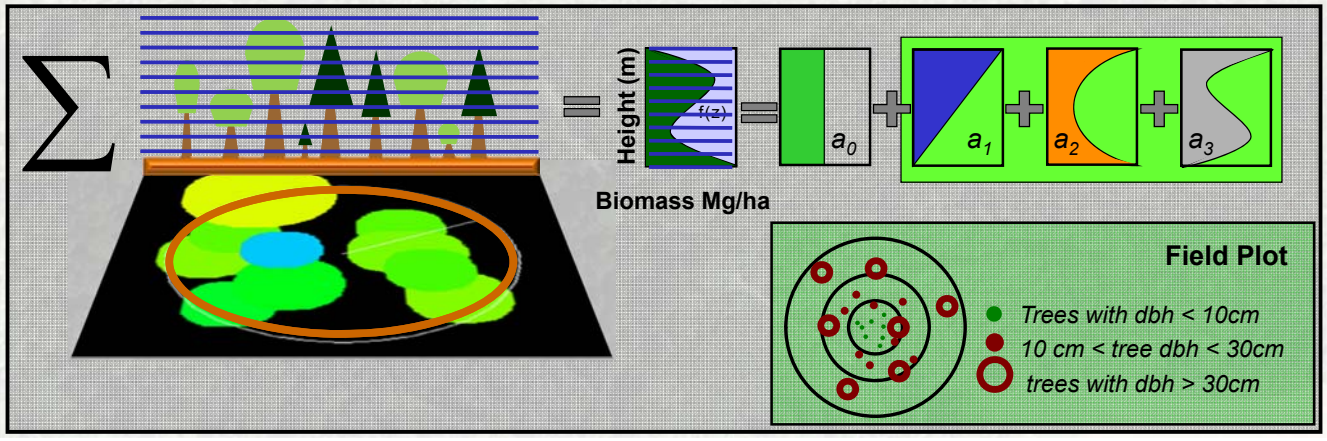

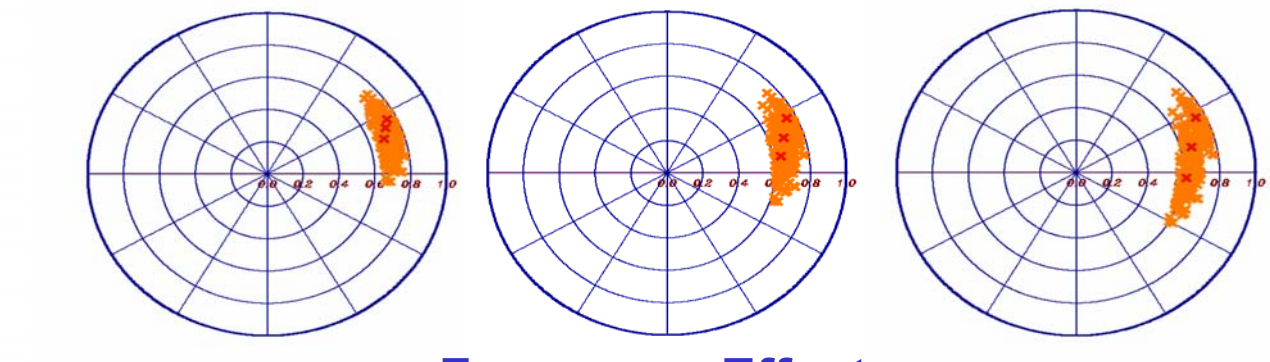

Frequency Effects

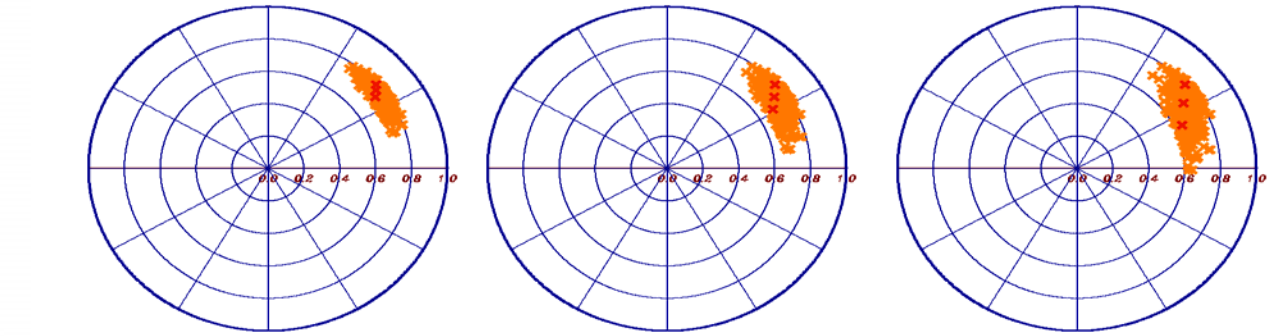

RVoG Model – Frequency Dependency

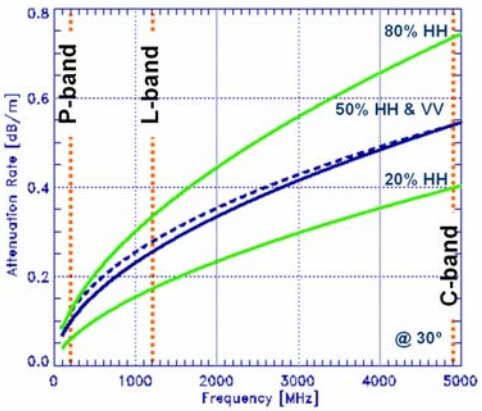

With degreasing frequency:

- The attenuation through the vegetation degreases;
- The Ground to Volume Scattering Ratio increases;
- The relative importance of the volume decreases;
- The relative importance of the ground increases;
- The effective scatterers change.

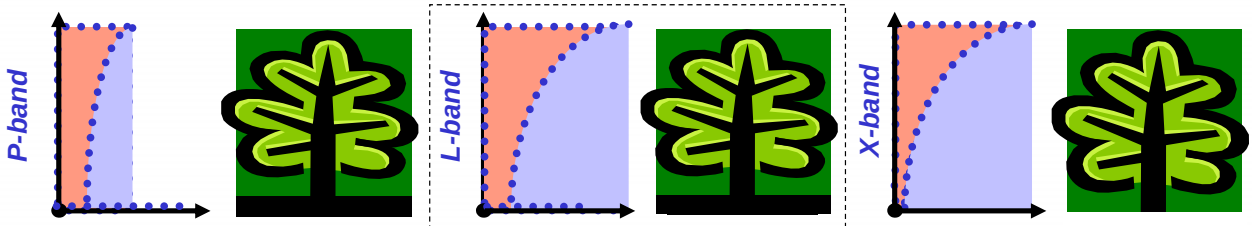

$$\tilde{\gamma}(\vec{w}) = \exp(i\varphi_0)\frac{\tilde{\gamma}_V + m(\vec{w})}{1 + m(\vec{w})} \qquad \tilde{\gamma}(\vec{w}) = \exp(i\varphi_0)\frac{\tilde{\gamma}_V + m(\vec{w})}{1 + m(\vec{w})} \qquad \tilde{\gamma}(\vec{w}) = \exp(i\varphi_0)\tilde{\gamma}_V$$

L.Bessette, S.Ayasli "Ultra Wide Band P-3 and Carabas II Foliage Attenuation and Backscatter Analysis", Proceedings of IEEE Radar Conference, 2001.

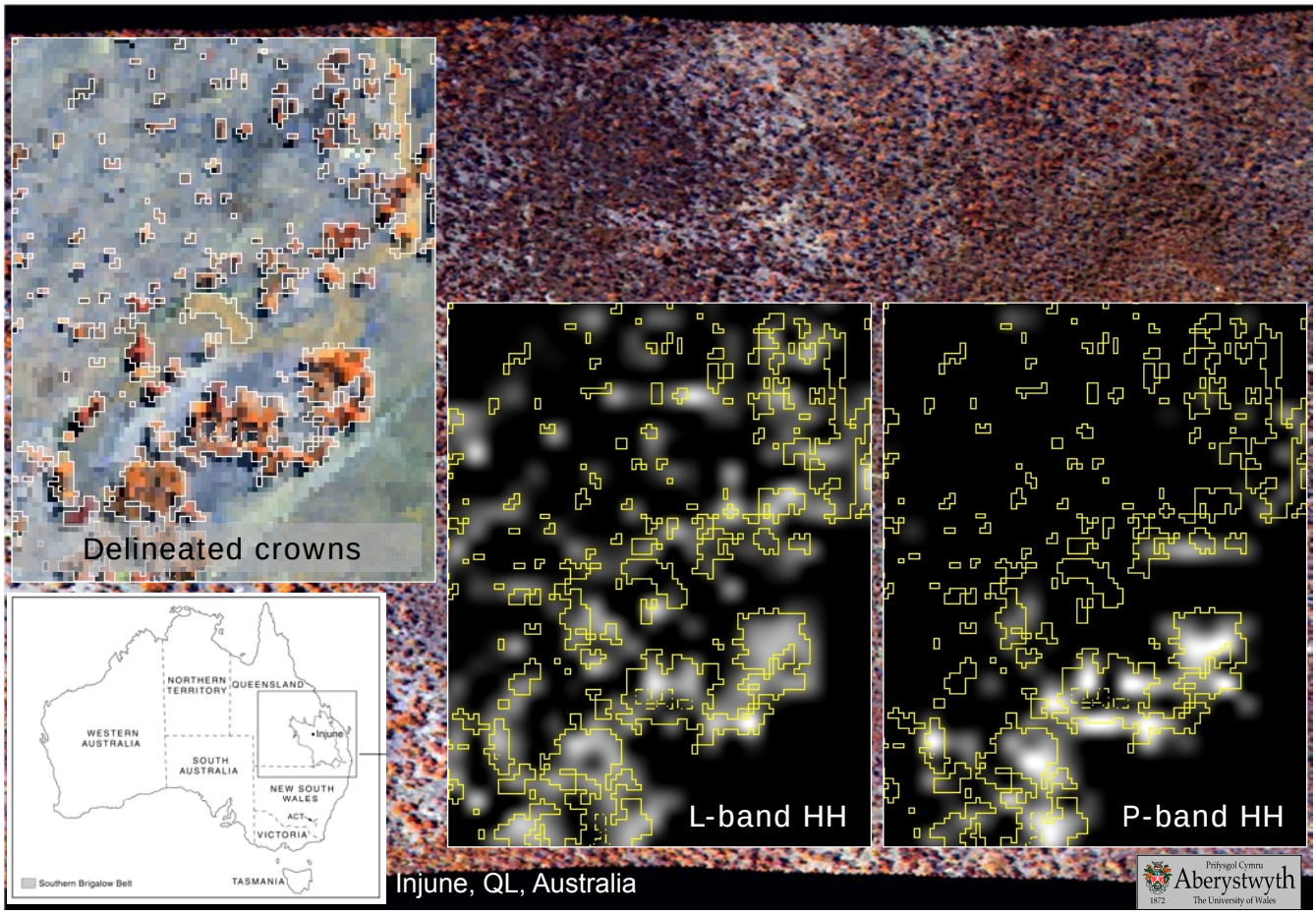

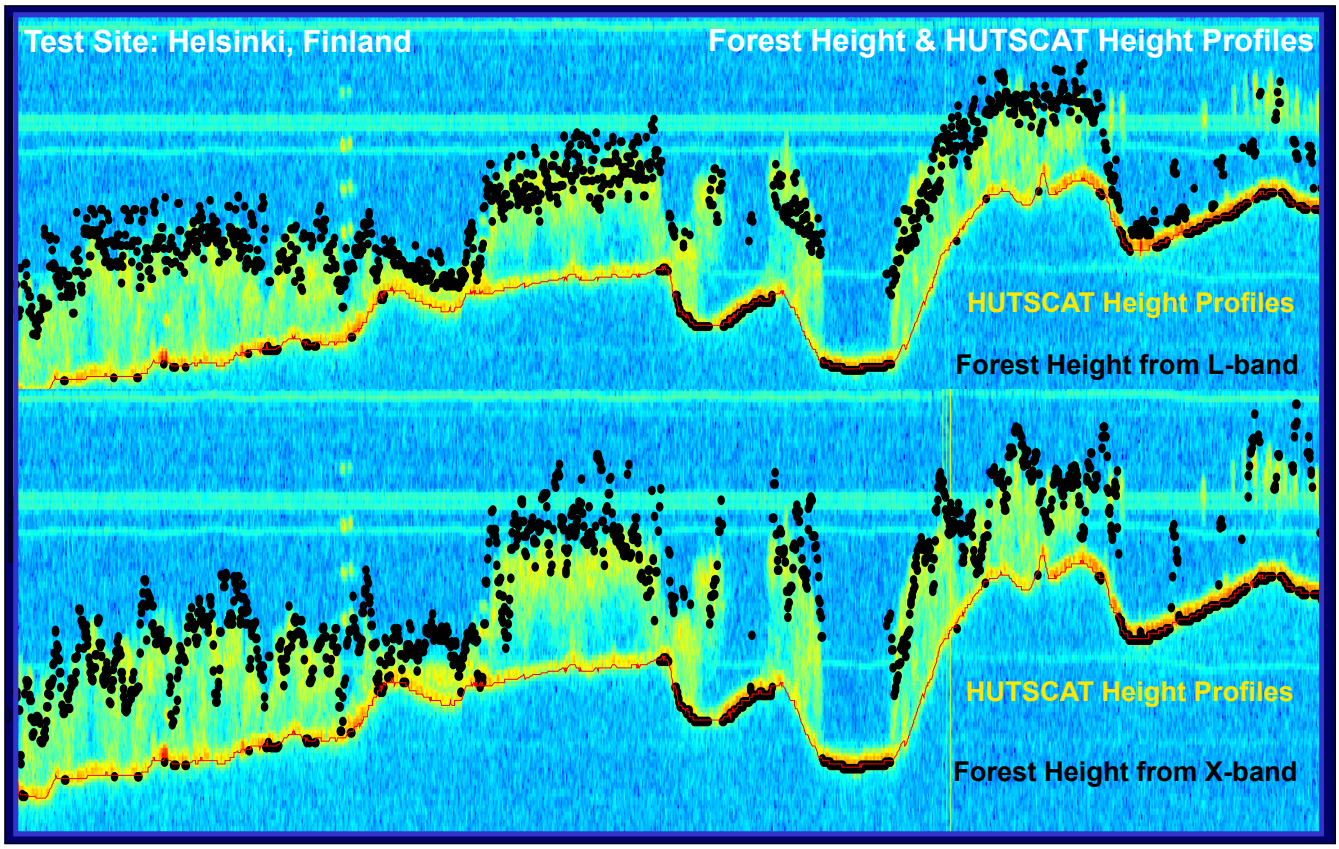

Deutsches Zentrum
DLR für Luft- und Raumfahrt e.V.
in der Helmholtz-Gemeinschaft

Traunstein Test Site

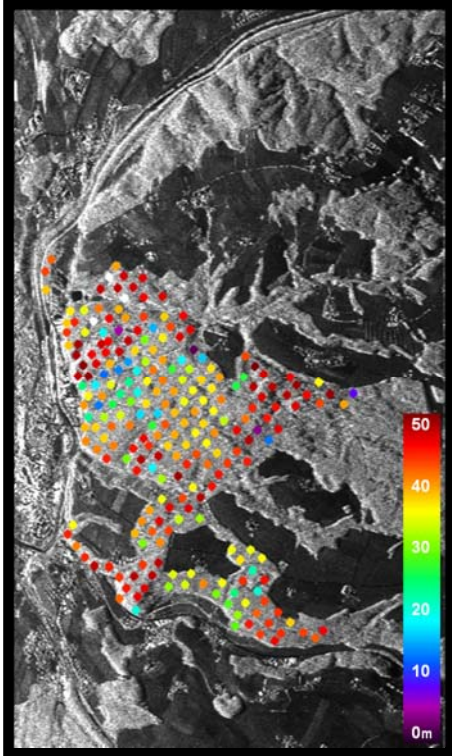

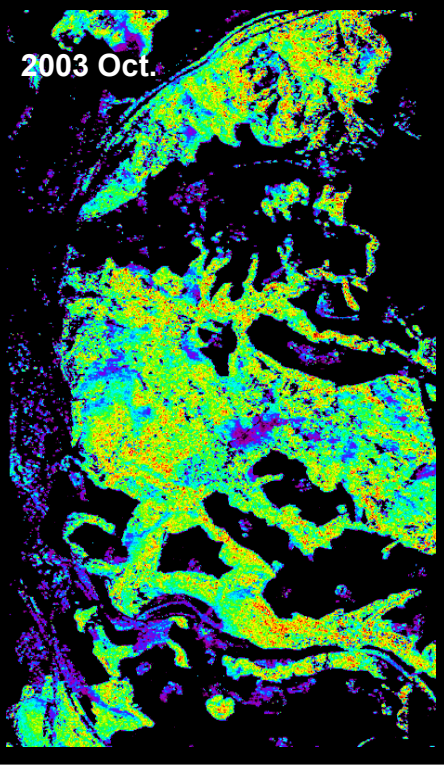

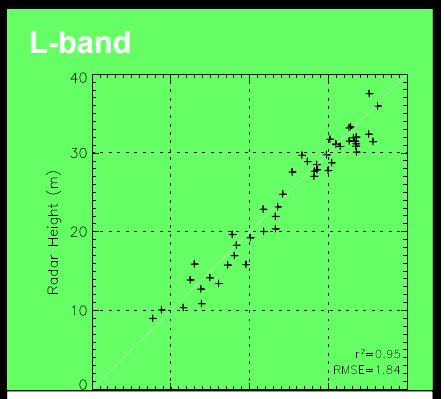

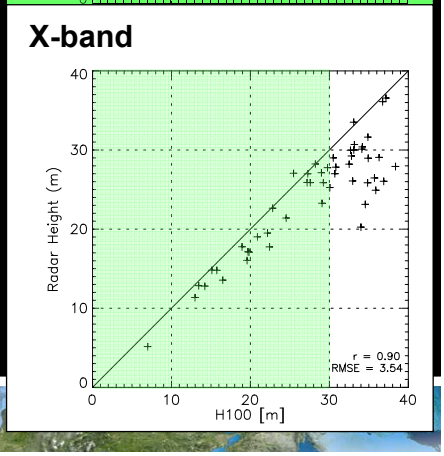

Deutsches Zentrum
DLR für Luft- und Raumfahrt e.V.
in der Helmholtz-Gemeinschaft

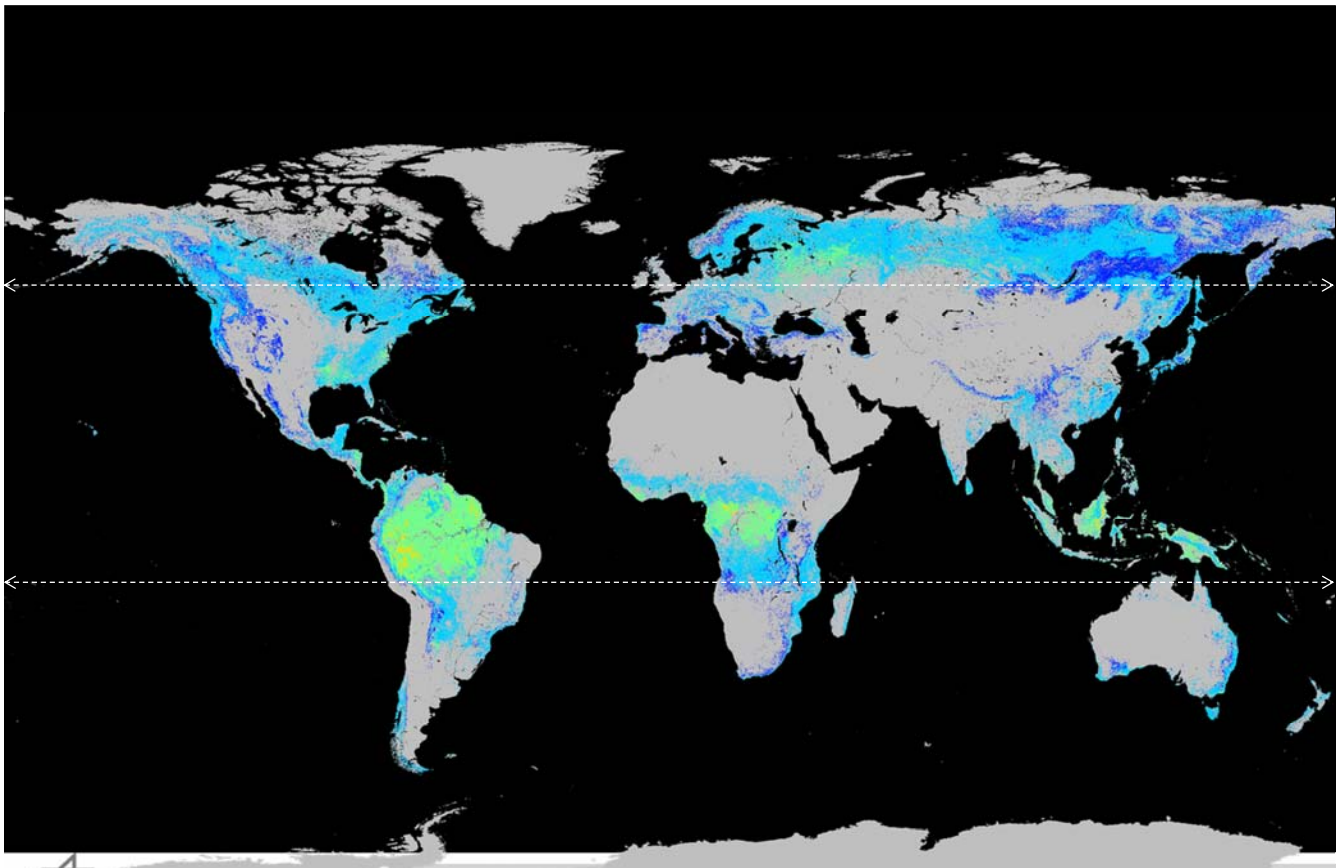

DLR

Source: Marc Simard, JPL, NASA

0 10 20 30 40 50 [m] 60

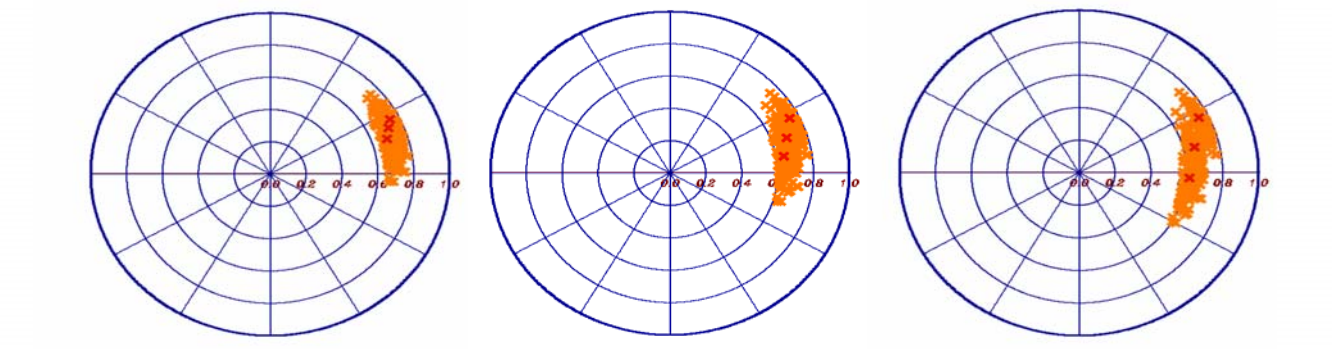

Non-Volumetric Decorrelation Effects

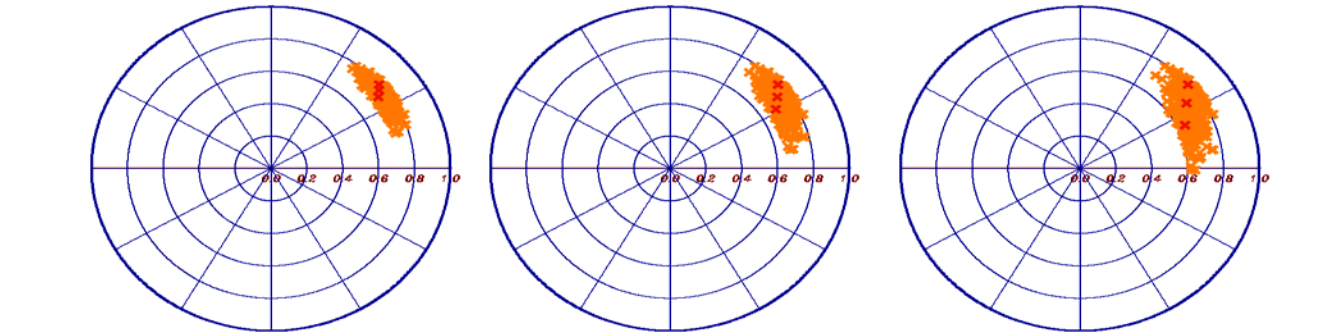

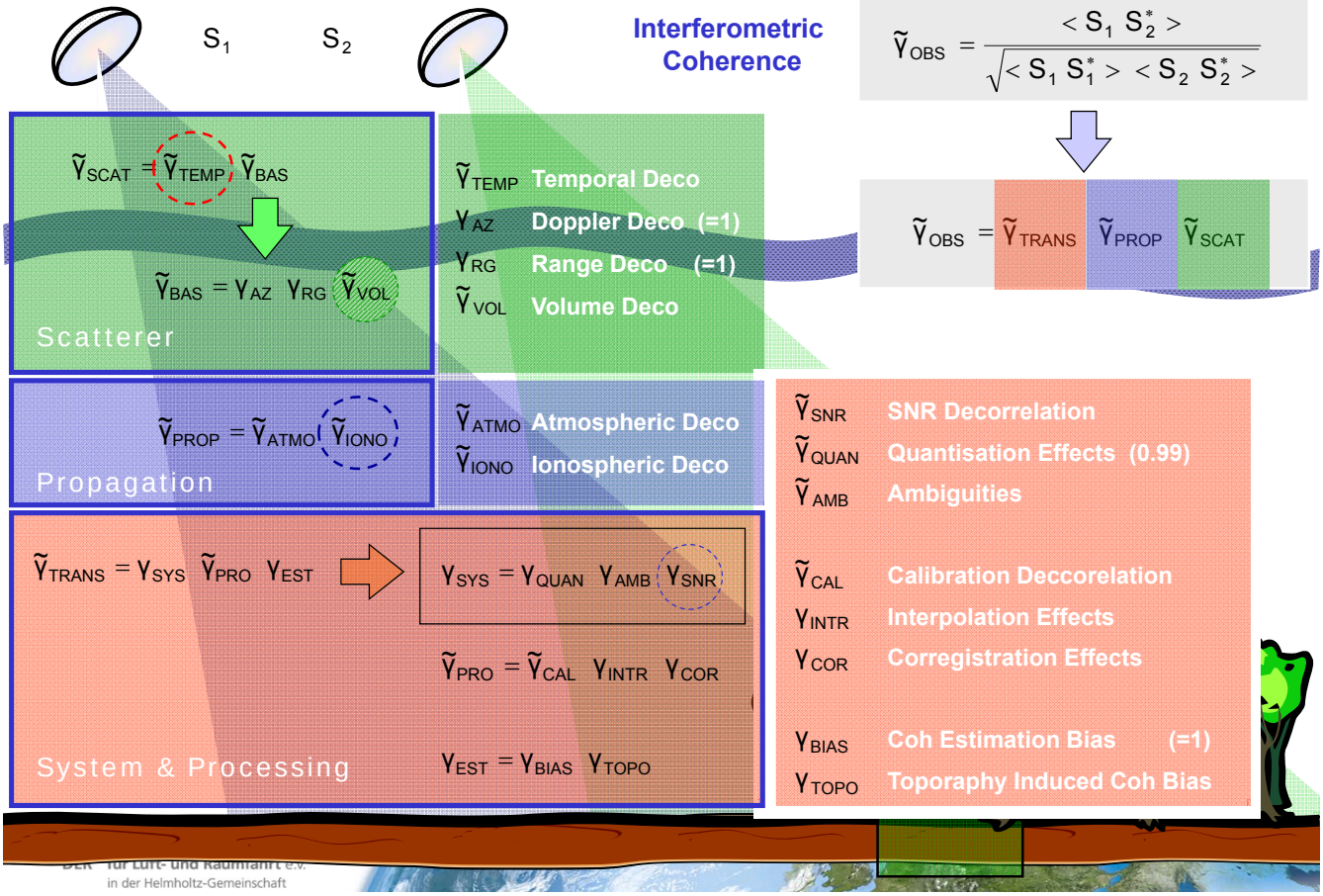

Amplitude Image

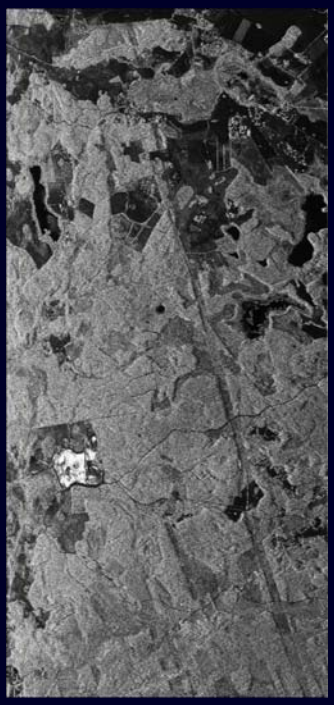

Amplitude Image HH

Interferometric Coherence: Volume vs Temporal Decorrelation

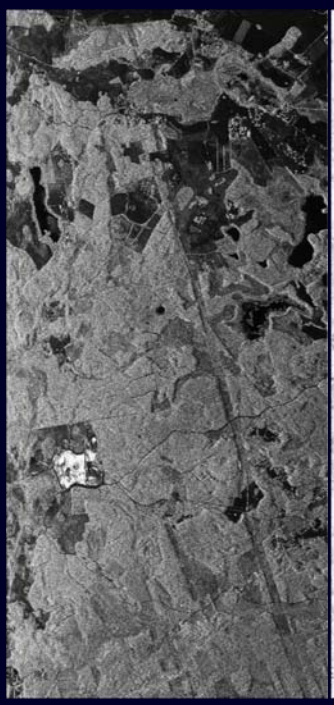

Amplitude Image HH

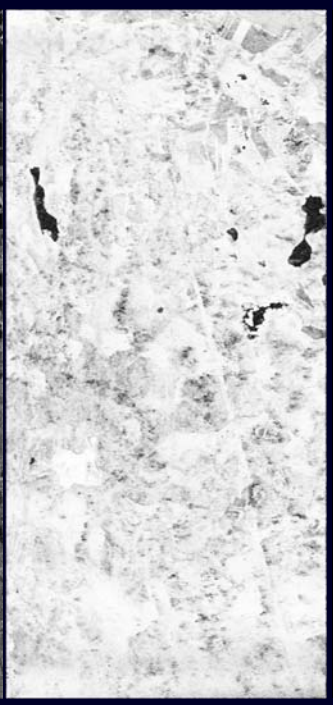

Volume Coherence

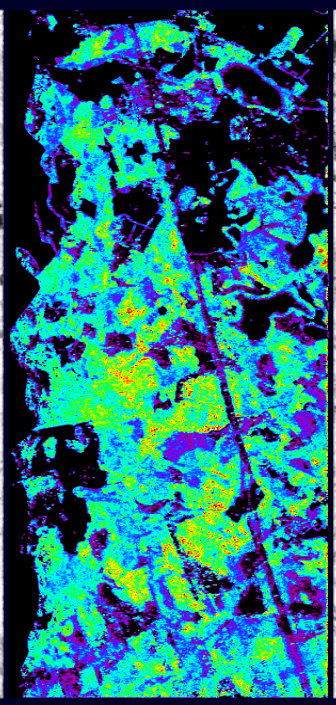

Forest Height Map

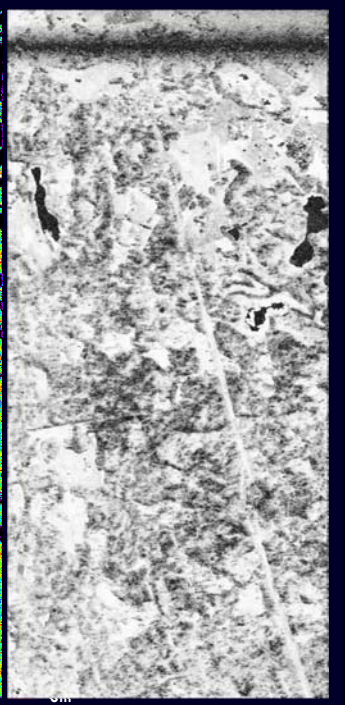

Volume + Temporal 24h

Interferometric Coherence: Volume vs Temporal Decorrelation

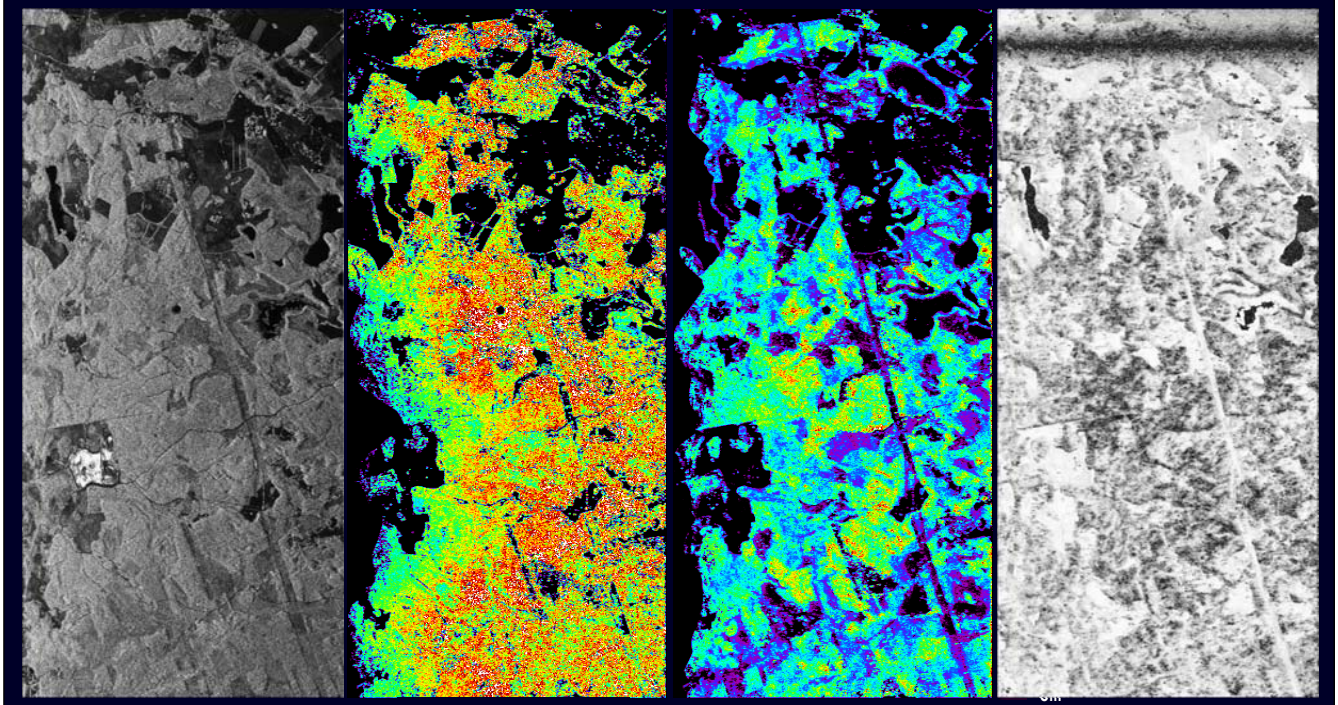

Deutsches Zentrum
DLR für Luft- und Raumfahrt e.V.
in der Helmholtz-Gemeinschaft

Forest Height Estimation & Decorrelation Effects

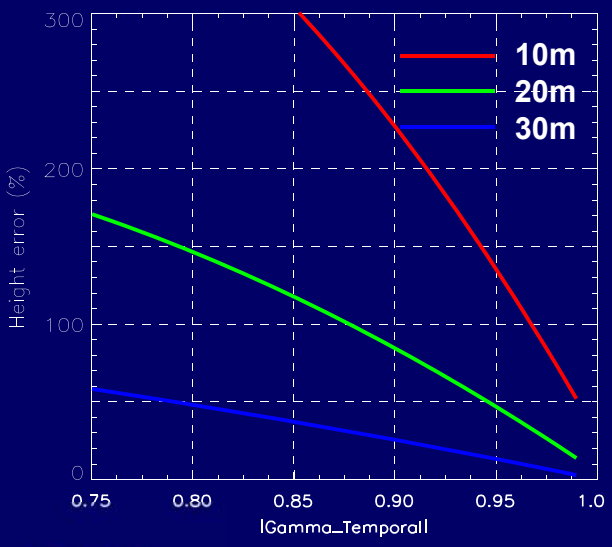

kz = 0.05

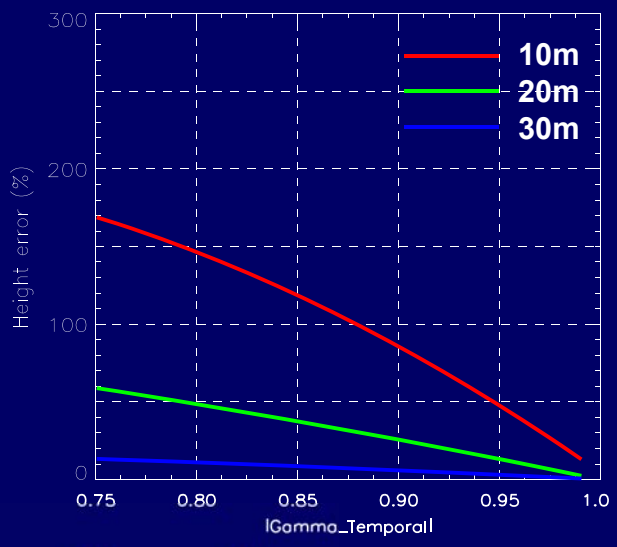

kz = 0.10

Incidence angle: 30°
Extinction: 0.1 dB/m

BIOSAR: Remningstorp Test Site

- Forest Heights: up to 25 -30m
- Predominantly Spruce but also Pine and Mixed stands.
- Homogenous and Managed.
- Biomass Level: up to 300t/ha
- Flat Topography

Remningstorp Test Site: The BIOSAR-I Campaign

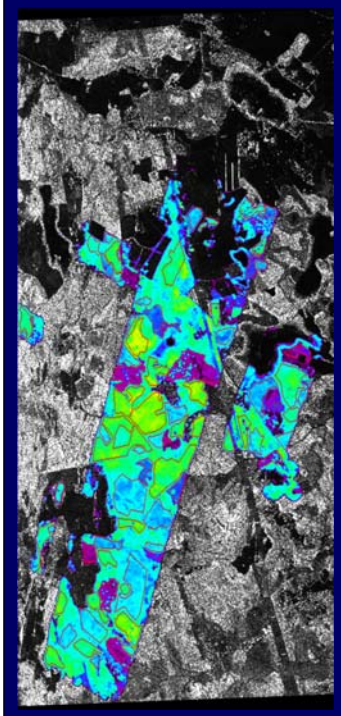

Amplitude Image HH

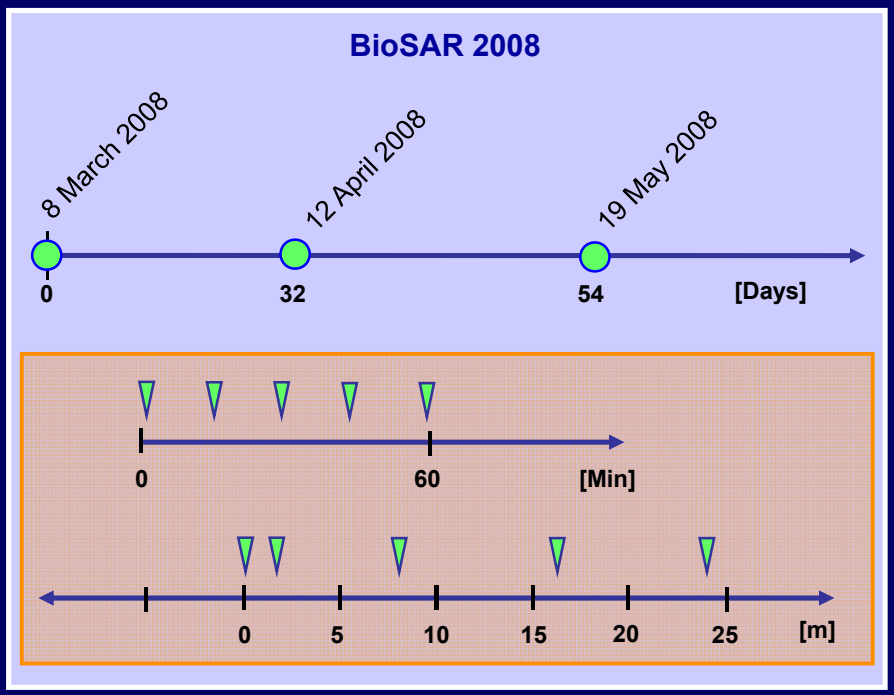

Remningstorp Test Site: Temporal Decorrelation: L-band

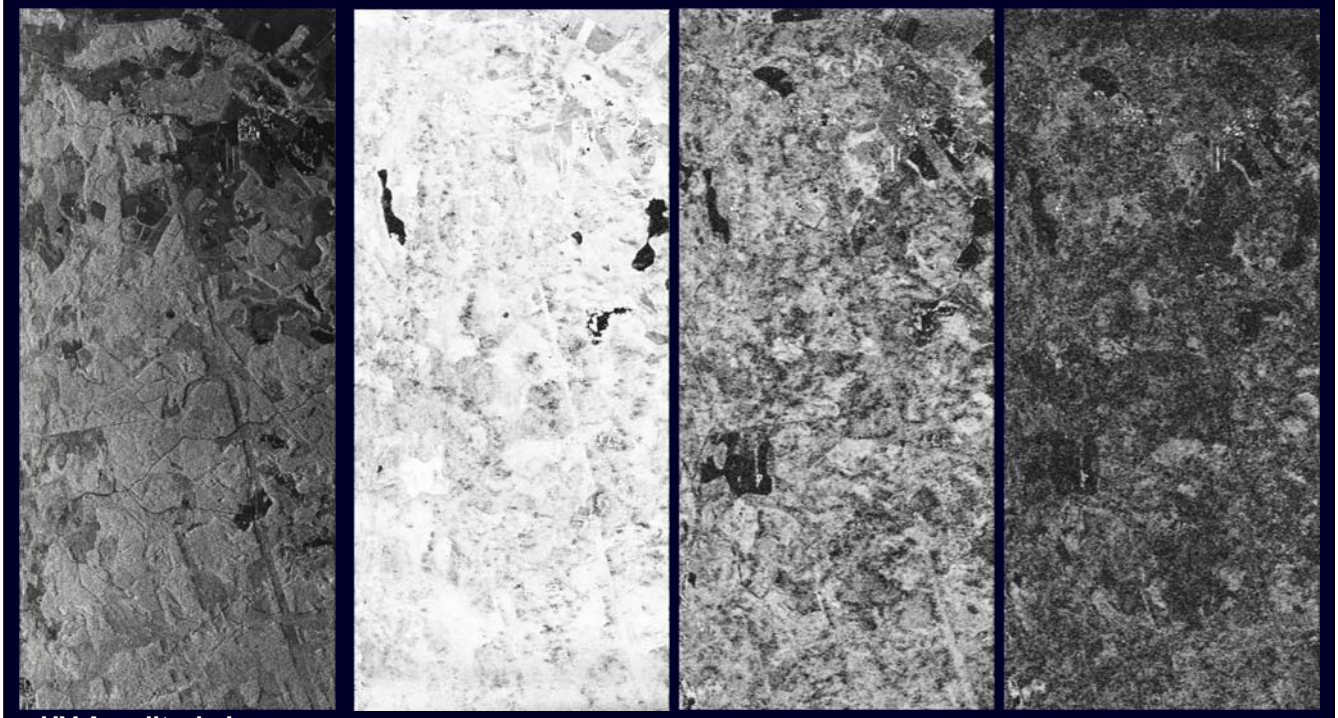

HV Amplitude Image | 0days | 30days | 58days

Remningstorp Test Site: Temporal Decorrelation: P-Band

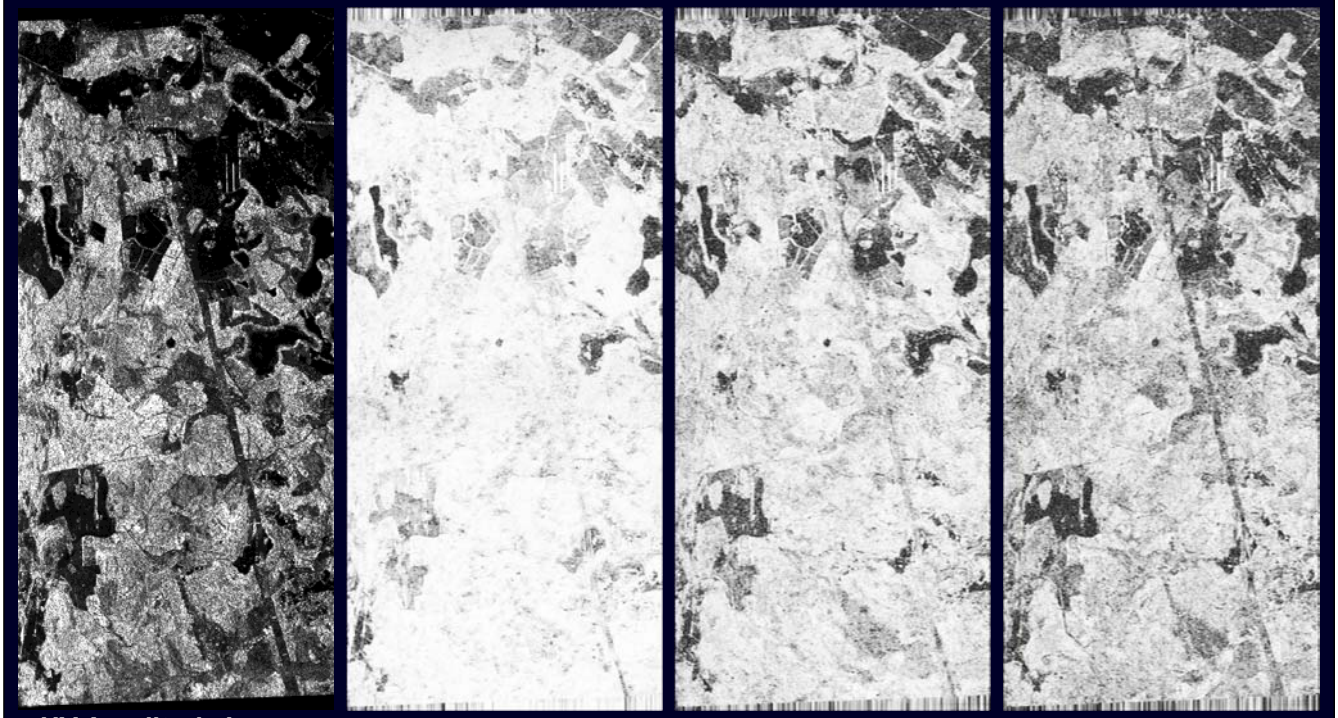

HV Amplitude Image | 0days | 30days | 58days

Remningstorp Test Site: Temporal Decorrelation: P-Band

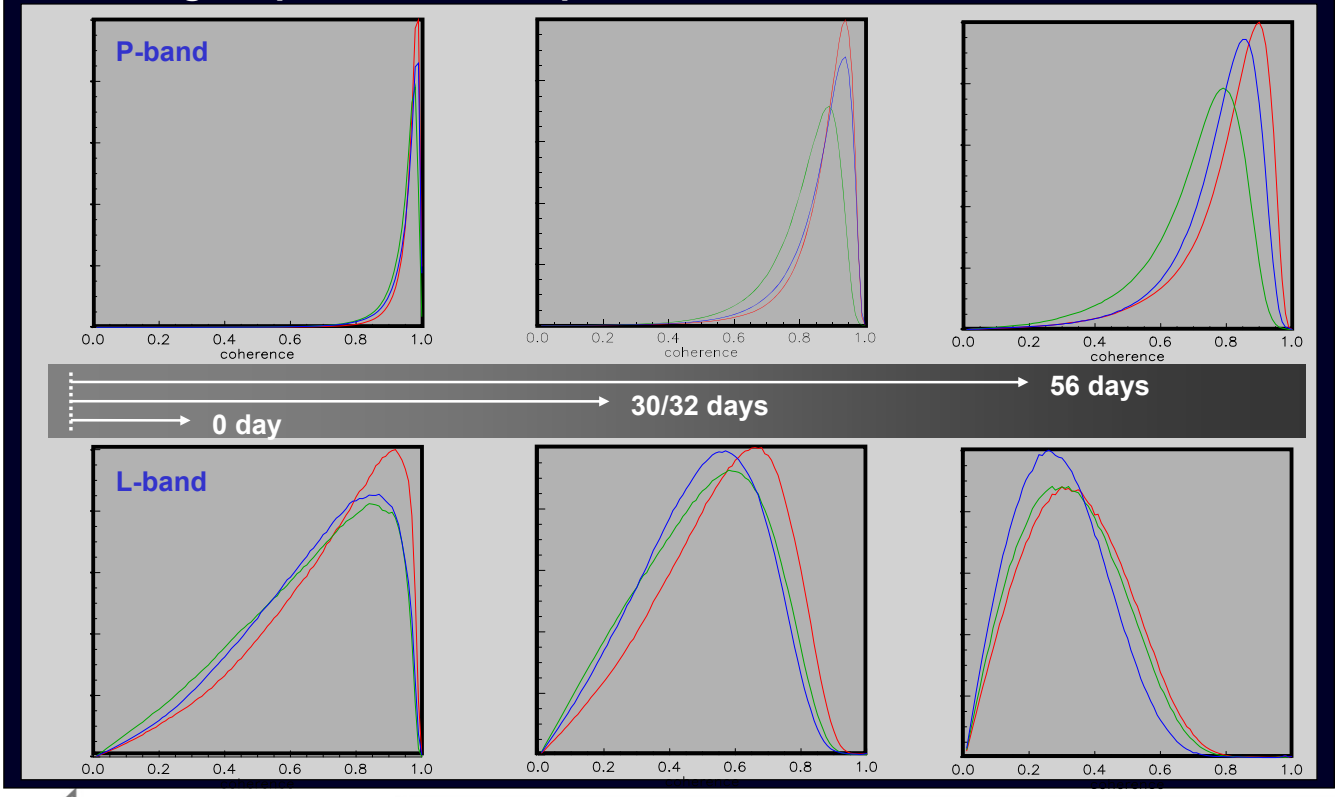

Deutsches Zentrum
DLR für Luft- und Raumfahrt e.V.
in der Helmholtz-Gemeinschaft

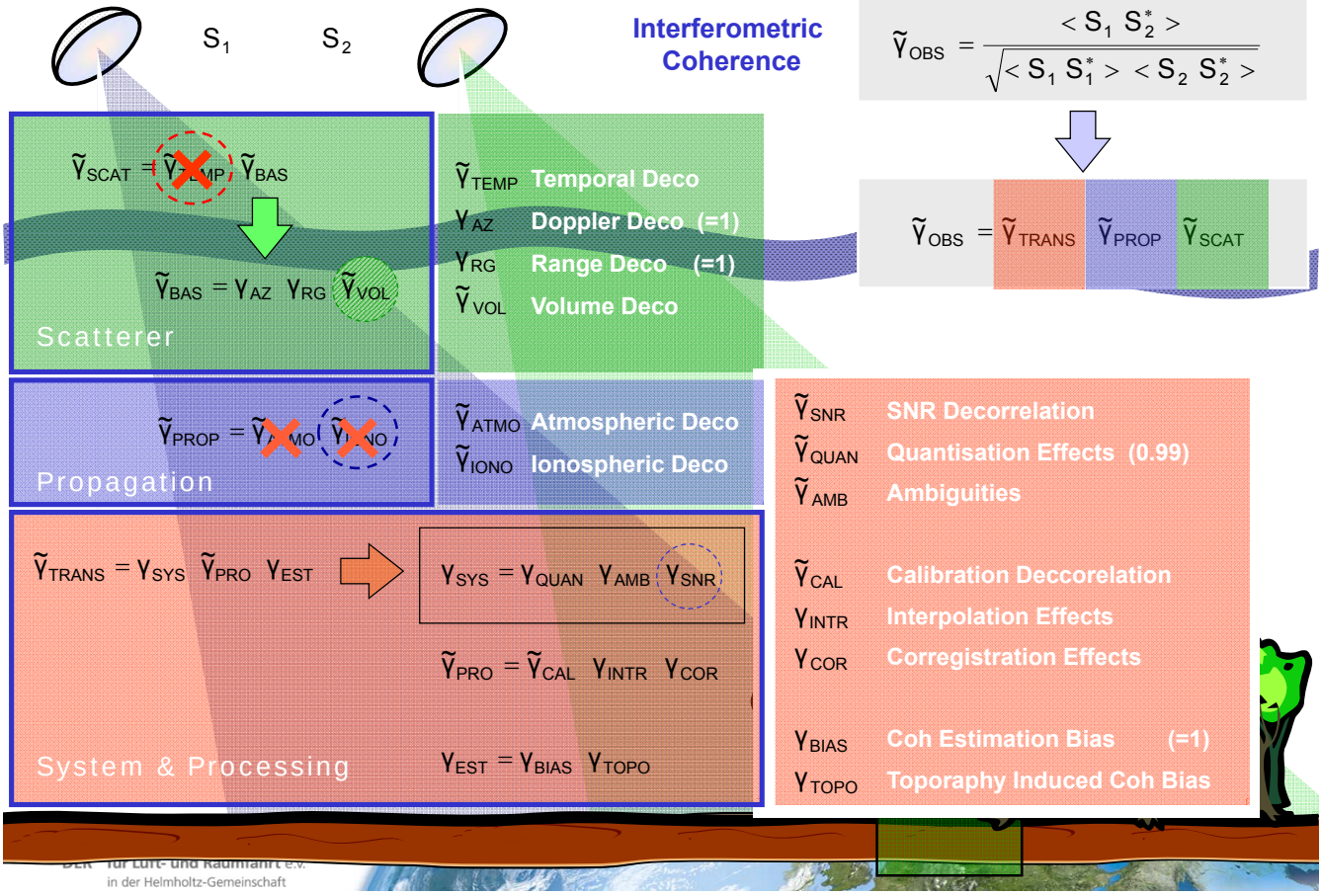

in der Helmholtz-Gemeinschaft

PolInSAR In Orbit

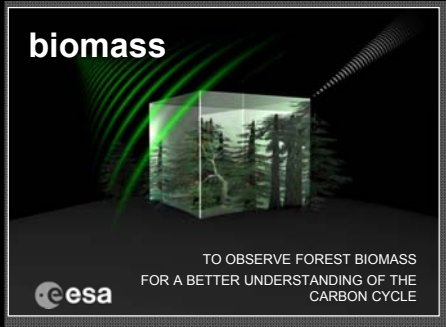

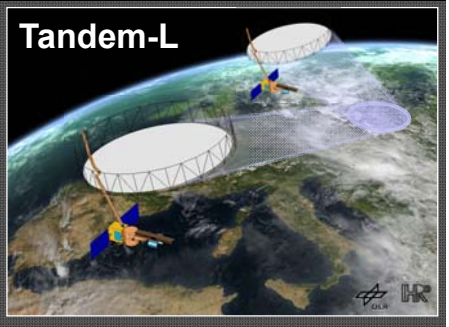

Deutsches Zentrum
DLR für Luft- und Raumfahrt e.V.
in der Helmholtz-Gemeinschaft

TanDEM-X: TerraSAR-X Add-on for Digital Elevation Measurements

DEMs	Spatial Resolution	Absolute Vertical Accuracy (90%)	Relative Vertical Accuracy (point-to-point in 1° cell, 90%
DTED-1	90m x 90m	< 30m	< 20m
DTED-2	30m x 30m	< 18m	< 12m
TanDEM-X DEM	12m x 12m	< 10m	< 2m
HDEM	6m x 6m	< 5m	< 0.8m

DLR ASTRIUM infoterra

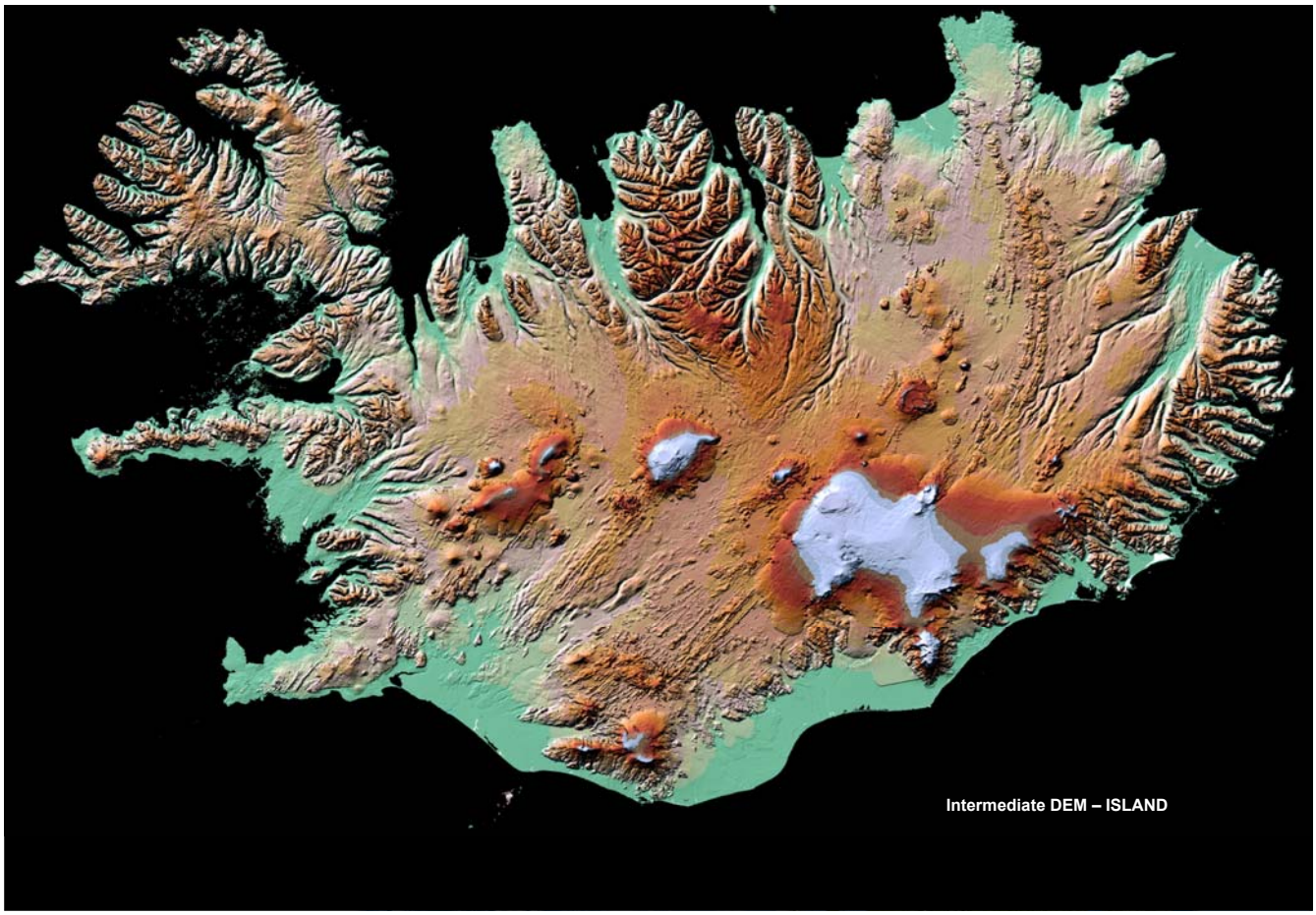

TanDEM-X Data Acquisition Modes

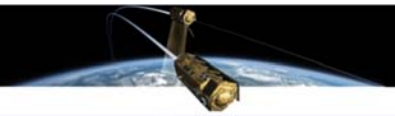

Pursuit Monostatic	July until October 2010	*Alternating Bistatic*
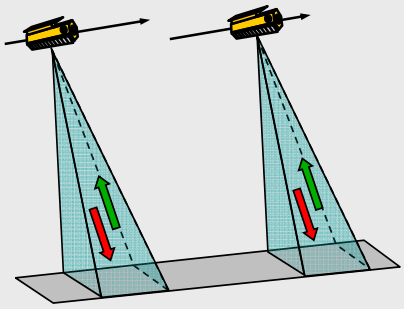	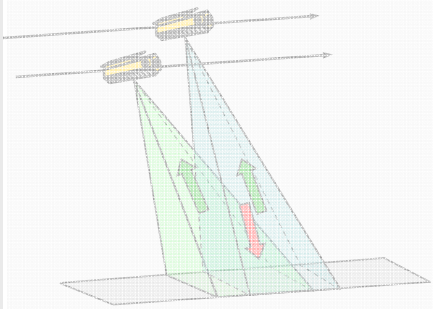	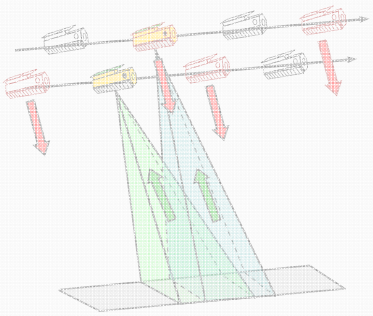
• **both satellites transmit and receive independently** • susceptible to temporal decorrelation & atmospheric disturbances • no PRF and phase synchronisation required (backup solution)	• one satellite transmits and both satellites receive simultaneously • small along-track displacement required for Doppler spectra overlap • requires PRF and phase synchronisation	• transmitter alternates between PRF pulses • provides three interferograms with two baselines in a single pass • enables precise phase synchronisation, calibration & verification

Standard DEM Mode

Temporal baseline: 2-3 sec (20-30Km Across Track separation)

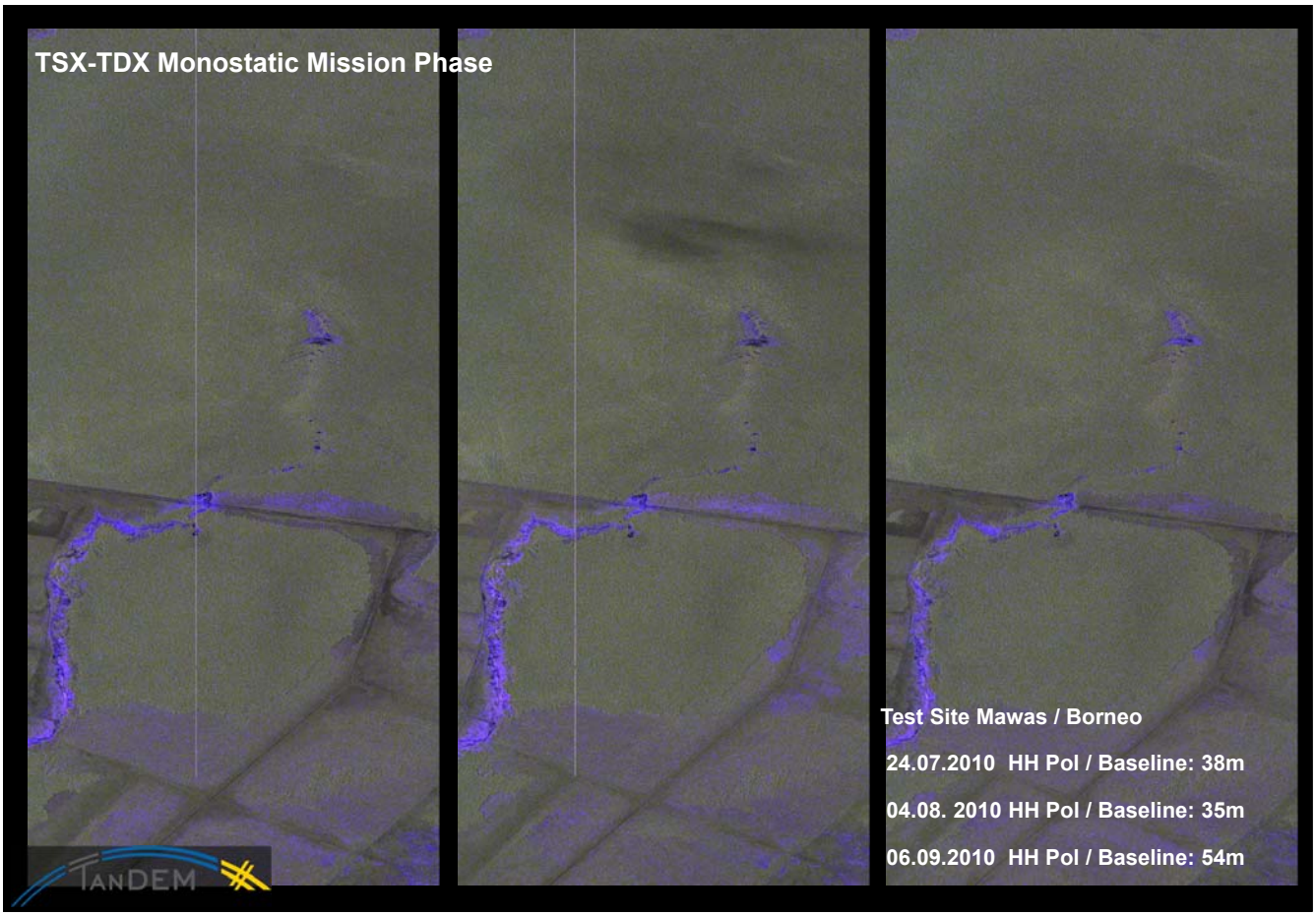
TSX-TDX Monostatic Mission Phase
TanDEM
Test Site Mawas / Borneo
24.07.2010 HH Pol / Baseline: 38m
04.08. 2010 HH Pol / Baseline: 35m
06.09.2010 HH Pol / Baseline: 54m

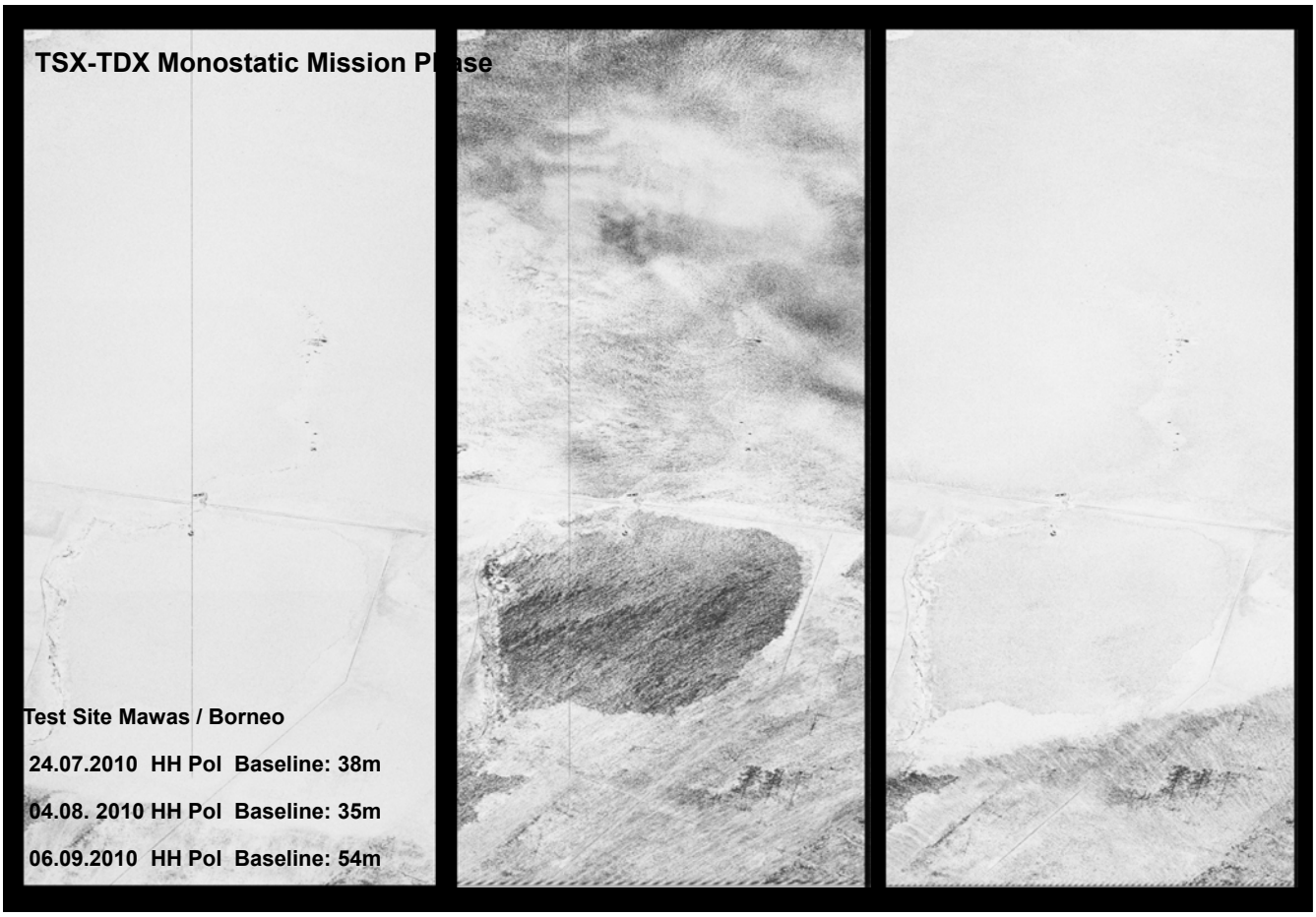
TSX-TDX Monostatic Mission Phase
Test Site Mawas / Borneo
24.07.2010 HH Pol Baseline: 38m
04.08. 2010 HH Pol Baseline: 35m
06.09.2010 HH Pol Baseline: 54m

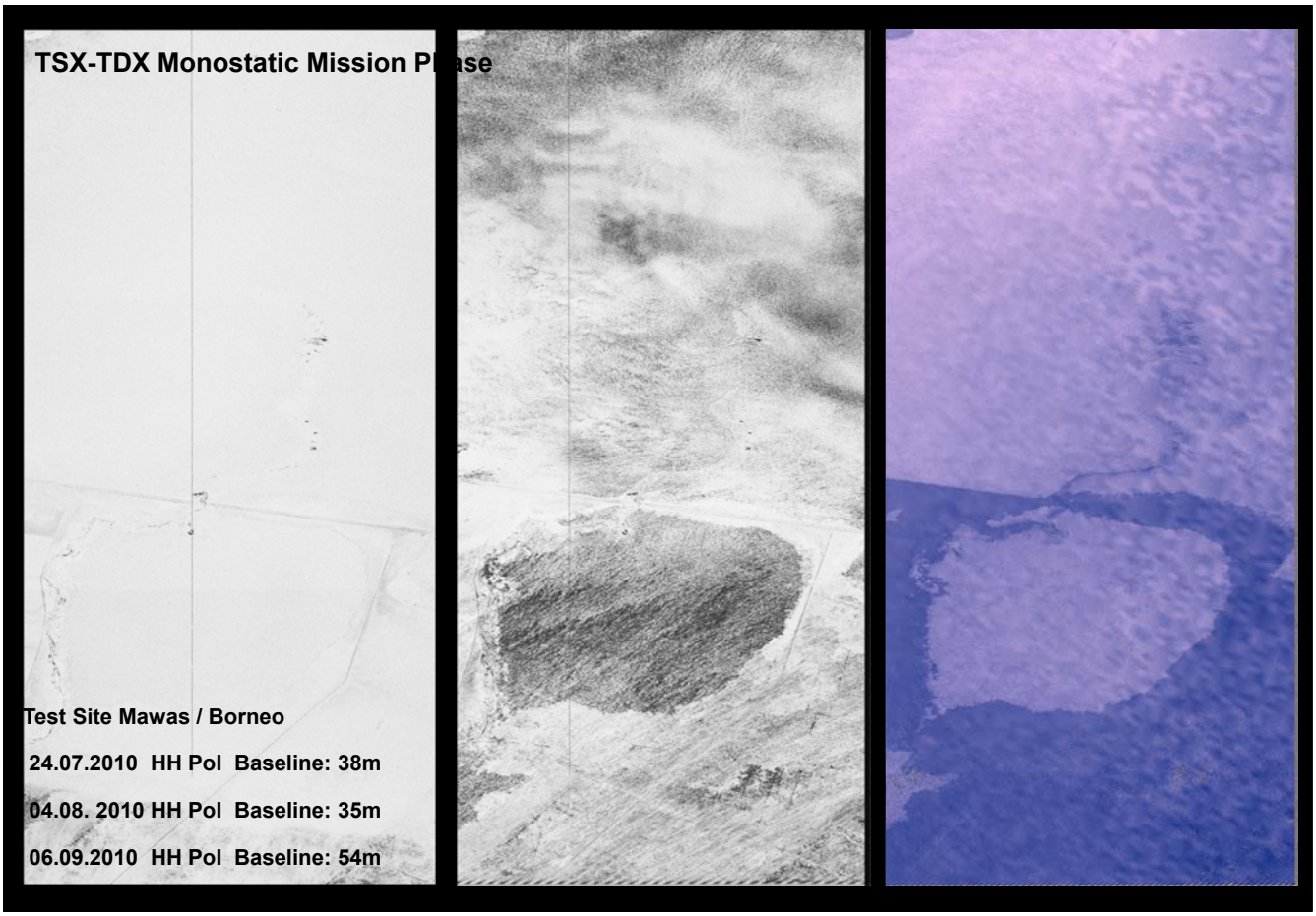

TanDEM-X Data Acquisition Modes

Pursuit Monostatic	Bistatic	Alternating Bistatic
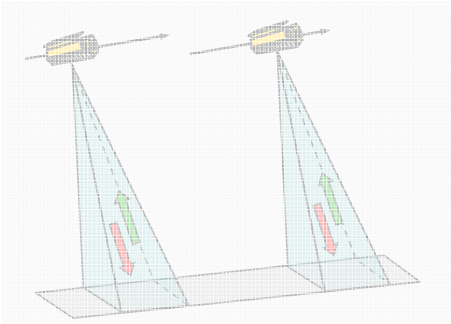	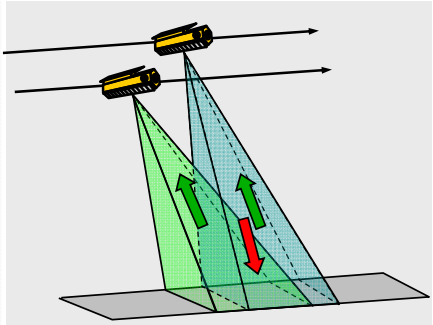	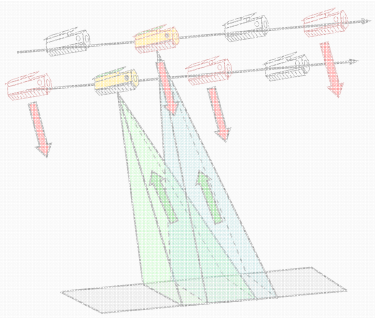
• both satellites transmit and receive independently • susceptible to temporal decorrelation & atmospheric disturbances • no PRF and phase synchronisation required (backup solution)	• **one satellite transmits and both satellites receive simultaneously** • small along-track displacement required for Doppler spectra overlap • requires PRF and phase synchronisation	• transmitter alternates between PRF pulses • provides three interferograms with two baselines in a single pass • enables precise phase synchronisation, calibration & verification

Standard DEM Mode

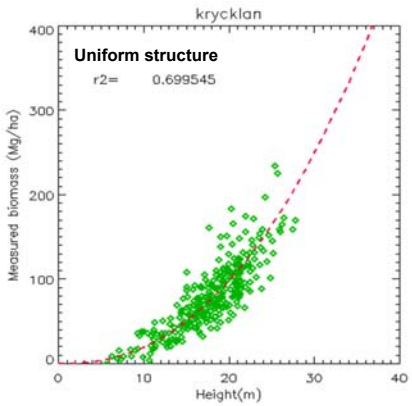

Test Site: Krycklan, Sweden

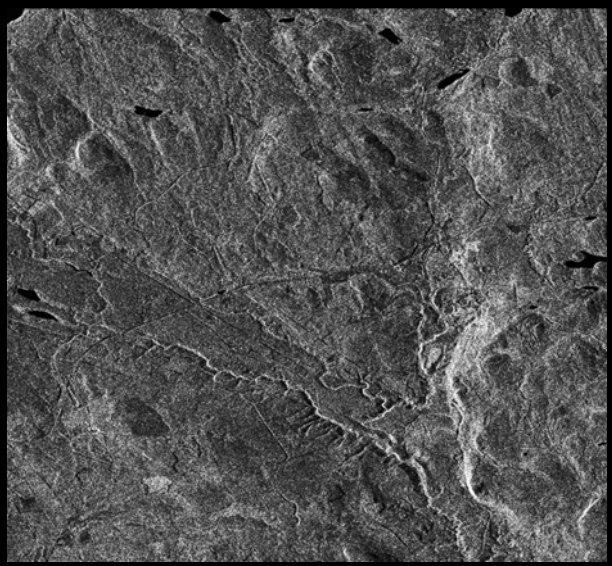

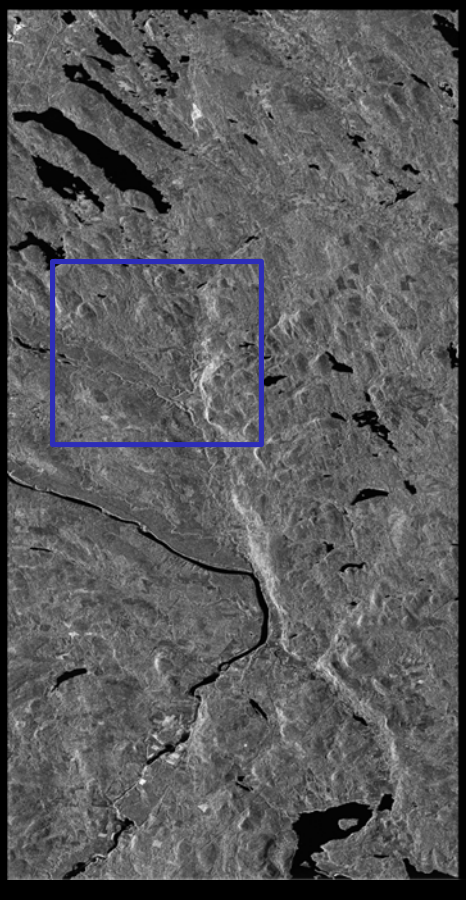

HH Amplitude

Test Site: Krycklan, Sweden

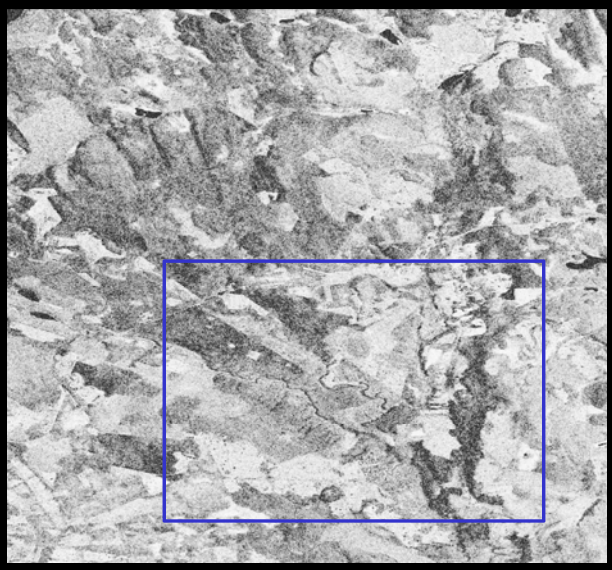

Interferometric Coherence HH

0 1

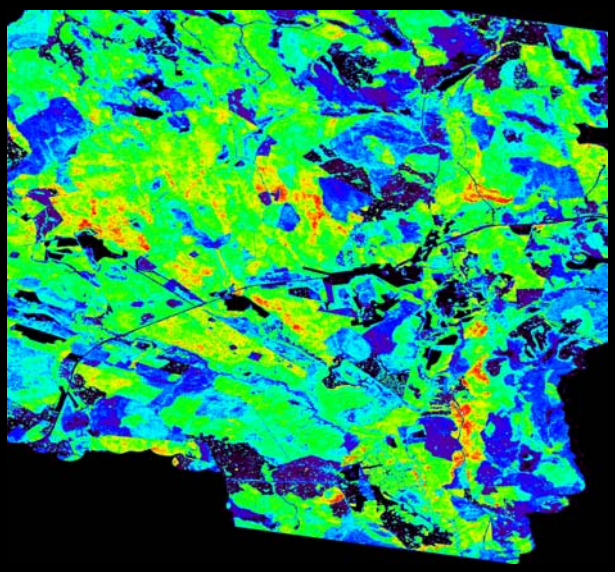

Lidar H100

0 [m] 30

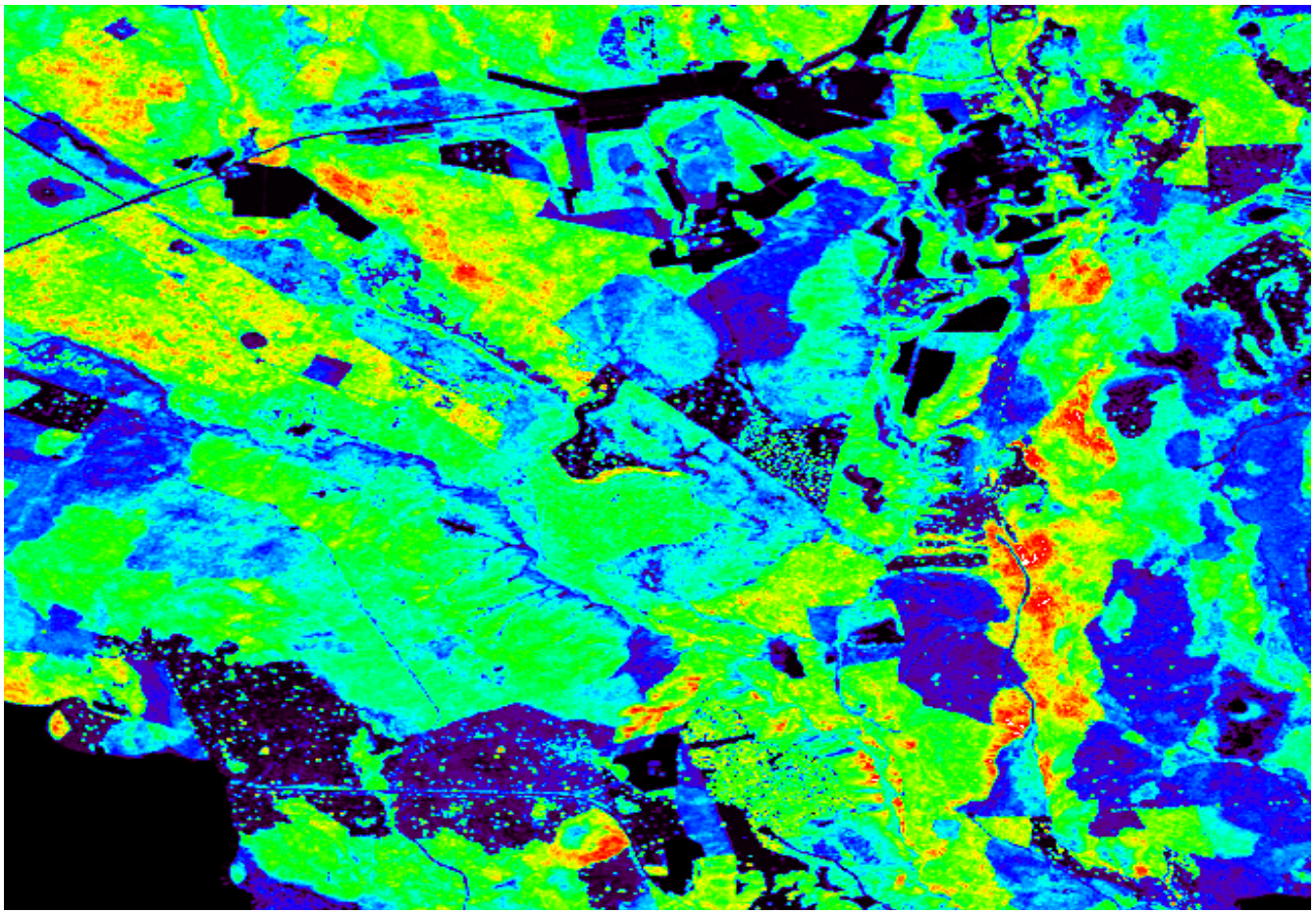

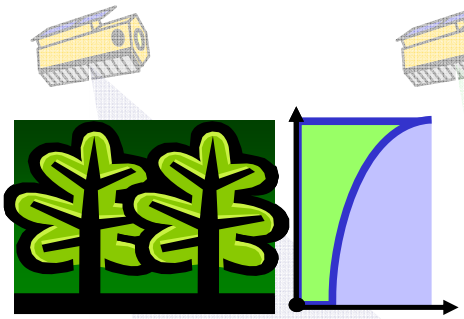

Single-Pol: 1 Layer Scattering Model

$$f(z) = \sigma_{V0} \exp\left(\frac{2\ \sigma\ z}{\cos\ \theta_0}\right)$$

$$\tilde{\gamma}(\vec{w}) = \exp(\,i\phi_0\,)\,\tilde{\gamma}_V$$

DEM ►Topography ϕ_0

Volume Height h_V Extinction σ

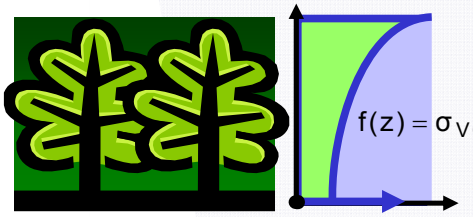

Dual-Pol: 2 Layer Scattering Model

$$f(z) = \sigma_{V0} \exp\left(\frac{2\ \sigma\ z}{\cos\ \theta_0}\right) + m'_G \delta(z - z_0)$$

$$\tilde{\gamma}(\vec{w}) = \exp(\,i\varphi_0\,)\,\frac{\tilde{\gamma}_V + m(\vec{w})}{1 + m(\vec{w})}$$

Volume Height h_V Extinction σ

Topography ϕ_0 G/V Ratio $m(\vec{w})$

$$\tilde{\gamma}_V = \frac{I}{I_0} \begin{cases} I = \int_0^{h_V} \exp(\,i\kappa_z z'\,) \exp\left(\frac{2\ \sigma\ z'}{\cos\ \theta_0}\right) dz' \\ I_0 = \int_0^{h_V} \exp\left(\frac{2\ \sigma\ z'}{\cos\ \theta_0}\right) dz' \end{cases}$$

G/V Ratio: $m(\vec{w}) = \frac{m_G(\vec{w})}{m_V(\vec{w}) I_0}$ Vertical Wavenumber: $\kappa_z = \frac{\kappa \Delta\theta}{\sin(\theta_0)}$

Test Site: Krycklan, Sweden

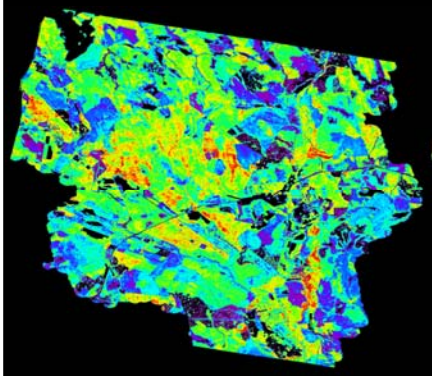

Lidar H100

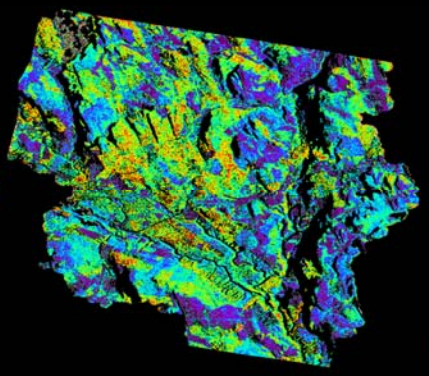

Single-Pol + DEM H100

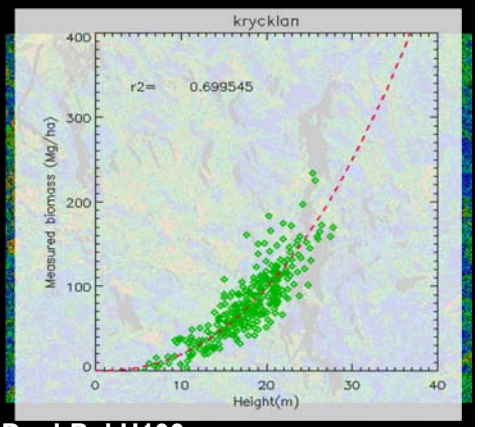

Dual-Pol H100

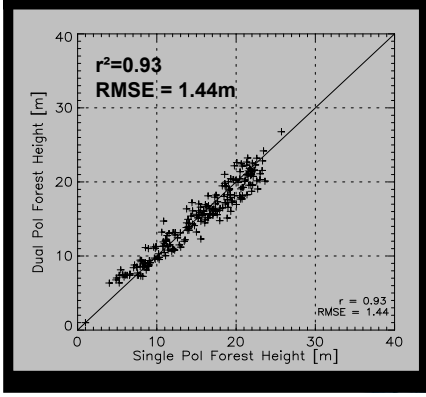

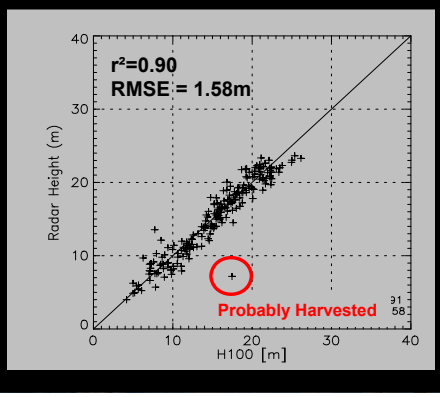

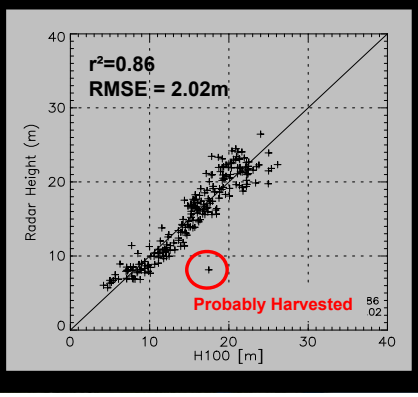

CORINE Land Cover Classes - Krycklan

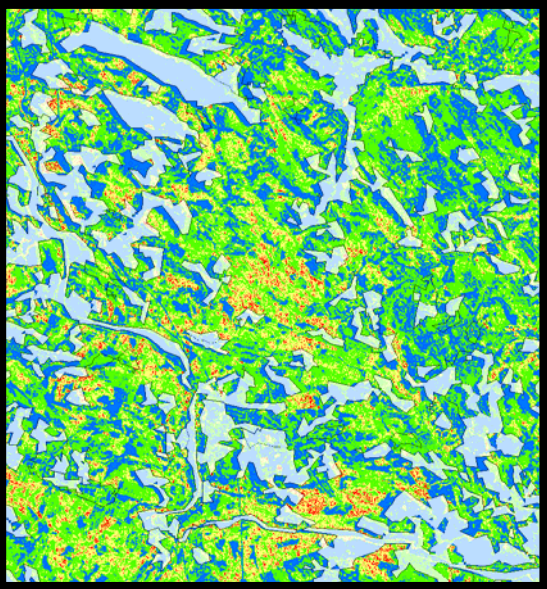

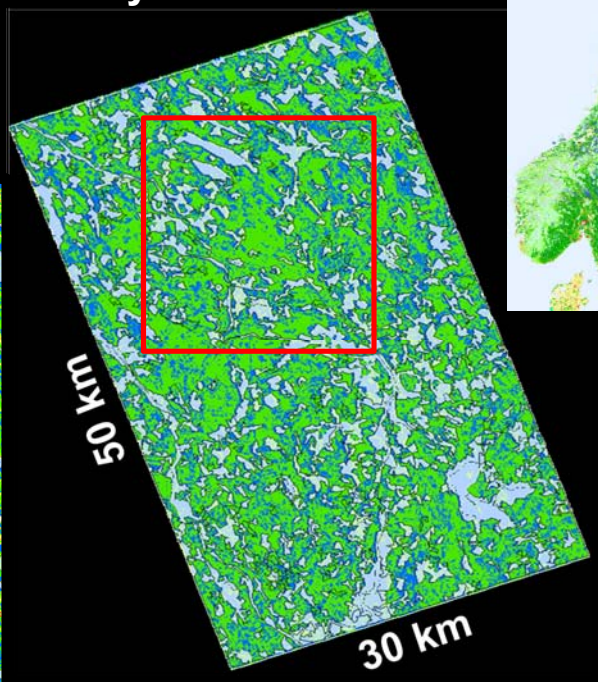

< 10 Mg/ha
10 - 50 Mg/ha
50 - 150 Mg/ha
> 150 Mg/ha

TanDEM

Test Site: Traunstein, Germany

HH Amplitude

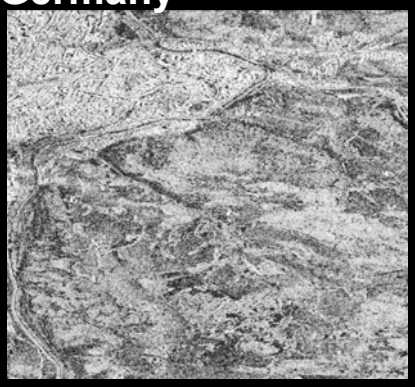

Interferometric Coherence HH

Interferometric Coherence Max

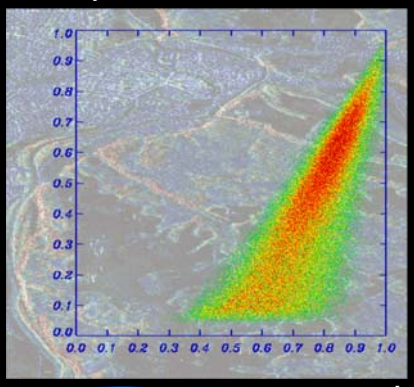

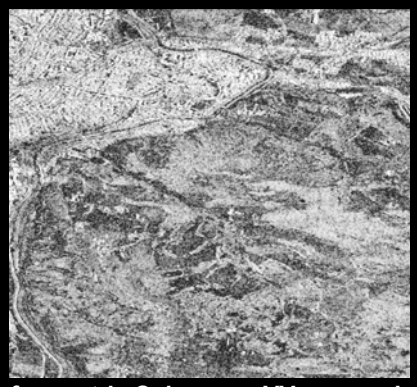

Interferometric Coherence VV

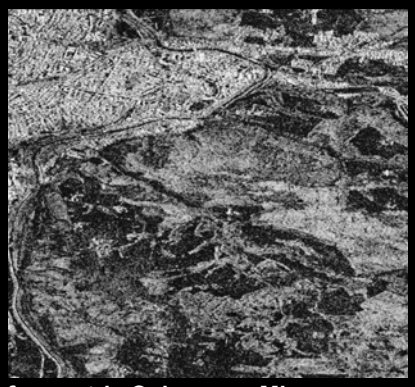

Interferometric Coherence Min

TanDEM

Test Site: Traunstein, Germany

ESAR Inversion Results

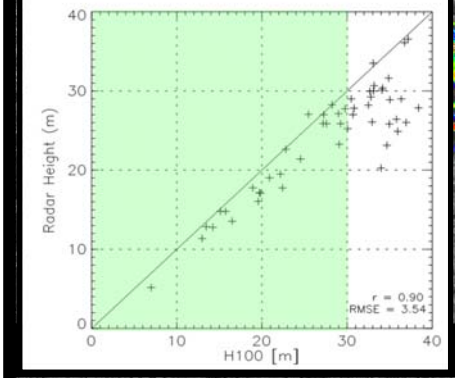

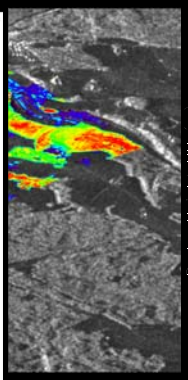

Single-Pol (HH) + DEM

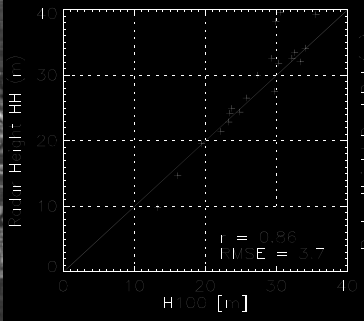

Dual-Pol

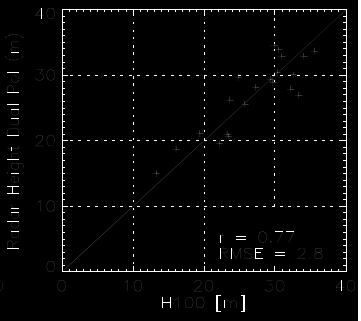

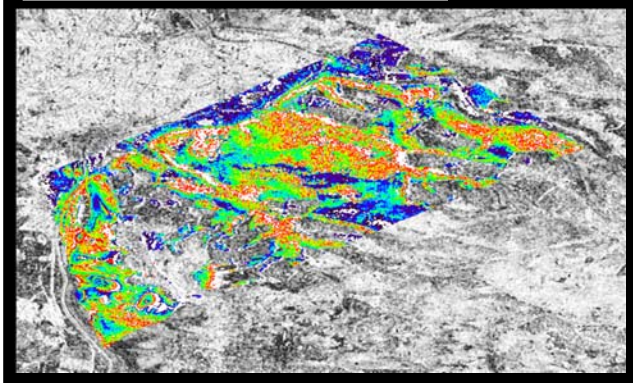

Single-Pol (HH) + DEM H100

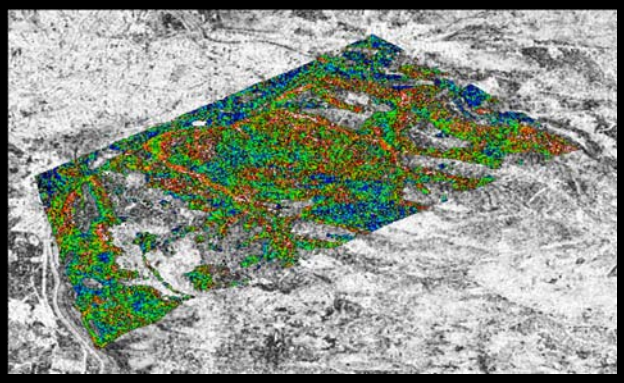

Dual-Pol H100

Test Site: Mawas, Indonesia

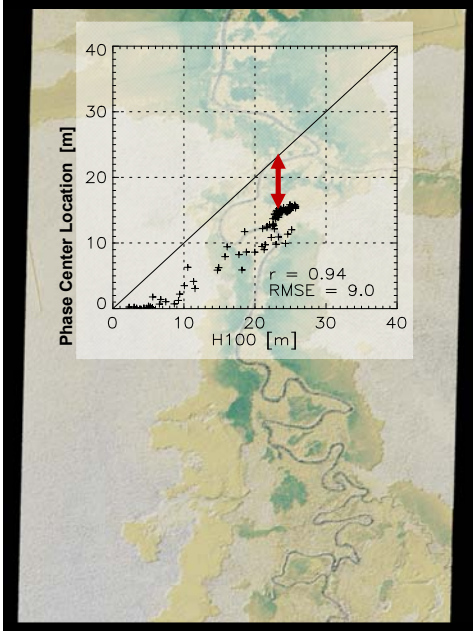

Tandem DEM

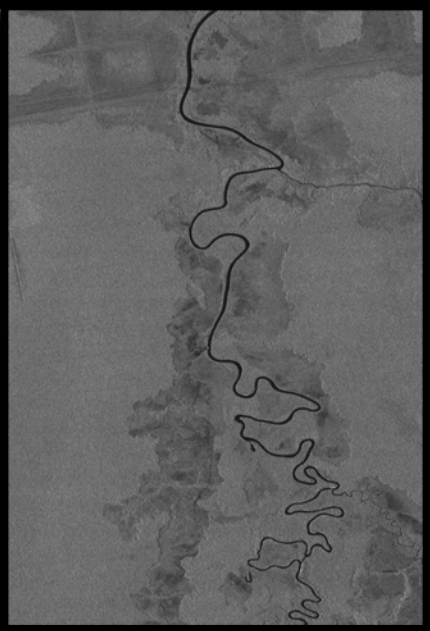

Amplitude HH

Interferometric Coherence HH

TanDEM

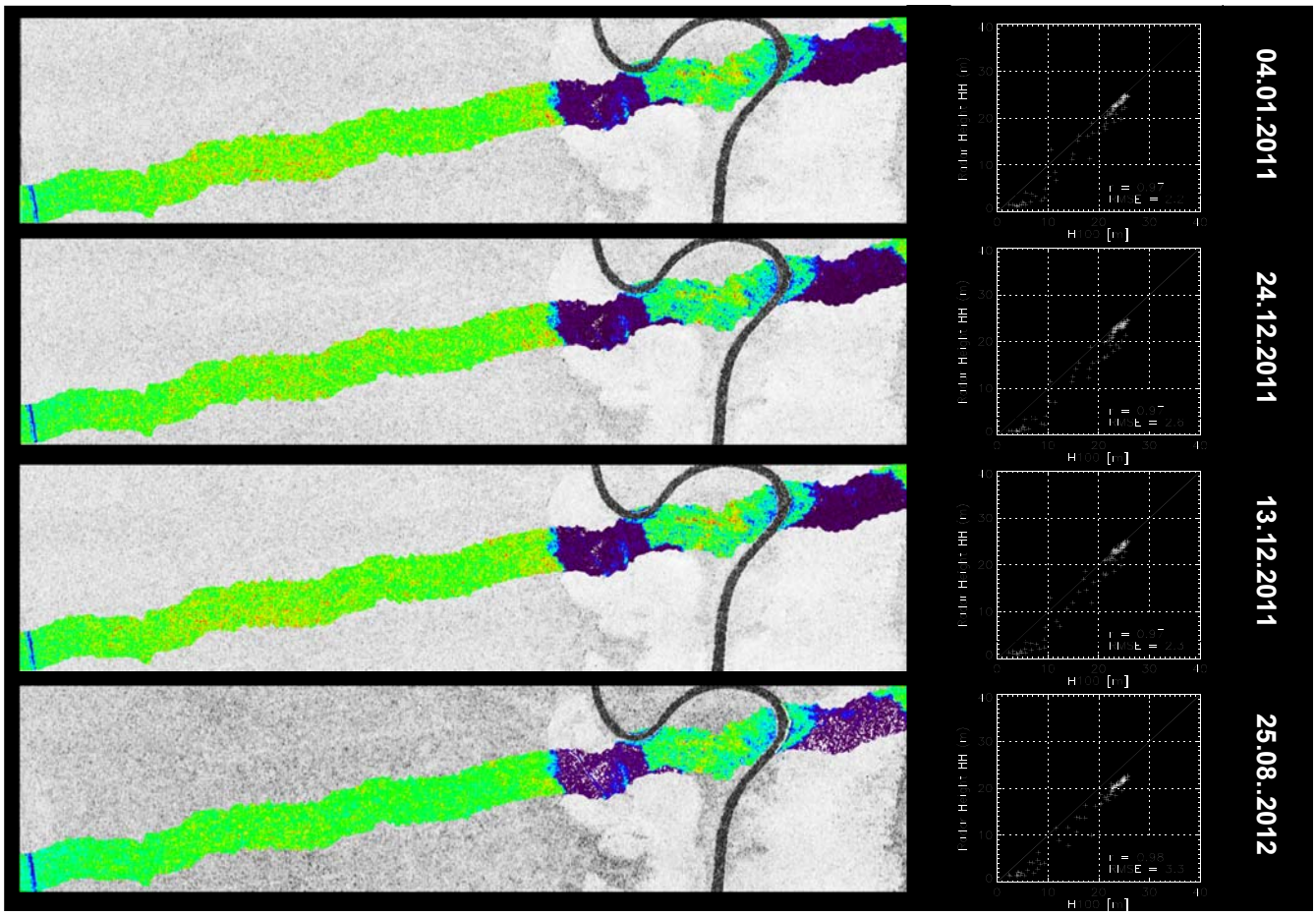

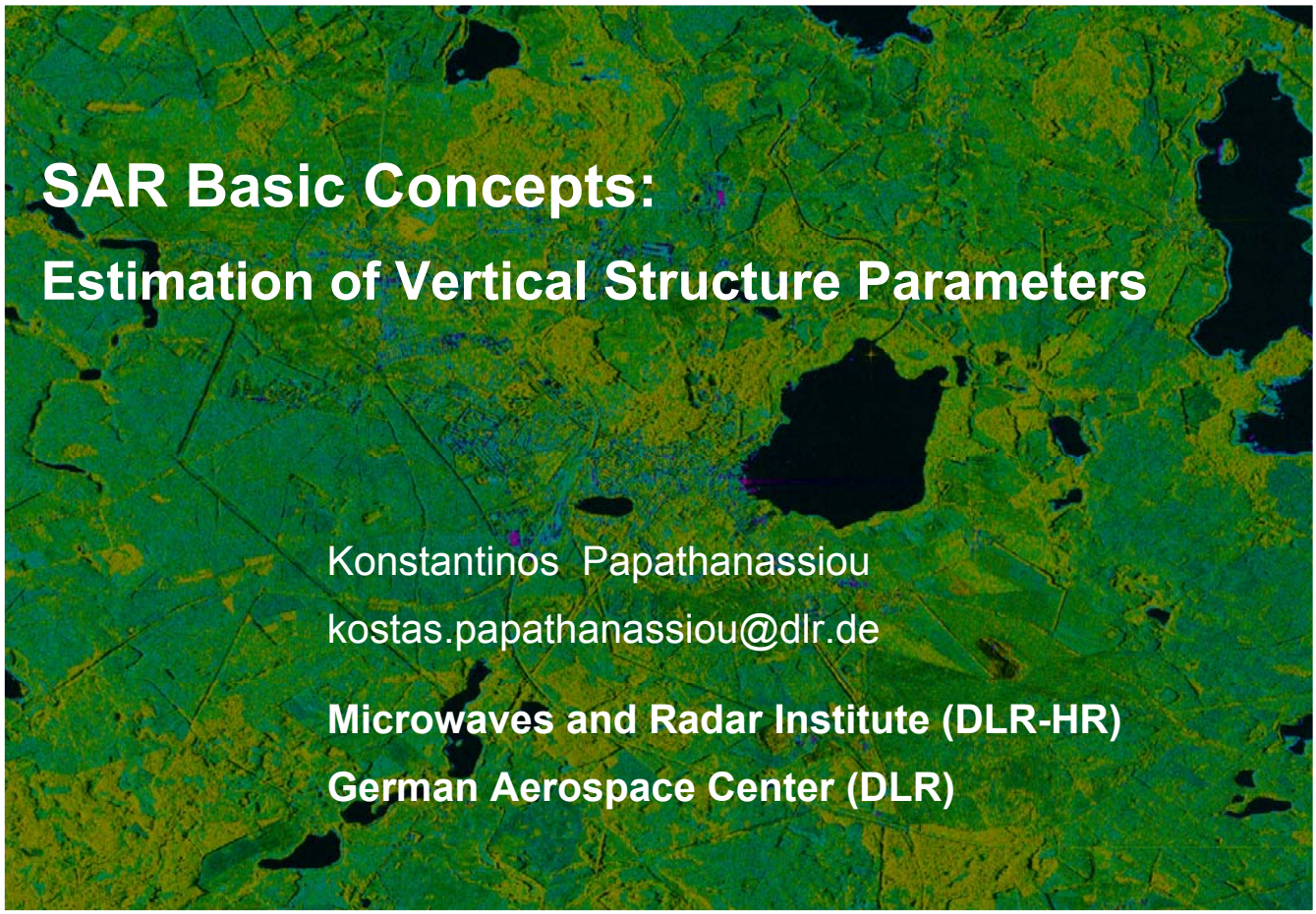

SAR Basic Concepts:

Estimation of Vertical Structure Parameters

Konstantinos Papathanassiou

kostas.papathanassiou@dlr.de

Microwaves and Radar Institute (DLR-HR)

German Aerospace Center (DLR)